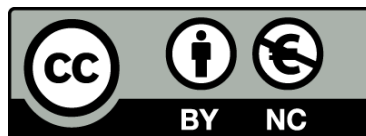




UNIVERSITAT_{DE}
BARCELONA

Correspondences in higher-dimensional gravity

Adriana Di Dato



Aquesta tesi doctoral està subjecta a la llicència **Reconeixement- NoComercial 3.0. Espanya de Creative Commons.**

Esta tesis doctoral está sujeta a la licencia **Reconocimiento - NoComercial 3.0. España de Creative Commons.**

This doctoral thesis is licensed under the **Creative Commons Attribution-NonCommercial 3.0. Spain License.**

Correspondences in higher-dimensional gravity

Maps between fluids, gravity and spacetimes

Adriana Di Dato

Departament de Física Fonamental

Universitat de Barcelona



July 2015

Programa de Doctorat en Física

Correspondences in higher-dimensional gravity

Adriana Di Dato

A dissertation submitted for the degree of

Doctor of Philosophy in Physics

This thesis was prepared under the supervision of Prof.

Roberto Emparan García de Salazar

Barcelona, July 2015

*To the person I will be,
my family and my love.*

“..AND ONCE THE STORM IS OVER YOU WON’T REMEMBER HOW YOU MADE IT THROUGH, HOW YOU MANAGED TO SURVIVE. YOU WON’T EVEN BE SURE, IN FACT, WHETHER THE STORM IS REALLY OVER. BUT ONE THING IS CERTAIN. WHEN YOU COME OUT OF THE STORM YOU WON’T BE THE SAME PERSON WHO WALKED IN. THAT’S WHAT THIS STORM’S ALL ABOUT.”

HARUKI MURAKAMI, *Kafka on the Shore*.

Acknowledgements

Todavía no puedo creer que este día haya llegado.

Mi primer agradecimiento va a la persona que ha permitido que todo esto haya sido posible, Roberto Emparan. Gracias por tu ayuda y disponibilidad. Ha sido un gran honor haber investigado en el límite del conocimiento de la física teórica aprendiendo de uno de los mejores. Gracias por todo lo que me has enseñado y por haberme indicado el camino.

I wish to express my sincere thanks to my collaborators Markus Fröb, Jakob Gath and Andreas Viegand. Without them this thesis would probably have been impossible. I would like to thank my hosts during my stays abroad Harvey Reall and Niels Obers for their warm hospitality. A special thanks to Niels for helping and inspiring me. Discussing with you is always a great pleasure, your passion for physics is amazing.

I would like to thank the members of our group, especially Jaume Garriga, Bartomeu Fiol, David Mateos, Enric Verdaguer, Javier Tarrío, Christiana Pantelidou, Miguel Zilhao and Antón Faedo for the interesting discussions during the Journal Clubs and for always being available for questions and sharing their experiences. Chris, me ha encantado conocerte. Es siempre muy divertido y estimulante estar contigo.

During this PhD I had the opportunity to travel a lot and meet great people who enriched me with interesting discussions as Jelle Hartong, Troels Harkmark, Marco Cardarelli, Oscar Dias and Joan Camps.

Un enorme agradecimiento a Bea, Elena y Cristina. No sé como habría resuelto la toda la complicada burocracia y los olvidos de llaves en casa. Sus sonrisas nunca faltan y es siempre un placer pasar por la secretaría.

Gracias a toda la gente maravillosa que he conocido durante estos cuatro años. Gracias Dani, Luis Cort, Genís, Carla, Roberta, Mirian, Miquel, Wilke, Alejandro, Paco, Paolo, Blai Pie, Isa, Oriol, Luis, Mariona, Pol, Carlos, María, Guille y Martin. Gente que sigue a mi lado y otra que desafortunadamente ha seguido su camino lejos de aquí que pero nunca olvidaré. Un placer haber compartido este trocito de vida juntos.

Gracias a los que considero mis hermanos mayores, Iván y Blabli. Siempre a mi lado, animándome y apoyándome. Gracias por ayudarme a ver la parte positiva de las cosas.

Gracias a Nuri. Por compartir nuestra pasión por la música , el cine, la naturaleza y la manera de vivir la vida. Por “Cinema paradiso” y por todos los proyectos que montaremos. Gracias a mi fantásticas amigas Mari y Chu. Ellas han hecho que mi camino fuera más divertido y que me sintiera menos sola. Gracias por la salsa, la música compartida, los vídeos divertidos, las comidas ricas, el billar y el ping pong (Chu, somos las campeonas). El tiempo con vosotras es siempre ¡Pura Vida!

Un Danke muy grande a mi amigo Markus. Por su ayuda, por todas las discusiones donde siempre aprendía algo y por todos los momentos divertidos pasados juntos. Gracias Albert por intentar mejorarme y por ayudarme cada vez que te lo pido. Sé que es tu manera de quererme. Gracias por todas las horas de tenis y los discursos interesantes mientras llegamos a esports, Vicente. Gracias Daddy por las risas, la música que fluye en tu sangre y por dejarme jugar a tu sabes qué.

A mis amigas Muriel e Isa, mi familia en Barcelona. Gracias por todos los momentos buenos y malos que hemos compartido, por las comidas juntas, por el ping pong antiestrés y las risas.

A Elsewhere che il destino ha voluto far tornare nel mio cammino y al super simpatico andalú Pablo...el que hace el mejor salmorejo que he probado nunca!

Un ringraziamento speciale con tutto il mio cuore va alla mia famiglia. Ai miei genitori che non hanno mai smesso di credere in me anche quando io ormai non lo facevo piú, per i loro consigli , il loro appoggio e per la loro presenza al mio fianco anche se a chilometri di distanza. E' anche per voi questo traguardo. Ai miei nonnini che aspettano con impazienza il mio ritorno ogni volta che me vado.

Alla mia sorellina un grazie dal profondo della mia anima. Senza di lei non so come sarebbe stata questa esperienza. Per essersi presa cura di me, sempre. Per il suo amore che mai é mancato e per le tante cose fatte insieme. Sempre mano nella mano affrontando la vita. Ovunque con te.

Alla mia momina per troppe cose. Per la cosa piú preziosa che mi poteva lasciare, la libertà. Grazie per esserti fidata di me e per aver appoggiato qualsiasi decisione avessi preso. Grazie per le lacrime che non hai pianto e per l'amore che non ho mai smesso mai di sentire. Questi quattro anni hanno significato tanto per me. Non possiamo tornare indietro ma possiamo pensare a quanti anni ancora avremmo da vivere insieme.

Al mio violino che ha saputo aspettare. Alla mia anima che ha avuto pazienza e non si é arresa.

List of Publications

- [1] A. Di Dato,
“*Kaluza-Klein reduction of relativistic fluids and their gravity duals*,”
JHEP **1312** (2013) 087, [arXiv:1307.8365 \[hep-th\]](#).
- [2] A. Di Dato and M. B. Fröb,
“*Mapping AdS to dS spaces and back*,”
Phys. Rev. D **91** (2015) 6, 064028, [arXiv:1404.2785 \[hep-th\]](#).
- [3] A. Di Dato, J. Gath and A. V. Pedersen,
“*Probing the Hydrodynamic Limit of (Super)gravity*,”
JHEP **1504** (2015) 171, [arXiv:1501.05441 \[hep-th\]](#).

Contents

1	Introduction	1
2	Effective theories of gravity	7
2.1	The fluid/gravity correspondence	7
2.1.1	Elements of fluid dynamics	8
2.1.2	Fluid dynamics from gravity	10
2.2	The Blackfold Approach	12
2.2.1	Applying the blackfold approach	14
3	Map for different spacetimes	19
3.1	AdS/Ricci flat correspondence	19
3.2	Mapping AdS to dS spaces and back	20
3.2.1	Introduction	20
3.2.2	Deriving the map	21
3.2.3	Applications	25
3.2.4	Discussion	38
4	Kaluza-Klein reduction of relativistic fluids and their gravity duals	41
4.1	Introduction	41
4.2	Hydrodynamic Kaluza-Klein ansatz and reduction of the perfect fluid	43
4.3	Reduction of dissipative terms	45
4.4	Charged black brane/fluid duals	49
5	Probing the Hydrodynamic Limit of (Super)gravity	53
5.1	Introduction	53
5.2	Hydrodynamics of black p -branes	56
5.2.1	The perturbative expansion	59
5.2.2	Transport coefficients	61
5.2.3	Dynamical stability	62

5.3	Hydrodynamics of dilatonic Maxwell charged branes	66
5.3.1	Transport coefficients	67
5.3.2	Dynamical stability	68
5.3.3	A check: Mapping to AdS	71
5.4	Discussion	74
6	Conclusions	79
7	Resumen en castellano	81
Appendix A	Curvature tensor from dimensional reduction	85
A.1	Curvature tensors for a product metric	85
A.2	Curvature tensors for asymptotically AdS with a CHS	86
Appendix B	Extracting transport coefficients	89
B.1	Equations of motion for the reduced theory	89
B.2	Dissipative transport coefficients	91
Appendix C	Details on the perturbative computation for Chapter 5	97
C.1	Setting up the perturbative problem	97
C.2	Solving the Maxwell system	100
C.3	Solving the fundametally charged system	106
C.4	Fixing the integration constants	109
References		111

Chapter 1

Introduction

One hundred years of General Relativity (GR) and there is still so much that remains to be understood. Einstein's celebrated theory of gravitation is a geometric description of the Universe fusing together space and time in a dynamical *spacetime* [4, 5]. GR is the base for modern cosmology and astrophysics and so far is our best theory of gravity. However we are still testing it out.

The most surprising prediction of Einstein's theory is the existence of black holes. These are regions of spacetime from which gravity prevents anything, including light, from escaping. The point of no return is defined by an event horizon. Amazingly, in contrast to their extremely complicated behaviour and description, black holes can be completely characterized by only three parameters: mass, electric charge, and angular momentum [6, 7]. This is what it is called the “no hair theorem”. Thermal nature of a black holes was another unexpected discovery. Black holes radiate and a finite temperature and entropy can be associated to it as derived by Bekenstein and Hawking [8, 9] in the context of quantum field theory. As result, a remarkable parallelism exists between the laws of black hole mechanics and the laws of thermodynamics [10].

Unfortunately, GR and quantum mechanic seem to be incompatible. For instance, the fact that black holes give off radiation leads to a non-unitary process. Quantum evolution, apparently, does not preserve information when black holes are present. The information is lost. This goes under the name of “information paradox” [11, 12]. An additional interesting puzzle arises once we pass the event horizon. Indeed, a singularity, a point where the spacetime curvature becomes pathological, is presumably hidden behind it. This anomalous behaviour should be seen as an indication that GR fails to provide a proper description. When the curvature of spacetime is around the Planck length we are probably outside the domain of applicability of Einstein's theory. It is

therefore necessary to find an adequate quantum description of gravity able to cure these problems.

In the last decade many improvements have been achieved in this direction but a satisfactory theory, which combines quantum theory and GR in a consistent way, still remains unknown. The great hope is string theory [13]. At fundamental level, this theory considers matter as tiny loops of string substituting hence the concept of point-particle. As any good theory of quantum gravity should do, at low-energies, string theory naturally gives rise to GR. Even if it is still experimentally untested, string theory provides an amazingly fruitful framework for physics exploring qualitatively new phenomena and trying to shed light on fundamental outstanding problems. However, there is a price to pay. String theory requires extra dimensions to keep its consistency. Spacetime with dimension higher than four seems to be an essential property of quantum gravity. This is one of fundamental reasons why people began to study gravity in higher dimensions and surprisingly many new interesting features came out that are absent in their four dimensional counterparts.

The dimensionality of the spacetime can be therefore seen as a parameter of the theory. Beyond doubt, four dimensional spacetime is extremely unique. For black holes this is particularly evident. Indeed, special characteristics that black holes possess in four dimensions, such as uniqueness, spherical topology, dynamical stability, do not hold more generally [14–16]. All these properties change drastically in more than four dimensions. Black holes can have non-spherical horizon topology [17], e.g. black rings [18], black branes [19], and their phase structure is incredibly richer [20]. Moreover dynamical instabilities may appear since these new black holes are not necessarily stable any more [21–23].

Among these new solutions, of particular interest in string theory are charged gravitational string and brane solutions [24]. These spatially extended geometries source a set of gauge potentials and are solutions of an appropriate supergravity (the extension of GR to include supersymmetry) that are exactly interpreted as the classical coherent state of a (large) stack of fundamental strings/branes each charged under the corresponding potentials. This simple, yet profoundly deep, observation lies at the very heart of the AdS/CFT correspondence [25–27]. Conjectured in 1997 by Juan Maldacena, this correspondence relates strongly coupled quantum field theories to gravity theories in higher dimensions (as classical theories). In its original form, it states that maximally supersymmetric $\mathcal{N} = 4$ Super Yang-Mills (SYM) theory, a conformal field theory (CFT), is dual to Type IIB string theory on $\text{AdS}_5 \times S^5$. Gravity solutions in AdS spacetime can be mapped to conformal field theories located at the asymptotic

timelike boundary giving an explicit realization of the “holographic principle” [28]. The two theories, indeed, live in a different number of dimensions. In this context, black objects correspond to finite temperature states on the gauge theory side. The AdS/CFT correspondence provides a practical way to answer complicated questions about strongly-coupled gauge theories translating these in terms of classical gravity problems. The same is true in the other way around as well, CFTs can help to a better understanding of higher dimensional gravity.

The powerful potentialities of this correspondence are the reasons for its huge success. Indeed, this duality has revealed surprising connections between unrelated phenomena and equations of physics. Notable are its applications to problems in a strongly coupled regimes as in certain condensed matter systems [29] or in quantum chromodynamics (QCD) [30]. For the latter, the most celebrated prediction concerns the calculation of the hydrodynamic properties of the quark-gluon plasma (produced in relativistic heavy ions collisions) [31] which is believed to be a locally thermalized phase of QCD and hence described by a relativistic fluid equation.

This result was obtained using the hydrodynamic limit of the AdS/CFT correspondence where the effective description of gravity as an hydrodynamic theory emerges naturally. Taking a certain limit, Einstein’s equations in a spacetime with negative cosmological constant are equivalent to relativistic Navier-Stokes equations as demonstrated in [32]. This is known as the “fluid/gravity correspondence”. The long-wavelength effective description of some conformal theory can be identified with a relativistic hydrodynamic theory and the dynamics of bulk spacetime is encoded in a fluid living on its boundary. Here the transport coefficients (for a review on relativistic fluid mechanics, see [33]) are directly computed from gravity using linear response theory in [34] and from a direct perturbative gravitational computation in [32]. Moreover, various generalizations including charged cases, have been carried out in these schemes, see e.g. [35–39].

Inspired in part by the fluid/gravity correspondence, the “blackfold approach” developed by [40, 41] is a long-wavelength effective theory that captures black holes dynamics. When the system exhibits two widely separated scales, as for instance rotating black holes in the ultra-spinning regime, the long-distance physics can be simplified integrating out the short-distance degrees of freedom. In other words, we are replacing the black hole with an effective source that, to leading order, takes the form of a fluid living on a membrane. Using the blackfold approach, the long-wavelength perturbations of black branes are hence described by an effective theory of viscous fluid flows. The effective dynamics of the fluid is expressed in terms of an effective

stress tensor computed in a derivative expansion. The dissipative transport coefficients are associated to fluctuations along the world-volume directions of the brane. This approach has previously been applied to the Schwarzschild black p -brane in [42], for the Reissner-Nordström black brane in [43] and for black $D3$ -branes in [44] where a hydrodynamical analysis was carried out. Another interesting application worth to mention is the study of fluctuations in the directions transverse to the brane. When the thickness of a black brane is much smaller than the characteristic length scale of the system the blackfold approach can be applied and one discovers that branes behave like elastic materials. The effect of bending a brane is encoded into new response coefficients which take into account its elastic deformation. Black branes are hydrodynamical objects but can also exhibit the properties of a solid as shown in [45–47]. Remarkably, besides being useful for describing black hole dynamics, the blackfold approach is also an excellent method for the construction of new approximate black hole solutions as shown in [48–51].

The main purpose of this thesis is to gain a more advanced understanding of higher dimensional gravity with a special focus on the study of black holes and black branes. We developed two leading lines of investigation: one is devoted to the analysis of the relation between different types of spacetime through maps which connect them and the other concerns the study of effective theories which allow to describe higher dimensional black holes and capture their dynamics. We are particularly interested in understanding the connections between fluids and black holes from a broad perspective. Using the blackfold approach we have investigated the effective hydrodynamics for several classes of black branes, including charged black branes, and we were able to extract their transport properties. The relevance of this analysis resides in the fact that on one hand one can approximately study the very complicated dynamics of black holes in terms of dissipative fluid flows and, conversely, by perturbation analysis of black holes one can probe the correct theory of hydrodynamics.

Outline:

The structure of this thesis is the following:

- In Chapter 2, we review some of the effective theories we used to study higher dimensional black holes. We will present the details of two of them: the fluid/gravity correspondence and the blackfold approach. We focus on how these effective descriptions capture the hydrodynamical behavior of the fluid dual to a certain gravity solution. Indeed, there exists an equivalence between the dynamics of

Einstein's equations and the dynamics of relativistic Navier-Stokes equations in a long-wavelength regime.

- In Chapter 3, we introduce the AdS/Ricci flat correspondence as developed in [52, 53], which is a map between asymptotically AdS spaces and Ricci-flat ones. We extend this work deriving a map between Einstein spaces of positive and negative curvature, including scalar matter. Starting from a space of positive curvature with some dimensions compactified on a sphere and analytically continuing the number of compact dimensions, we obtain a space of negative curvature with a compact hyperbolic subspace, and vice versa. Prime examples of such spaces are de Sitter (dS) and anti-de Sitter (AdS) space, as well as black hole spacetimes with (A)dS asymptotics and perturbed versions thereof, which play an important role in holography. Such a map can also be used as a solution generator, and we obtain a Kerr/AdS solution with hyperbolic horizon from a known Kerr/dS one. The results are based on [2].
- In Chapter 4, we study the hydrodynamics of relativistic fluids with several conserved global charges (i.e., several species of particles) by performing a Kaluza-Klein dimensional reduction of a neutral fluid on a N -torus. Via fluid/gravity correspondence, this allows us to describe the long-wavelength dynamics of black branes with several Kaluza-Klein charges. We obtain the equation of state and transport coefficients of the charged fluid directly from those of the higher-dimensional neutral fluid. We specialize these results for the fluids dual to Kaluza-Klein black branes. The analysis is based on [1].
- In Chapter 5, we study the long-wavelength effective description of two general classes of charged dilatonic (asymptotically flat) black p -branes including D/NS/M-branes in ten and eleven dimensional supergravity. In particular, we consider gravitational brane solutions in a hydrodynamic derivative expansion (to first order) for arbitrary dilaton coupling and for general brane and co-dimension

and determine their effective electro-fluid-dynamic descriptions by exacting the characterizing transport coefficients. The results are based on [3].

- In Chapter 6, we conclude with an overview of the work elaborated in the thesis and show the main results.
- In Chapter 7, a summary of the thesis in Spanish is provided.

Notation: The notation we have used in this thesis will be explicitly specified for each chapter. It is important to stress that the conventions and the terminology we have adopted can be different in the Chapters 3, 4 and 5, and for this reason we will make it clear as necessary to avoid possible confusion.

Chapter 2

Effective theories of gravity

2.1 The fluid/gravity correspondence

Understanding the early evolution of our universe is one of the main reasons to study the state of matter known as quark-gluon plasma (QGP). This state, produced from the collision of heavy-ions (e.g. at RHIC) at extremely high temperature and density, consists of asymptotically free quarks and gluons. QGP is the deconfined phase obtained when QCD is at strongly coupling. For this reason perturbation theory is not appropriated to study such a system and it is necessary a new method to achieve that.

Holography provides a possible way out mapping strongly coupled systems to some classical theory of gravity as mentioned in the introduction. Even though the AdS/CFT correspondence is shown to work only for some special class of gauge theories quite different from QCD, one can at least get qualitative features about the QGP. The most successful prediction of holography for strongly coupled systems is the value for the shear viscosity η which is probably the most relevance transport coefficient characterizing these. Indeed, in [34] they were able to compute the entropy density to shear viscosity ratio of strongly coupled $N = 4$ supersymmetric Yang-Mills plasma. Comparing their result with numerical fits to RHIC data one finds a remarkable agreement. Superconformal field theories can therefore be treated as toy models providing new insights into QGP. In [34] it was also conjectured that for any CFT with a gravity dual there exists a universal lower bound for the entropy density to shear viscosity ratio, that is

$$\frac{\eta}{s} \geq \frac{1}{4\pi} . \tag{2.1.1}$$

Interestingly, the QGP is characterized by a very small ratio near the saturation value of the bound.

If quantum field theory is in a local thermal equilibrium hydrodynamics is the appropriated effective theory to describe it. Holography then translates the dynamics of the effective fluid into classical gravitational dynamics. The long-wavelength limit of the AdS/CFT correspondence can be therefore seen as the duality between an AdS gravity solution in the bulk and a conformal fluid at thermal equilibrium living at the boundary of AdS. This equivalence, known as *the fluid/gravity correspondence*, was originally introduced by [32]. Later an extension to classes of non-conformal fluids was presented in [54]. A review of the fluid/gravity correspondence and its extensions can be found in [55].

Even if fluids and black holes seem to be completely unrelated, in a certain regime, there exists a strong and extremely useful relation between them. Long wavelength dynamics of black holes governed by Einstein's equations with a negative cosmological constant is equivalent to fluid dynamics described by Navier-Stokes equations in one dimension less as demonstrated in [56]. In other words, the long wavelength limit of D dimensional Einstein's equations in an asymptotically AdS space reduces to $(D - 1)$ -dimensional relativistic fluid dynamics. Hence, remarkably, hydrodynamics enables us to understand various aspects of the dynamics and the phase structure of black holes.

Before entering into the details of the fluid/gravity correspondence we will give a brief review of fluid dynamics since we will widely use these in the following chapters.

2.1.1 Elements of fluid dynamics

Hydrodynamics is the effective description of interacting systems nearly thermal equilibrium at long enough distance. To be more precise, consider a quantum system in a global thermal equilibrium characterized by a temperature field \mathcal{T} and a fluid velocity field u_A . We now allow these fluid parameters to vary slowly, perturbing the system with fluctuations whose wavelengths are large compared to the scale set by the thermodynamic variables. Under this condition the system is well described by fluid dynamics. In some sense one is examining it at a length scale where is not important the movement of single elements. Therefore, the dynamics simplifies substantially and the effective description of its variables is completely captured by fluid dynamics. The long-wavelength physics of any interacting quantum field theory in a local thermal equilibrium can be described in terms of a relativistic fluid flow.

Hydrodynamics is governed by conservation laws of the stress-energy tensor T^{AB} and the charge currents J_I^A with index $I = \{1, 2, \dots\}$ corresponding to the number of

conserved charges characterizing the system. These are

$$\nabla_A T^{AB} = 0, \quad \nabla_A J_I^A = 0, \quad (2.1.2)$$

where ∇_A is the covariant derivative corresponding to the background metric g_{AB} on which this fluid lives. From now on, for simplicity, we consider only one conserved current ($I = 1$ and $J_1^A \equiv J^A$) since the extension is trivial. It is also necessary to define the equation of state which allow to express the stress-energy tensor and the charge current as functions of the fluid variables. In general, one constructs these in a derivative expansion of the fluid dynamical fields. Order by order, it is possible to determine their form using thermodynamics and symmetry arguments. At zeroth order in the derivative expansion, the stress tensor is simply that of a perfect fluid given by

$$T_{AB} = (\varrho + P)u_A u_B + P g_{AB}, \quad (2.1.3)$$

in terms of the energy density ϱ , the pressure P and the normalized velocity field u^A ($g_{AB}u^A u^B = -1$). The velocity field is chosen to be aligned to the direction of energy flow. The charge current takes the form

$$J_A = \mathcal{Q}u_A, \quad (2.1.4)$$

where \mathcal{Q} is the charge density. Since for a perfect fluid there is not production of entropy another current conserved exists, the entropy current. This is expressed as

$$J_s^A = s u^A, \quad (2.1.5)$$

with entropy density s .

When one allows the fluid variables to fluctuate as result entropy is produced and dissipative corrections must be added. So, the stress tensor and the charge current are corrected by extra contributions as

$$T_{AB} = (\epsilon + P)u_A u_B + P g_{AB} + T_{AB}^{diss}, \quad J_A = \mathcal{Q}u_A + J_A^{diss}. \quad (2.1.6)$$

Dissipation is the effect of the equilibration of the fluid trying to recover an equilibrium configuration. This is reflected on T_{AB} and J_A where the extra terms added, T_{AB}^{diss} and J_A^{diss} account for the viscous corrections.

Before giving the explicit form of the dissipative corrections it is required to choose a frame. We consider the one in which the velocity field is orthogonal to the dissipative

contributions, called the Landau frame, satisfying the conditions

$$T_{AB}^{diss} u^A = 0, \quad J_A^{diss} u^A = 0. \quad (2.1.7)$$

We are now able to express the dissipative part of the stress tensor that, to first order, takes the form

$$T_{AB}^{diss} = -2\eta\sigma_{AB} - \zeta P_{AB}\theta, \quad (2.1.8)$$

where η and ζ are the *shear* and *bulk viscosities*. The determination of these coefficients for certain systems will be part of the main results shown in the following chapters. In D dimensions, the expansion θ , the projector P_{AB} and the shear viscosity tensor σ_{AB} are defined as

$$\theta = \partial_A u^A, \quad P_{AB} = g_{AB} + u_A u_B, \quad \sigma_{AB} = P_A^C P_B^D \partial_{(C} u_{D)} - \frac{1}{D-1} \theta P_{AB}. \quad (2.1.9)$$

For a conformal fluid the bulk viscosity is null.

The charge current at leading order in gradient expansion it is written in terms of the temperature \mathcal{T} and chemical potential μ as

$$J_A^{diss} = -\kappa P_A^B \partial_B \left(\frac{\mu}{\mathcal{T}} \right), \quad (2.1.10)$$

where κ is the charge diffusion coefficient.

The first order contribution to the entropy current is given by

$$J_s^{A,diss} = -\frac{1}{\mathcal{T}} u_B T_{diss}^{AB}. \quad (2.1.11)$$

From the positivity of the entropy current one can demonstrate that the shear and the bulk viscosities must satisfy $\eta \geq 0$ and $\zeta \geq 0$.

After this brief overview on relativistic hydrodynamics, we are now able to connect the effective fluid to the corresponding black hole using the fluid/gravity correspondence as follows.

2.1.2 Fluid dynamics from gravity

As presented at the beginning of this section, the fluid/gravity duality describes the relation between gravity solutions of a certain AdS spacetime and a fluid living on its time-like boundary. At any order in a derivative expansion, a solution of Einstein's equations with a negative cosmological constant can be mapped to some

effective fluid configuration and vice versa. A perturbed fluid flow corresponds to an inhomogeneous, time-dependent black hole with a slowly varying horizon. This black hole approximates a black brane in AdS in a long-wavelength limit. Thanks to the fluid/gravity correspondence we have a practical way to compute the transport coefficients of the fluid associated to some class of strongly coupled field theories from the analysis of classical perturbation equations of black holes.

At zeroth order or equivalently in a global thermal equilibrium a static solution of AdS-Einstein equations with regular horizon is described by the stress-energy tensor of a perfect fluid of the form in Eq. (2.1.3). The temperature associated to the fluid is the Hawking temperature of the black hole, while its horizon boost velocity corresponds to the fluid velocity.

To study the dynamics of this black brane we promote the temperature \mathcal{T} (or equivalently the radius of the horizon) and the boost velocity u_A to functions of the x^A coordinates on the boundary spacetime on which the fluid lives. These parameters $\mathcal{T}(x^A), u_A(x^A)$ are required to vary sufficiently slowly. The perturbed black brane is not a solution of the Einstein's equations any more. For this reason we have to correct it order by order in a derivatives expansion. Once we determine the complete bulk metric at a give order we are then able to compute the corresponding effective T_{AB} at the boundary which will be of the form expressed in (2.1.6). In order to do this we use the prescription presented by Brown-York in [57]. In Chapt. 3 we will give more details about the construction of this effective stress tensor. To summarize, from black brane's deformations we can compute the corresponding effective stress energy tensor and extract the transport coefficients characterizing the viscous fluid flow at the boundary which in turn, in a long wavelength regime, encodes the behaviour of some strongly coupled field theory.

The mathematical details used to obtained the corrected metric and the stress energy tensor from a perturbed black hole solution will be outlined in Sec. 5.2.1 and more specifically in App. C. Even if there we have considered a charged black brane in an asymptotically flat space the procedure is substantially equivalent to the one valid in solutions AdS.

In the next section, we will introduce another long-wavelength effective theory used to study black holes dynamics but in a generic spacetime.

2.2 The Blackfold Approach

In four dimensions, asymptotically flat black holes possess necessarily a spherical S^2 event horizon [58]. In contrary, for higher dimensional gravity the topology of the event horizon can differ from the spherical one. The presence of black holes with a non-trivial horizon topology is probably one of the most surprising peculiarity of gravity in $D \geq 5$. Higher is the dimension of the spacetime richer is the phase structure of the possible black holes but unfortunately, as one can imagine, the difficulty of finding such solutions increases as well.

In five dimensions an extension of the Kerr black hole, a Myers-Perry (MP) black hole, was presented in [59] maintaining the spherical horizon topology (that is S^3). Lately, Emparan and Reall in [60] succeeded in finding a five dimensional regular rotating asymptotically flat black ring. A generalization to a charged black ring, solution of $D = 5$ Einstein-Maxwell theory, was presented in [61]. The topology of the black ring horizon is $S^1 \times S^2$ where the rotation is along S^1 identified by a radius R and the horizon radius is r_0 . An interesting feature of this solution is that its angular momentum, for a given mass, is unbounded from above. In four dimensions this is forbidden. There exists a regime in which the ring can rotate so fast that it can reach the condition $R \gg r_0$.

The presence of horizons with characteristic lengths of very different size is a novel property exclusive of higher dimensional gravity. Generally, in D dimensions a black hole is characterized by two length scales ℓ_M and ℓ_J as

$$\ell_M \sim (GM)^{\frac{1}{D-3}}, \quad \ell_J \sim \frac{J}{M}, \quad (2.2.1)$$

delineated by its mass M and angular momentum J . These scales can differ arbitrarily. Consequently, we identify three possible regimes for the phase structure of stationary black holes. Nothing new is believed to happen when $\ell_M \gg \ell_J$, the only stable phase is the Myers-Perry solution. Black holes qualitatively behave similarly to the four dimensional spherical black hole. Things get more interesting when $\ell_M \approx \ell_J$. A variety of new solutions is expected together with the manifestation of possible instabilities (in four dimensions black holes are stable).

The last condition refers to the *ultra-spinning regime* obtained when $\ell_J \gg \ell_M$. As evident, for this limit a clear hierarchy of scales is present and one can treat the system in terms of an effective theory. In order to understand what we mean by this, let us analyse the behaviour of black hole solutions when the ultra-spinning limit is reached.

Consider for instance a black ring and, as before, spin it very fast. Due to the centrifugal force the radius R begins to increase, the black ring becomes very thin and eventually we reach the regime $R \gg r_0$. Here a peculiar characteristic appears: in a region very near to the horizon the ultra-spinning black ring looks locally like a boosted black string. The same argument can be applied to MP black holes as shown in [23]. When the angular momentum is very large, the MP black hole “pancakes” along the direction of the rotation and looks locally as a flat boosted black brane.

So, the main lesson from these examples is that when a generic black hole presents a wide separation of scales we can describe it in terms of black string or brane. Integrating out the short-distance physics of the system and replace it with a long-distance effective theory. Essentially, it is the same principle behind hydrodynamics as explained for the fluid/gravity correspondence. Finding solutions of higher dimensional gravity or analysing their dynamics can be a very difficult task but when the length scales characterizing the system differ substantially the model simplifies and we can use approximate methods for studying these.

Assuming that black holes in a certain limit become locally black branes we can instead change the perspective and consider black branes as the starting point to construct new black hole solutions. One can indeed solve perturbatively Einstein equations order by order from a wrapped or bent black branes. This is conceptually the basis of the blackfold approach developed in [40, 41, 62] (a review can be found in [63]). Indeed, a *blackfold* is defined as a *black* brane (possibly locally boosted) whose worldvolume is bent into the shape of a submanifold of a background spacetime. The blackfold approach describes the way in which a black brane can be bent into a given background spacetime.

We can therefore use it to study the space of solutions and possibly construct new ones. Applications of this method to black ring in different backgrounds are given in [48] for flat space, in [49] for (A)dS, and in [64] for Taub-Nut asymptotics. Note that the blackfold approach is not a peculiarity of flat space. Blackfolds embedded in (A)dS background were studied by [49, 50].

Since the blackfold method captures the long-wavelength effective physics of black holes it is also very useful for probing their dynamics and analysing their stability properties. When the system presents a separation of scales one can integrate out the short-distance degrees and the physics is then captured by an effective stress tensor. A possible way to compute this tensor is using the Brown-York procedure as mentioned previously for the fluid/gravity correspondence. Once again hydrodynamics is the appropriate theory capturing the effective description of worldvolume theory. So, in

a long wavelength regime, the black brane behaves like an effective fluid. At leading order, a stationary solution will correspond to a perfect fluid with stress energy tensor (2.1.3).

This blackfold approximation to study black brane dynamics is based on the assumption that fluctuations considered along the worldvolume of the brane possess a wavelength λ much larger than r_0 . In other words, we want that the perturbation scale is large enough compared to the microscopic scale of the brane geometry that, in our case, is set by the horizon radius. Blackfolds capture the long-distance dynamics of higher-dimensional horizons that in turn is captured by viscous fluid dynamics and elasticity of a brane. A black p -brane, hence, take the form of a fluid flow living on a dynamical worldvolume. The main difference with the fluid/gravity correspondence is that the fluid is not located at boundary of AdS space time but lives on a dynamical worldvolume of arbitrary co-dimension.

From a given gravitational solution, order by order in a derivative expansion, we are able to construct the effective stress energy tensor (and vice versa) which encodes the effect of the perturbations at long-distances $r \gg r_0$. Once we have computed the stress tensor we are then able to extract the transport coefficients that characterize the effective theory of the black brane under analysis. We are basically replacing the problem of investigating complicated gravitational physics by an achievable computation of response coefficients.

The method was developed in [42] to study the hydrodynamical properties of a neutral black brane and later extended to the charged case by [43] for a Reissner-Nordström black brane and in [44] for the Black D3-brane solution. In Chapt.5 the blackfold approach will be used for the analysis of the fluid dual to charged dilatonic black branes. In App.C we give the details of the computation.

An interesting outcome of having the dissipative corrections of the system is that one can therefore analyse the response to small long-wavelength perturbations and deduce the stability of the brane. This is a very straightforward method to examine the phase structure of possible solutions. In Sec.5.2.3 and 5.3.2 we will perform the stability analysis for the Maxwell and fundamentally charged branes.

In the following section we will give an example of how the blackfold approach works illustrating the procedure for a perturbed neutral black brane.

2.2.1 Applying the blackfold approach

As outlined very much repeatedly, the key ingredient to applied the blackfold approach is the existence of a wide separation of scale. Blackfolds, indeed, capture the long-

distance dynamics of higher-dimensional horizons which will be constructed from solving Einstein equations using a matched asymptotic expansion (MAE). MAE is a common approach to solve differential equations when the system exhibit two regions where the equations simplify. In these regions we are then able to solve the equations and each solution provides the appropriate boundary condition for the other in the intermediate region. This leads to a systematic approach for constructing an approximated solution correcting it order by order in a perturbative expansion.

To give an idea of the blackfold construction we analyse the long wavelength description of a flat, boosted black p -brane in $D = p + n + 3$ spacetime dimensions with metric

$$ds^2 = \left(\eta_{ab} + \frac{r_0^n}{r^n} u_a u_b \right) d\sigma^a d\sigma^b + \frac{dr^2}{1 - r_0^n/r^n} + r^2 d\Omega_{n+1}, \quad (2.2.2)$$

where η_{ab} is the Minkowski metric and the coordinates $\sigma^a = (t, z^i)$, $i = 1, \dots, p$, span the brane worldvolume where z^i are flat spacial directions of the brane. The volume of the transverse unit sphere is labeled with Ω_{n+1} . This solution is parametrized by the horizon radius r_0 , the normalized boost velocity u^a and the $D - p - 1$ transverse coordinates X^\perp to the worldvolume of the brane which we identify as collective coordinates $\phi = \{X^\perp, r_0, u^i\}$.

We now perturb this metric with a long-wavelength perturbation and examine two possible regions of the system:

- **the near horizon region:** $R \gg r$, where R delineates a characteristic scale length of the system, typically given by the smallest intrinsic or extrinsic curvature radius of the worldvolume. This region is well described by (2.2.2) when $R \rightarrow \infty$ (at zeroth order) but when R is finite the collective coordinates become functions of the worldvolume coordinates, that is $\phi(\sigma^a)$. Near the horizon this metric captures the distortion caused by the background curvature on the black brane. The appropriate metric describing the near region then takes the form

$$ds^2 = \left(\eta_{ab}(\sigma) + \frac{r_0(\sigma)^n}{r^n} u_a(\sigma) u_b(\sigma) \right) d\sigma^a d\sigma^b + \frac{dr^2}{1 - r_0(\sigma)^n/r^n} + r^2 d\Omega_{n+1} + \dots \quad (2.2.3)$$

where the dots indicate we have to correct it since it is not a solution of the Einstein's equations any more. For this reason we perform a derivative expansion of the equations and correct the solution order by order. It is important to remark that we need to preserve the regularity of the horizon after the perturbations.

- **the far region:** $r \gg r_0$. To zeroth order in r_0/R , the far region geometry is determined by the background metric. We then need to consider backreaction for the next order. The metric deviates from its form and the variation is sourced by the appropriate blackfold effective stress energy tensor. This effective stress tensor solves the conservation equations

$$\nabla^a T_{ab} = 0 . \quad (2.2.4)$$

which will give the blackfold effective equations of motion.

So, once we obtain the corrected metric (2.2.3) to a given order using the Brown-York prescription we are able to compute T_{ab} in the overlap region $R \gg r \gg r_0$ where the gravitational field is weak.

At leading order, for the boosted black p -brane this tensor is given by

$$T^{ab} = \frac{\Omega_{n+1}}{16\pi G} r_0^n (n u^a u^b - \eta^{ab}) . \quad (2.2.5)$$

Comparing it with the stress tensor of an isotropic fluid in (2.1.3) we obtain the values of the pressure and the energy density of the effective fluid. These are

$$\varrho = \frac{\Omega_{n+1}}{16\pi G} r_0^n , \quad P = -\frac{1}{n+1} \varrho . \quad (2.2.6)$$

The first order corrections can be found in [42].

Computing the horizon area and the surface gravity one can determine the entropy density and the local temperature, respectively, associated to the fluid in its rest frame that are

$$s = \frac{\Omega_{n+1}}{4G} r_0^{n+1} , \quad \mathcal{T} = \frac{n}{4\pi r_0} \quad (2.2.7)$$

using the Bekenstein-Hawking identifications. It is easy to verify that the Euler-Duhem relation

$$\varrho + P = \mathcal{T} s \quad (2.2.8)$$

is satisfied.

So, in this section we have shown how to apply the blackfold method to construct the effective theory that capturing the brane dynamics. This effective long-wavelength theory is expressed in term of a fluid living on a dynamical worldvolume which satisfies the conservation equations in (2.2.4). This method is an efficient way to investigate new solutions of higher dimensional gravity and to determine the properties of black branes in a certain limit.

In the next section we turn our attention to another kind of correspondence. We discuss how to connect different spacetimes with very few ingredients: a dimensional reduction and an analytic continuation. This can help in the perspective of obtaining a holographic description for a spacetime different from AdS.

Chapter 3

Map for different spacetimes

3.1 AdS/Ricci flat correspondence

Holography works extremely well in AdS and it seems that the structure of such spacetime is a key ingredient for the correspondence to work. During the last fifteen years people have been trying to develop an holographic dictionary that applies to spacetimes other than AdS. Unfortunately we are still quite far from a clear understanding of holographic duality for these cases. Recent progress towards holography for asymptotically flat spacetimes has been achieved in [52, 53]. They derived a map, called “AdS/Ricci flat correspondence”, between solutions of the Einstein equations with negative cosmological constant and Ricci-flat solutions using generalized dimensional reduction, a diagonal Kaluza-Klein (KK) dimensional reduction [65, 66] followed by an analytic continuation in the number of dimensions [52, 53, 67, 68], which in particular includes a map between asymptotically AdS and asymptotically flat spacetimes. This map does not involve an analytic continuation in the complex plane, but instead rests on a suitable compactification of some coordinates in each space. It is important to stress that the correspondence works not only for the equations of motion, but also at the level of the action. The basic procedure of the AdS/Ricci flat correspondence is the same as the one used for developing the map between de Sitter (dS) spaces and AdS shown in Sec.3.2. For this reason we omit the explication of the derivation of the map and its applications.

We want to stress the importance of this correspondence for holography. In [52, 53] a relevant result was found: the holographic stress tensor in AdS is mapped to a brane situated at $r = 0$ in Minkowski spacetime, which serves as the source for the metric perturbations. This is in contrast to previous works that, in analogy with the AdS

case, studied holography at various boundaries of flat space [69–71]. Such result can therefore possibly give hints for understanding how to set up holography in flat space.

In the next section, we present the generalization of the AdS/Ricci flat map for dS including moreover matter fields.

3.2 Mapping AdS to dS spaces and back

3.2.1 Introduction

Since the discovery of the AdS/CFT correspondence, a concrete realization of the holographic idea that theories with gravity can be described by theories without gravity in one dimension less, a lot of effort has been invested in the study of this and other holographic dualities. An area in which a holographic duality would be very useful is for the description of the early Universe, especially for inflation. However, the geometry of the Universe at that time is close to dS space [72], and also today the measured cosmological constant is positive [73], so that the AdS/CFT correspondence is not directly applicable. A dS/CFT correspondence has been proposed by Strominger [74, 75] (see also Refs. [76–81]), but the boundary CFT can be nonunitary and contain complex conformal weights (e. g., for sufficiently massive scalars in dS). Another approach to use holography in inflation has been put forward by McFadden and Skenderis [82–85], where correlators are calculated using the standard AdS/CFT correspondence and then analytically continued to complex momenta to obtain results for de Sitter spacetime. This construction has been tested to give the right predictions for correlators of gravitons and inflaton perturbations, which are both massless fields, but it is not assured that it works for massive fields as well.

Recently, as presented in Sec.3.1 a map between solutions of the Einstein equations with negative cosmological constant and Ricci-flat solutions was derived [52, 53]. In this section, we generalize such construction to solutions of the Einstein equations with positive and negative cosmological constants, including matter in the form of a scalar field — a map that can bring AdS to dS and vice versa. The possibility of such a map had already been mentioned in [53], but only the matter-free reduced action in the Jordan frame was calculated there. We organized this section as follows: First, we derive the map using a diagonal KK dimensional reduction of the action. Reducing also the higher-dimensional Einstein equations (which leads to the same result), we then show that the reduction ansatz is consistent. Afterwards, we give some examples: the maps between empty AdS and dS spaces, between black holes with AdS/dS asymptotics and

for perturbations near the boundary of AdS, which are relevant for holography. For this last case, we calculate the Brown-York stress tensor and compare with holographic expectations. By mapping a known Kerr/dS black hole, we also find a (most probably new) solution for a rotating black hole in AdS with a hyperbolic horizon, showing the feasibility of using the map as a solution generator.

For the metric and curvature tensors, we use the “+++” convention of Ref. [4]. Capital latin indices denote coordinates in the higher-dimensional space before reduction, and lowercase latin (greek) indices denote coordinates in the reduced (compact) directions. Quantities which refer to (asymptotic) dS space are indicated by a prime, while quantities without a prime either are general or refer to (asymptotic) AdS space.

3.2.2 Deriving the map

In this section, we show how the map can be derived by a diagonal KK dimensional reduction of a higher-dimensional system, once directly at the level of the action and once by reducing the higher-dimensional Einstein equations. We start from a $(n + \nu)$ -dimensional spacetime that is a solution of the Einstein equations with a cosmological constant (which can be either positive or negative) and matter. Of these coordinates, ν will be compactified, with the size of the compactification determined by a scalar field ϕ (a dilaton) that only depends on the n reduced coordinates. That is, we start from a metric

$$d\bar{s}^2 = \bar{g}_{MN} dX^M dX^N, \quad M, N = 0, \dots, n + \nu - 1 \quad (3.2.1)$$

that solves the Einstein equations with matter

$$\bar{G}_{MN} + \Lambda \bar{g}_{MN} = 8\pi G_N^{n+\nu} \bar{T}_{MN} \quad (3.2.2)$$

in $n + \nu$ dimensions. We perform dimensional reduction by taking the ansatz

$$d\bar{s}^2 = e^{2\alpha\phi(x)} ds^2 + e^{2\beta\phi(x)} d\sigma^2 \quad (3.2.3)$$

with the n -dimensional reduced metric

$$ds^2 = g_{ab}(x) dx^a dx^b \quad (3.2.4)$$

and the ν -dimensional compact metric

$$d\sigma^2 = \gamma_{\alpha\beta}(y) dy^\alpha dy^\beta. \quad (3.2.5)$$

We take the metric of the compact space $\gamma_{\alpha\beta}$ to be fixed, while the reduced metric g_{ab} is dynamical and, like the scalar ϕ , only depends on the coordinates x^a . The parameters α and β are constants and can be chosen at will; however, β cannot be zero for a consistent reduction, as can be seen later on from the reduced equations (3.2.15).

Generalized dimensional reduction of the action

The $(n+\nu)$ -dimensional action is the Einstein-Hilbert action with cosmological constant Λ and a free, canonically normalized scalar field χ

$$S = \int \left[\frac{\bar{R} - 2\Lambda}{16\pi G_N^{n+\nu}} - \frac{1}{2} \bar{g}^{AB} \partial_A \bar{\chi} \partial_B \bar{\chi} \right] \sqrt{-\bar{g}} d^{n+\nu} X, \quad (3.2.6)$$

where $G_N^{n+\nu}$ is Newton's constant in $n + \nu$ dimensions. For the dimensional reduction, the scalar $\bar{\chi}$ is taken to only depend on the reduced coordinates, and to simplify the formulas we rescale it

$$\chi = \sqrt{16\pi G_N^{n+\nu}} \bar{\chi}. \quad (3.2.7)$$

Calculating the curvature tensors for the ansatz (3.2.3), which is done in App. A.1, and substituting them into the action (3.2.6), we obtain (after integration by parts and ignoring surface terms)

$$\begin{aligned} S = & \frac{1}{16\pi G_N^{n+\nu}} \int e^{[(n-2)\alpha + \nu\beta]\phi} \left[R - 2e^{2\alpha\phi} \Lambda \right. \\ & + e^{2(\alpha-\beta)\phi} R[\gamma] - \frac{1}{2} \nabla^a \chi \nabla_a \chi \\ & + \left((n-1)(n-2)\alpha^2 + 2(n-1)\nu\alpha\beta \right. \\ & \left. \left. + \nu(\nu-1)\beta^2 \right) \nabla^a \phi \nabla_a \phi \right] \sqrt{-g} \sqrt{\gamma} d^n x d^\nu y. \end{aligned} \quad (3.2.8)$$

In this expression, $R[\gamma]$ is the Ricci scalar of the compact metric $\gamma_{\alpha\beta}$, and ∇ is the covariant derivative with respect to the reduced metric g_{ab} . Setting $\alpha = 0$, $\beta = 1/\nu$ and $\chi = 0$, we recover the matter-free reduced action in the Jordan frame derived in Ref. [53].

Now take the compact space to be an Einstein space which has $R_{\mu\nu}[\gamma] = k(\nu - 1)H^2\gamma_{\mu\nu}$, where H is a constant with dimensions of inverse length related to the radius of the compact space (e. g., for a sphere, the radius would be H^{-1}). The constant k takes the values ± 1 , and the compact space has volume $V_\nu^k \propto H^{-\nu}$. We express the cosmological constant as $\Lambda = \lambda(n + \nu - 1)(n + \nu - 2)/(2\ell^2)$ with $\lambda = \pm 1$, and a constant ℓ with dimensions of length (e. g., in pure AdS, ℓ is the AdS radius). Integrating out the compact coordinates, we get

$$\begin{aligned}
S = & \frac{V_\nu^k}{16\pi G_N^{n+\nu}} \int \left[R - \lambda \frac{(n + \nu - 1)(n + \nu - 2)}{\ell^2} \right] e^{2\alpha\phi} \\
& + \nu(\nu - 1)kH^2 e^{2(\alpha-\beta)\phi} - \frac{1}{2} \nabla^a \chi \nabla_a \chi \\
& + \left((n - 1)(n - 2)\alpha^2 + 2(n - 1)\nu\alpha\beta \right. \\
& \left. + \nu(\nu - 1)\beta^2 \right) \nabla^a \phi \nabla_a \phi \Big] e^{[(n-2)\alpha + \nu\beta]\phi} \sqrt{-g} \, d^n x.
\end{aligned} \tag{3.2.9}$$

To construct a map between a space which is a solution for $\Lambda > 0$ and one for $\Lambda < 0$, we perform this reduction twice, with different internal spaces. On one hand, we consider the reduced action S with $\Lambda < 0$ (and thus $\lambda = -1$), and on the other hand a second reduced action S' (denoted by primes) with $\Lambda' > 0$ (and thus $\lambda' = +1$). The actions S and S' are proportional to each other,

$$S = \frac{G_N^{n'+\nu'}}{V_\nu^{k'}} \frac{V_\nu^k}{G_N^{n+\nu}} S', \tag{3.2.10}$$

if and only if $k = -1$, $k' = +1$ and

$$\ell = 1/H', \quad H = 1/\ell', \tag{3.2.11a}$$

$$\alpha = \alpha' - \beta', \quad \beta = -\beta', \tag{3.2.11b}$$

$$n = n', \quad \nu = 2 - n' - \nu'. \tag{3.2.11c}$$

This is consistent with the AdS/Ricci-flat correspondence [52, 53], where, however, the constants α and β were fixed (choosing a specific frame and a canonical normalization for the scalar field).

That is, given a solution of the Einstein equations with negative cosmological constant of the form

$$d\bar{s}^2 = e^{2\alpha\phi(x)} g_{ab}^{(n)} dx^a dx^b + e^{2\beta\phi(x)} \gamma_{\alpha\beta}^{(\nu)-} dy^\alpha dy^\beta, \tag{3.2.12}$$

where we have shown explicitly the dimensions of the metrics and denoted the negative curvature of the compact space by a minus sign, and a scalar field χ , the line element

$$\begin{aligned} d\tilde{s}^2 &= e^{2\alpha'\phi(x)} g_{ab}^{(n')} dx^a dx^b + e^{2\beta'\phi(x)} \gamma_{\alpha\beta}^{(\nu)'} dy^\alpha dy^\beta \\ &= e^{2(\alpha-\beta)\phi(x)} g_{ab}^{(n)} dx^a dx^b \\ &\quad + e^{-2\beta\phi(x)} \gamma_{\alpha\beta}^{(2-n-\nu)} dy^\alpha dy^\beta \end{aligned} \quad (3.2.13)$$

with the *same* metric $g_{ab}^{(n)}$ and scalar field ϕ as well as the *same* scalar χ gives a solution of the Einstein equations with positive cosmological constant. This map is valid in general dimensions, and while the dimensions of the reduced spaces are the same, the dimension of the compact space changes. For sufficiently large n and ν , ν' will be negative and must be analytically continued to a positive value. This poses no problem as long as no factors of $1/\nu'$ (or similar) appear.

It is important to note that any explicit factors of n , ν , ℓ or H appearing in the metric and the scalar fields (or α and β) must be identified as well using (3.2.11), so that one needs to know the solution for arbitrary ν (since $n' = n$, one may fix n). If one wants to work in a specific frame (Einstein or Jordan), one may fix α or β , but this is not necessary for the map. Furthermore, exchanging primed and unprimed quantities in (3.2.11), we see that the map works likewise both ways.

Since the actions are equal up to an overall constant (3.2.10), the equations of motion for the reduced space and the scalar field are the same. However, we need to check the consistency of the reduction, i. e., that the Einstein equations that follow from the reduced action (3.2.9) can be obtained by reducing the equations that follow from the starting action (3.2.6). This will be done in the next section.

Reduction of the Einstein equations

The Einstein equations that follow from the original $(n + \nu)$ -dimensional action (3.2.6) are

$$\begin{aligned} \bar{R}_{AB} - \frac{1}{2} \bar{R} \bar{g}_{AB} + \Lambda \bar{g}_{AB} \\ = \frac{1}{2} \left[\bar{\nabla}_A \chi \bar{\nabla}_B \chi - \frac{1}{2} \bar{g}_{AB} \bar{\nabla}^C \chi \bar{\nabla}_C \chi \right], \end{aligned} \quad (3.2.14)$$

and the scalar field equation reads $\bar{\nabla}^A \bar{\nabla}_A \chi = 0$. Using the product space metric ansatz (3.2.3), they can be decomposed using the formulas from App. A.1. Imposing (as in the last section) that the compact metric is Einstein with Ricci tensor $R_{\mu\nu}[\gamma] = k(\nu - 1)H^2 \gamma_{\mu\nu}$ and taking $\Lambda = \lambda(n + \nu - 1)(n + \nu - 2)/(2\ell^2)$, we obtain after some

algebraic manipulations

$$\begin{aligned}
R_{mn} - \lambda(n + \nu - 1)/\ell^2 e^{2\alpha\phi} g_{mn} - \alpha g_{mn} \nabla^a \nabla_a \phi \\
- [(n - 2)\alpha + \nu\beta] \nabla_m \nabla_n \phi \\
+ [(n - 2)\alpha^2 + 2\nu\alpha\beta - \nu\beta^2] \nabla_m \phi \nabla_n \phi
\end{aligned} \tag{3.2.15a}$$

$$\begin{aligned}
- \alpha [(n - 2)\alpha + \nu\beta] g_{mn} \nabla^a \phi \nabla_a \phi = \frac{1}{2} \nabla_m \chi \nabla_n \chi, \\
\beta \left[\nabla^a \nabla_a \phi + [(n - 2)\alpha + \nu\beta] \nabla^a \phi \nabla_a \phi \right]
\end{aligned} \tag{3.2.15b}$$

$$\begin{aligned}
+ \left[\lambda(n + \nu - 1)/\ell^2 - k(\nu - 1)H^2 e^{-2\beta\phi} \right] e^{2\alpha\phi} = 0, \\
\nabla^a \nabla_a \chi = [(n - 2)\alpha - \nu\beta] (\nabla^a \phi) \nabla_a \chi.
\end{aligned} \tag{3.2.15c}$$

These are exactly the equations that follow by varying the reduced action (3.2.9). We thus conclude that the reduction is consistent. Here we also see why the restriction $\beta \neq 0$ is important: for $\beta = 0$, the second equation does not give any restriction on the dilaton, but instead relates the sizes of the extended and the compact space.

In the Einstein frame, we have $(n - 2)\alpha + \nu\beta = 0$, and the equations reduce to the simpler ones

$$\begin{aligned}
R_{mn} - \lambda(n + \nu - 1)/\ell^2 e^{2\alpha\phi} g_{mn} - \alpha g_{mn} \nabla^a \nabla_a \phi \\
+ \nu\beta(\alpha - \beta) \nabla_m \phi \nabla_n \phi = \frac{1}{2} \nabla_m \chi \nabla_n \chi,
\end{aligned} \tag{3.2.16a}$$

$$\begin{aligned}
\beta \nabla^a \nabla_a \phi = \\
- \left[\lambda(n + \nu - 1)/\ell^2 - k(\nu - 1)H^2 e^{-2\beta\phi} \right] e^{2\alpha\phi},
\end{aligned} \tag{3.2.16b}$$

$$\nabla^a \nabla_a \chi = 0. \tag{3.2.16c}$$

Note that while α , β and ν individually change under the map (3.2.11), “being in the Einstein frame” is a condition that is preserved, as can be easily seen from the term-by-term comparison of the corresponding actions. However, it is almost always easier to work with $\alpha = 0$ or ± 1 and $\beta = \pm 1$, as we will do in the following.

3.2.3 Applications

In this section, we apply the map derived above to concrete examples. First, we give a short introduction to compact hyperbolic spaces, which are an example of Riemannian Einstein manifolds of constant negative curvature, and which are the simplest space of negative Ricci curvature to use in the map. Afterwards, we show that we can map

pure dS to pure AdS. The next subsection then treats small perturbations on top of AdS, which arise in holography in the AdS/CFT correspondence, in order to explore a possible dS/CFT correspondence via our map. Lastly, we show how to map the Schwarzschild-dS black hole to the Schwarzschild-AdS black hole, and map a rotating Kerr/dS black hole to AdS, obtaining a (probably new) Kerr/AdS black hole solution with hyperbolic horizon.

Compact hyperbolic spaces

Hyperbolic spaces are the analogue of AdS in Riemannian geometry, in the same way that the sphere is the Riemannian analogue of dS. It is well known that the ν -dimensional unit sphere can be defined by embedding it into a $(\nu + 1)$ -dimensional flat Euclidean space known as ambient space, where it arises as the submanifold

$$\delta_{AB}X^AX^B = 1, \quad A, B = 1, \dots, \nu + 1. \quad (3.2.17)$$

The metric of the sphere is then the induced metric obtained by restricting the flat ambient metric δ_{AB} to this submanifold. In the same way, hyperbolic spaces (of unit radius) are obtained from an ambient space with flat Lorentzian metric η_{AB} as the submanifold

$$\eta_{AB}X^AX^B = -1. \quad (3.2.18)$$

Choosing

$$X^1 = \frac{4\delta_{\alpha\beta}y^\alpha y^\beta - 1}{4y^1}, \quad X^A = \frac{y^\alpha}{y^1}, \quad A = \alpha = 2, \dots, \nu \quad (3.2.19)$$

and solving equation (3.2.18) for X^0 , one obtains the induced metric

$$\gamma_{\alpha\beta} = \eta_{AB} \frac{dX^A}{dy^\alpha} \frac{dX^B}{dy^\beta} = \frac{\delta_{\alpha\beta}}{(y^1)^2}. \quad (3.2.20)$$

In these coordinates, it is clear that hyperbolic space is the Riemannian analogue of AdS (identifying y^1 with r , where r is the radial coordinate). Another coordinate system which will be more suited for the purposes of the map later on is obtained by choosing

$$X^1 = \sinh y_1 \cos y_2 \quad (3.2.21)$$

and taking the coordinates X^A for $A = 2, \dots, \nu$ to be spherical coordinates with radius $\sinh y_1 \sin y_2$. This choice gives the induced metric

$$\gamma_{\alpha\beta} dy^\alpha dy^\beta = dy_1^2 + \sinh^2 y_1 d\Omega_{\nu-1}^2. \quad (3.2.22)$$

Spaces which do not have unit radius are then obtained by simply multiplying the metric by the (constant) radius.

One now has to compactify this space, which is done by taking the quotient by a discrete subgroup of isometries (which are the isometries of the ambient space that leave invariant the submanifold (3.2.18)). Of course, the local metric does not change under this compactification, and one easily calculates that

$$R_{abcd}[\gamma] = -H^2(\gamma_{ac}\gamma_{bd} - \gamma_{ad}\gamma_{bc}) \quad (3.2.23)$$

for all compact hyperbolic spaces (CHSs). An example of such a compactification can easily be given: take the two-dimensional hyperbolic space with metric

$$ds^2 = \frac{dx^2 + dy^2}{(Hy)^2}. \quad (3.2.24)$$

The isometry group of this metric is formed by the transformations

$$(x + iy) \rightarrow \frac{a(x + iy) + b}{c(x + iy) + d} \quad (3.2.25)$$

with $ad - bc = 1$ (the Möbius transformations), as one can easily check. A discrete subgroup of this group is the modular group, where the parameters a , b , c and d are restricted to be integers. One then identifies points which are mapped one into the other by the action of this subgroup, which e. g. includes $x \rightarrow x + k$, $k \in \mathbb{Z}$ (for $a = d = 1$, $b = k$ and $c = 0$). A fundamental domain for this group action is given by points which have $x^2 + y^2 \geq 1$ and $|x| \leq \frac{1}{2}$, and the CHS is obtained by identifying the borders, just like the torus can be obtained by identifying the sides of a rectangle. The volume of this space is given by

$$V_2^- = \int_{-\frac{1}{2}}^{\frac{1}{2}} \int_{\sqrt{1-x^2}}^{\infty} (Hy)^{-2} dy dx = \frac{\pi}{3H^2}, \quad (3.2.26)$$

which is finite, showing that this CHS really is compact. In higher dimensions, there are plenty of CHSs [86–88], and so there is no problem using them in our map.

AdS/dS spacetimes

Of course, the simplest examples for the map are empty dS/AdS spaces. Taking $\chi = 0$, it turns out to be easier to start from the dS side, where the $(n' + \nu')$ -dimensional

metric (in the Poincaré patch) takes the form

$$d\tilde{s}^2 = \frac{(\ell')^2}{\eta^2} \left(-d\eta^2 + d\vec{x}_{n'-2}^2 + dr^2 + r^2 d\Omega_{\nu'}^2 \right), \quad (3.2.27)$$

where we compactified ν' coordinates on a sphere, with metric $d\Omega_{\nu'}^2$. Comparing with the general formula (3.2.13), the most economic choice is to take $\alpha' = 0$ and $\beta' = -1$, which means $\alpha = \beta = 1$. The reduced metric then reads (using the identification (3.2.11) for the second equality)

$$\begin{aligned} g_{ab}^{(n)} dx^a dx^b &= \frac{(\ell')^2}{\eta^2} \left(-d\eta^2 + d\vec{x}_{n'-2}^2 + dr^2 \right) \\ &= \frac{1}{(H\eta)^2} \left(-d\eta^2 + d\vec{x}_{n-2}^2 + dr^2 \right), \end{aligned} \quad (3.2.28)$$

and the scalar field is given by

$$\phi = \ln \left(\frac{\eta}{H'\ell'r} \right) = \ln \left(\frac{H\ell\eta}{r} \right) \quad (3.2.29)$$

(recall that the compact space was taken to be of radius $1/H'$ in the map (3.2.11), which needs to be compensated by the scalar field since there is no H' in the metric (3.2.27)). The map tells us that the metric obtained from equation (3.2.12)

$$\begin{aligned} d\bar{s}^2 &= e^{2\phi} g_{ab}^{(n)} dx^a dx^b + e^{2\phi} d\sigma_\nu^2 \\ &= \frac{\ell^2}{r^2} \left(-d\eta^2 + d\vec{x}_{n-2}^2 + dr^2 + \eta^2 d\Upsilon_\nu^2 \right), \end{aligned} \quad (3.2.30)$$

with $d\Upsilon_\nu^2$ the ν -dimensional line element of a CHS of unit radius, is a solution of the Einstein equations with negative cosmological constant. To recover the metric of the Poincaré patch of AdS, we take the metric of the CHS in the form (3.2.22)

$$d\Upsilon_\nu^2 = dy_1^2 + \sinh^2 y_1 d\Omega_{\nu-1}^2 \quad (3.2.31)$$

and perform the coordinate transformation

$$\eta^2 = t^2 - \vec{z}_\nu^2, \quad \sinh^2 y_1 = \frac{\vec{z}_\nu^2}{t^2 - \vec{z}_\nu^2}. \quad (3.2.32)$$

Then we obtain (analogous to the Milne universe [72])

$$-d\eta^2 + \eta^2 d\Upsilon_\nu^2 = -dt^2 + d|\vec{z}_\nu|^2 + \vec{z}_\nu^2 d\Omega_{\nu-1}^2 = -dt^2 + d\vec{z}_\nu^2, \quad (3.2.33)$$

so that the metric (3.2.30) reduces to

$$d\tilde{s}^2 = \frac{\ell^2}{r^2} \left(-dt^2 + d\vec{x}_{n-2}^2 + dr^2 + d\vec{z}_\nu^2 \right) \quad (3.2.34)$$

which is AdS in $n + \nu$ dimensions, with r the radial/holographic coordinate. By compactifying ν' coordinates of de Sitter space on a sphere and applying the map, we thus find AdS space.

An interesting feature of the map concerns the position of the AdS boundary, which is located at $r = 0$. Since the extended metric does not change under the mapping, this surface is located in the bulk of dS, and has itself the geometry of a dS space: an $(n - 1)$ -dimensional dS brane. This happens in a similar manner in the AdS/Ricci-flat correspondence [52, 53], where the AdS boundary is mapped to a flat brane in the bulk of Minkowski spacetime, and we will discuss implications of this fact in Sec. 3.2.3, where we treat perturbations in AdS/dS.

Just like AdS, empty dS enjoys a conformal symmetry. Of special importance are dilatations and special conformal transformations. We undo the compactification in (3.2.27), writing

$$dr^2 + r^2 d\Omega_{\nu'}^2 = d\vec{r}_{\nu'+1}^2, \quad (3.2.35)$$

so that the metric takes the form

$$d\tilde{s}^2 = \frac{(\ell')^2}{\eta^2} \left(-d\eta^2 + d\vec{x}_{n'-2}^2 + d\vec{r}_{\nu'+1}^2 \right). \quad (3.2.36)$$

The dilatations are given by

$$\eta \rightarrow \lambda\eta, \quad \vec{x} \rightarrow \lambda\vec{x}, \quad \vec{r} \rightarrow \lambda\vec{r}. \quad (3.2.37)$$

The invariance of the metric under this transformation is clear. Defining $\vec{z} = \{\vec{x}, \vec{r}\}$, special conformal transformations read

$$\eta \rightarrow \eta - 2\eta(\vec{b}\vec{z}), \quad (3.2.38a)$$

$$\vec{z} \rightarrow \vec{z} + \vec{b}(\vec{z}^2) - 2\vec{z}(\vec{b}\vec{z}) - \eta^2\vec{b}, \quad (3.2.38b)$$

with \vec{b} an infinitesimal constant vector. One can easily verify that (3.2.36) is invariant. After the compactification, we are only interested in the transformation of the reduced part. We decompose therefore $\vec{b} = \{\vec{b}^x, \vec{b}^r\}$ and define $c \equiv (\vec{b}^r \vec{r})/r$. The transformation of the reduced coordinates then only depends on \vec{b}^x and c , and we calculate

$$\eta \rightarrow \eta - 2\eta(\vec{b}^x \vec{x} + cr), \quad (3.2.39a)$$

$$\vec{x} \rightarrow \vec{x} + \vec{b}^x(\vec{x}^2 + r^2 - \eta^2) - 2\vec{x}(\vec{b}^x \vec{x} + cr), \quad (3.2.39b)$$

$$r \rightarrow r + c(\vec{x}^2 + r^2 - \eta^2) - 2r(\vec{b}^x \vec{x} + cr). \quad (3.2.39c)$$

The reduced metric (3.2.28) is invariant under this transformation, but the dilaton (3.2.29) changes as

$$\phi \rightarrow \phi - \frac{c}{r}(\vec{x}^2 + r^2 - \eta^2). \quad (3.2.40)$$

We see that the compactification breaks the original conformal symmetry, but the resulting transformations can be seen as a generalized conformal structure — the reduced metric is conformally invariant, but the dilaton introduces a scale in the theory. These transformations are, however, solution generating transformations, as can be checked from the equations (3.2.15). Since the map brings solutions to solutions, the same transformations are valid in AdS space.

Asymptotic AdS with perturbations

In the AdS/CFT correspondence, the large N and large 't Hooft coupling limit of the conformal field theory corresponds to a weakly coupled gravity theory that can be described by supergravity in an asymptotically AdS space. The dictionary, the precise relation between these theories including renormalization, is known [89, 90], and in this section we calculate how perturbations near the AdS boundary, which are relevant in this holographic dictionary, are mapped to perturbations around dS. Again, we treat vacuum solutions and take $\chi = 0$.

We therefore approach the mapping from the other direction: take $\alpha = 0$ and $\beta = 1$, and a reduced metric and dilaton of the form

$$g_{ab}^{(n)} = \frac{\ell^2}{r^2} (\eta_{ab} + h_{ab}(\eta, \vec{x}, r)) \quad (3.2.41a)$$

$$\phi = \ln \left(\frac{H\ell\eta}{r} \right) + \psi(\eta, \vec{x}, r), \quad (3.2.41b)$$

where we take the Fefferman-Graham gauge [91]: h_{ab} does not have components in the radial direction, and both h_{ab} and ψ vanish as $r \rightarrow 0$. Both h_{ab} and ψ can be

considered as perturbations on top of the background AdS metric, and we retain the correct asymptotic behavior as $r \rightarrow 0$. The full metric then reads

$$d\bar{s}^2 = \frac{\ell^2}{r^2} \left[(\eta_{ab} + h_{ab}) dx^a dx^b + e^{2\psi} \eta^2 d\Upsilon_\nu^2 \right], \quad (3.2.42)$$

with $d\Upsilon_\nu^2$ the line element of a CHS of unit radius (3.2.31). We thus leave the compact space unperturbed, and only vary its radius. For $h_{ab} = \psi = 0$, the map gives the same de Sitter metric (3.2.27), showing that α and β can be chosen freely and in a suitable way for the problem at hand.

Since our boundary metric is flat (we just have the Poincaré patch of AdS in the unusual coordinates (3.2.32)), the relevant corrections are of the form [53, 90] ($n + \nu \geq 4$)

$$h_{ab} = r^d h_{ab}^{(d)}(\eta, \vec{x}) + r^{d+2} h_{ab}^{(d+2)}(\eta, \vec{x}) + \mathcal{O}(r^{d+3}), \quad (3.2.43a)$$

$$\psi = r^d \psi^{(d)}(\eta, \vec{x}) + r^{d+2} \psi^{(d+2)}(\eta, \vec{x}) + \mathcal{O}(r^{d+3}), \quad (3.2.43b)$$

where we defined $d \equiv n + \nu - 1$. The (reduced) Einstein equations (3.2.15) then give

$$h^{(d)} = -2\nu \psi^{(d)}, \quad (3.2.44a)$$

$$h^{(d+2)} = -2\nu \psi^{(d+2)}, \quad (3.2.44b)$$

$$\eta \partial^m h_{mn}^{(d)} = \nu h_{n0}^{(d)} - \delta_n^0 h^{(d)}, \quad (3.2.44c)$$

$$2(d+2)\eta^2 h_{mn}^{(d+2)} = -\eta^2 \partial^2 h_{mn}^{(d)} + \nu \eta \partial_\eta h_{mn}^{(d)} - 2\nu \delta_{(m}^0 h_{n)0}^{(d)} + 2\delta_m^0 \delta_n^0 h^{(d)}. \quad (3.2.44d)$$

For $\nu = 0$ (i. e., no compact dimensions), we should recover perturbations around pure AdS, and we indeed obtain

$$h^{(d)} = 0, \quad (3.2.45a)$$

$$\partial^m h_{mn}^{(d)} = 0, \quad (3.2.45b)$$

$$2(d+2)h_{mn}^{(d+2)} = -\partial^2 h_{mn}^{(d)}, \quad (3.2.45c)$$

which are the well-known conditions for asymptotically AdS spaces with a flat boundary [53, 90].

After performing the map (3.2.13), (3.2.11), we obtain the de Sitter metric with perturbations of the form

$$d\tilde{s}^2 = \frac{(\ell')^2}{\eta^2} e^{-2\psi} [(\eta_{ab} + h_{ab}) dx^a dx^b + r^2 d\Omega_{\nu'}^2]. \quad (3.2.46)$$

However, due to the now singular factor $r^d = r^{1-\nu'}$ in the perturbations, they no longer fulfill the source-free Einstein equations (3.2.15). On the de Sitter side after the map, we have $\alpha' = \beta' = -1$, so that the reduced Einstein equations (with a general source (A.1.3)) read

$$\begin{aligned} R_{mn} + g_{mn} \nabla^a \nabla_a \phi - (n' + \nu' - 1)/(\ell')^2 e^{-2\phi} g_{mn} \\ + (n' + \nu' - 2) (\nabla_m \nabla_n \phi + \nabla_m \phi \nabla_n \phi - g_{mn} \nabla^a \phi \nabla_a \phi) \end{aligned} \quad (3.2.47a)$$

$$\begin{aligned} = 8\pi G_N^{n'+\nu'} \left(T_{mn} - \frac{1}{(n' + \nu' - 2)} g_{mn} T \right), \\ - \nabla^a \nabla_a \phi + (n' + \nu' - 2) \nabla^a \phi \nabla_a \phi - (\nu' - 1)(H')^2 \\ + (n' + \nu' - 1)/(\ell')^2 e^{-2\phi} = \frac{8\pi}{(n' + \nu' - 2)} G_N^{n'+\nu'} T, \end{aligned} \quad (3.2.47b)$$

where $T = g^{mn} T_{mn} = (H')^2 r^2 \eta^{mn} T_{mn}$. Putting the perturbations (3.2.43) into these equations and using the conditions (3.2.44) (taking care to replace $n \rightarrow n'$, $\nu \rightarrow 2 - n' - \nu'$ and $d \rightarrow 1 - \nu'$ according to the map), we obtain

$$\begin{aligned} T_{mn} &= -\frac{(1 - \nu')}{16\pi G_N^{n'+\nu'}} h_{mn}^{(d)} r^{-\nu'} \delta(r) \\ &= -\left[\left(\frac{1}{H'} \right)^{d-1} \frac{d}{16\pi G_N^{d+1}} h_{mn}^{(d)} \right] \delta^{1+\nu'}(\vec{r}), \end{aligned} \quad (3.2.48)$$

where we have ‘‘uncompactified’’ the compact coordinates as in (3.2.35), and defined the $(d + 1)$ -dimensional Newton’s constant as

$$G_N^{d+1} \equiv \frac{G_N^{n'+\nu'}}{V_{\nu'}^+} = \frac{G_N^{n'+\nu'}}{(H')^{-\nu'} \Omega_{\nu'}}. \quad (3.2.49)$$

We thus see that the perturbations after the map are sourced by a stress tensor situated on a brane (with intrinsic de Sitter geometry) located in the bulk of de Sitter at $r = 0$. This map is shown in Fig. 3.1. Furthermore, if the conformal field theory living at the $(n + \nu - 1)$ -dimensional boundary of AdS before the compactification can be consistently reduced to an n -dimensional theory plus an additional scalar operator, the expectation

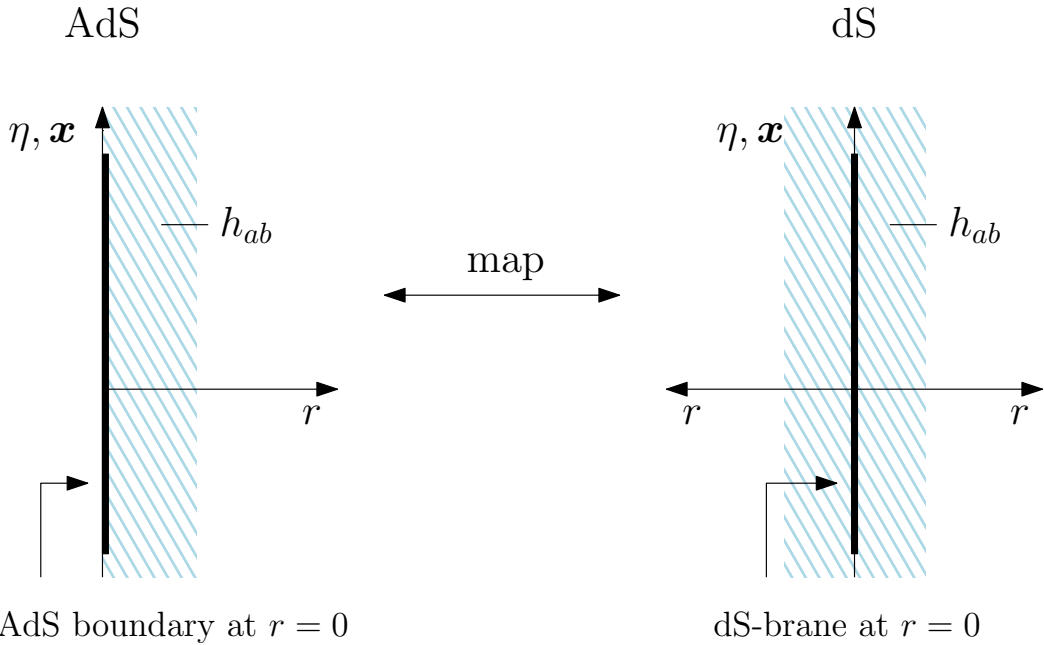


Fig. 3.1 The map for perturbations around (anti-)de Sitter spacetime. On the AdS side, the perturbations live near the boundary at $r = 0$, while the map puts them near a brane located in the bulk of dS at $r = 0$.

value of the n -dimensional holographic stress tensor would be given by the term in brackets in (3.2.48),

$$\langle T_{mn}^{\text{CFT}} \rangle = \frac{d\ell^{d-1}}{16\pi G_N^{d+1}} h_{mn}^{(d)} \quad (3.2.50)$$

(taking into account the map: $n = n'$ and $H' = 1/\ell$). This is the same conclusion that has been reached in the AdS/Ricci-flat correspondence [52, 53]: the (negative) dual stress tensor of the holographic CFT serves as a source for the metric perturbations after the map, with support on a brane situated in the bulk of Minkowski spacetime.

To reinforce these indications, we calculate the (subtracted and rescaled) quasilocal Brown-York stress tensor [57, 89, 90, 92] associated with a surface $r = \text{const.}$ in the metric (3.2.42). The normal vector to this surface is given by

$$n^A = \frac{r}{\ell} \delta_r^A \quad (3.2.51)$$

and normalized to $n^A n_A = 1$. The extrinsic curvature tensor K_{AB} of the surface is defined by

$$K_{AB} = (\delta_A^M - n_A n^M)(\delta_B^N - n_B n^N) \nabla_M n_N, \quad (3.2.52)$$

and we calculate

$$\nabla_M n_N = \frac{\ell}{r^2} \delta_M^r \delta_N^r + \frac{r}{2\ell} \partial_r g_{MN} \quad (3.2.53)$$

and from this

$$\begin{aligned} K_{ab} &= -\frac{\ell}{r^2} (\eta_{ab} - \delta_a^r \delta_b^r) + \frac{\ell r}{2} \partial_r \left(\frac{1}{r^2} h_{ab} \right) \\ &= -\frac{\ell}{r^2} \left(\eta_{ab} - \delta_a^r \delta_b^r - \frac{(d-2)}{2} r^d h_{ab}^{(d)} \right) + \mathcal{O}(r^d), \end{aligned} \quad (3.2.54a)$$

$$K_{a\beta} = 0, \quad (3.2.54b)$$

$$\begin{aligned} K_{\alpha\beta} &= \frac{\ell r}{2} \eta^2 \gamma_{\alpha\beta}^{(-1)} \partial_r \left(\frac{1}{r^2} e^{2\psi} \right) \\ &= -\frac{\ell}{r^2} \eta^2 \gamma_{\alpha\beta}^{(-1)} \left(1 - (d-2) r^d \psi^{(d)} \right) + \mathcal{O}(r^d), \end{aligned} \quad (3.2.54c)$$

where $\gamma_{\alpha\beta}^{(-1)}$ is the metric of a CHS of unit radius, $d\Upsilon_\nu^2 = \gamma_{\alpha\beta}^{(-1)} dy^\alpha dy^\beta$. The trace of the extrinsic curvature follows as (using the conditions (3.2.44))

$$K = g^{MN} K_{MN} = -\frac{d}{\ell} + \mathcal{O}(r^{d+2}). \quad (3.2.55)$$

The unsubtracted Brown-York stress tensor can be shown to be equal to [89, 92]

$$8\pi G_N^{n+\nu} T_{MN}^{\text{BY}} = K_{MN} - K g_{MN}, \quad (3.2.56)$$

and the counterterms that one needs to subtract from the stress tensor to make it well defined as $r \rightarrow 0$ depend on the dimension. For dimensions up to four, they are given by [89, 90]

$$\begin{aligned} 8\pi G_N^{n+\nu} T_{MN}^{\text{CT}} &= -\frac{(d-1)}{\ell} g_{MN} \\ &\quad - \frac{\ell}{d-2} \left(\mathcal{R}_{MN} - \frac{1}{2} \mathcal{R} g_{MN} \right), \end{aligned} \quad (3.2.57)$$

where \mathcal{R}_{MN} is the Ricci tensor of the induced boundary metric $g_{MN}(r = \text{const})$. In even dimensions, there is an additional term (related to the conformal anomaly) which we do not consider here. The Ricci tensor for the induced boundary metric can be found in App. A.2, and using the perturbation (3.2.43) and the conditions (3.2.44), we find up to corrections of order $\mathcal{O}(r^d)$

$$8\pi G_N^{n+\nu} T_{ab}^{\text{BY}} = \frac{\ell}{r^2} \left[(d-1) \eta_{ab} + \frac{(3d-2)}{2} r^d h_{ab}^{(d)} \right], \quad (3.2.58a)$$

$$8\pi G_N^{n+\nu} T_{a\beta}^{\text{BY}} = 0, \quad (3.2.58b)$$

$$8\pi G_N^{n+\nu} T_{\alpha\beta}^{\text{BY}} = \frac{\ell}{r^2} \eta^2 \gamma_{\alpha\beta}^{(-1)} \left[(d-1) + (3d-2)r^d \psi^{(d)} \right], \quad (3.2.58c)$$

$$8\pi G_N^{n+\nu} T_{ab}^{\text{CT}} = -(d-1) \frac{\ell}{r^2} \left(\eta_{ab} + r^d h_{ab}^{(d)} \right), \quad (3.2.58d)$$

$$8\pi G_N^{n+\nu} T_{a\beta}^{\text{CT}} = 0, \quad (3.2.58e)$$

$$8\pi G_N^{n+\nu} T_{\alpha\beta}^{\text{CT}} = -(d-1) \frac{\ell}{r^2} \eta^2 \left(1 + 2r^d \psi^{(d)} \right) \gamma_{\alpha\beta}^{(-1)}. \quad (3.2.58f)$$

Note that to leading order, only the first counterterm in (3.2.57) contributes, while the others are of order $\mathcal{O}(r^d)$. The subtracted and rescaled stress tensor is then given by [90]

$$T_{MN}^{\text{SR}} = \lim_{r \rightarrow 0} \left[\left(\frac{\ell}{r} \right)^{d-2} \left(T_{MN}^{\text{BY}} + T_{MN}^{\text{CT}} \right) \right], \quad (3.2.59)$$

and we finally obtain

$$T_{ab}^{\text{SR}} = \frac{d\ell^{d-1} h_{ab}^{(d)}}{16\pi G_N^{n+\nu}}, \quad (3.2.60a)$$

$$T_{a\beta}^{\text{SR}} = 0, \quad (3.2.60b)$$

$$T_{\alpha\beta}^{\text{SR}} = 2\eta^2 \gamma_{\alpha\beta}^{(-1)} \frac{d\ell^{d-1} \psi^{(d)}}{16\pi G_N^{n+\nu}}. \quad (3.2.60c)$$

This is consistent with our earlier remarks around equation (3.2.50), and shows explicitly what form the stress tensor expectation value in the dual CFT would have to take.

Black holes

In the case of black objects, solutions for general n are much more difficult to obtain. Since the AdS/Ricci-flat map has been used to study hydrodynamics of black branes, we would also like to apply the AdS/dS map to a (planar, vacuum) black brane, with the metric

$$d\bar{s}^2 = \frac{\ell^2}{r^2} \left(-f(r) dt^2 + d\vec{x}_{n-2}^2 + \frac{dr^2}{f(r)} + d\vec{z}_\nu^2 \right) \quad (3.2.61)$$

and $f(r) = 1 - (r/b)^{n+\nu-1}$ with a constant b . However, if we try to compactify \vec{z}_ν using the coordinate transformation (3.2.32), the dilaton depends on the compactified coordinates, in contrast to our initial ansatz.

If we start from the dS side, a (vacuum) black brane solution is not known. Nevertheless, we can consider the Schwarzschild-dS black hole with fixed $n' = 2$, since the dimension of the reduced space does not change under the map. This solution is

given in static coordinates by [93, 94]

$$d\tilde{s}^2 = -f(r) dt^2 + \frac{dr^2}{f(r)} + r^2 d\Omega_{\nu'}^2, \quad (3.2.62)$$

with

$$f(r) = 1 - \left(\frac{r_S}{r}\right)^{\nu'-1} - \frac{r^2}{(\ell')^2} = 1 - \left(\frac{r}{r_S}\right)^{\nu+1} - H^2 r^2, \quad (3.2.63)$$

and where r_S is the Schwarzschild radius of the black hole, while ℓ' is the dS radius. Again, we already used the identification (3.2.11) for the second equality. Comparison with (3.2.13), taking $\alpha' = 0$ and $\beta' = -1$ and thus $\alpha = \beta = 1$, gives us

$$g_{ab}^{(n)} dx^a dx^b = -f(r) dt^2 + \frac{dr^2}{f(r)}, \quad (3.2.64a)$$

$$\phi = -\ln(H'r) = -\ln(r/\ell), \quad (3.2.64b)$$

and the corresponding AdS metric obtained via the map (3.2.12) reads

$$d\bar{s}^2 = \frac{\ell^2}{r^2} \left(-f(r) dt^2 + \frac{dr^2}{f(r)} + H^{-2} d\Upsilon_{\nu}^2 \right). \quad (3.2.65)$$

Changing coordinates to $z = \ell/(Hr)$ and $t = \tau/(H\ell)$, we obtain

$$d\bar{s}^2 = -\bar{f}(z) d\tau^2 + \frac{dz^2}{\bar{f}(z)} + z^2 d\Upsilon_{\nu}^2 \quad (3.2.66)$$

with

$$\bar{f}(z) = \frac{z^2}{\ell^2} f(\ell/(Hz)) = -1 - (Hr_S)^{-(\nu+1)} \left(\frac{\ell}{z}\right)^{\nu-1} + \frac{z^2}{\ell^2}, \quad (3.2.67)$$

which is the metric for an AdS black hole with hyperbolic horizon geometry [95, 96].

What happens to the horizons? We concentrate on the case of a small black hole, where $r_S \ll \ell'$. The black hole horizon is situated at $r_{\text{BH}} \approx r_S$, while the cosmological horizon is at $r_{\text{CH}} \approx \ell'$. The map gives $\ell' = 1/H$, so that we have $Hr_S \ll 1$. After the coordinate transformation, the black hole horizon is mapped to $z_{\text{BH}} \approx \ell/(Hr_S) \gg \ell$, and the cosmological horizon to $z_{\text{CH}} \approx \ell$. Plugging these values into $\bar{f}(z)$, we see that for the black hole horizon we have $\bar{f}(z_{\text{BH}}) \approx 0$ (since we can neglect the -1 in comparison with the huge term $(Hr_S)^{-2}$), but for the cosmological horizon we obtain $\bar{f}(z_{\text{CH}}) \approx -(Hr_S)^{-(\nu+1)} \neq 0$. This can be understood from the map: the term $-(r_S/\ell')^{\nu'-1}$, which was negligible at the cosmological horizon for positive ν' , became $-(Hr_S)^{-(\nu+1)}$, which is large for positive ν .

We see that the black hole horizons are mapped to each other, while the cosmological horizon disappears because of the analytic continuation in the number of dimensions.

Another class of black hole solutions which are interesting to analyze are rotating ones. Kerr/dS black holes have been constructed in higher dimensions with any number of rotation parameters [97], but to show examples of the map one rotation parameter is enough. We use the metric given in Ref. [98], which describes a rotating black hole with mass parameter M and (one) angular momentum parameter a . This metric reads

$$\begin{aligned} d\tilde{s}^2 = & -\frac{\Delta_r}{\rho^2} \left(dt - \frac{a}{\Xi} \sin^2 \theta d\phi \right)^2 + \frac{\rho^2}{\Delta_r} dr^2 + \frac{\rho^2}{\Delta_\theta} d\theta^2 \\ & + \frac{\Delta_\theta \sin^2 \theta}{\rho^2} \left(a dt - \frac{r^2 + a^2}{\Xi} d\phi \right)^2 + r^2 \cos^2 \theta d\Omega_{\nu'}^2, \end{aligned} \quad (3.2.68)$$

where

$$\Delta_r = (r^2 + a^2) \left(1 - \frac{r^2}{(\ell')^2} \right) - 2Mr^{3-\nu'}, \quad (3.2.69a)$$

$$\Delta_\theta = 1 + \frac{a^2}{(\ell')^2} \cos^2 \theta, \quad (3.2.69b)$$

$$\Xi = 1 + \frac{a^2}{(\ell')^2}, \quad (3.2.69c)$$

$$\rho^2 = r^2 + a^2 \cos^2 \theta. \quad (3.2.69d)$$

The reduction proceeds in the same way as before, and again taking $\alpha' = 0$ and $\beta' = -1$, we have

$$g_{ab} dx^a dx^b = d\tilde{s}^2 - r^2 \cos^2 \theta d\Omega_{\nu'}^2, \quad (3.2.70a)$$

$$\phi = -\ln(H'r \cos \theta) = -\ln \left(\frac{r}{\ell} \cos \theta \right). \quad (3.2.70b)$$

The mapped rotating black hole in AdS is then given by

$$\begin{aligned} d\bar{s}^2 = & \frac{\ell^2}{r^2 \cos^2 \theta} \left[-\frac{\tilde{\Delta}_r}{\rho^2} \left(dt - \frac{a}{\tilde{\Xi}} \sin^2 \theta d\phi \right)^2 + \frac{\rho^2}{\tilde{\Delta}_r} dr^2 \right. \\ & + \frac{\rho^2}{\tilde{\Delta}_\theta} d\theta^2 + \frac{\tilde{\Delta}_\theta \sin^2 \theta}{\rho^2} \left(a dt - \frac{r^2 + a^2}{\tilde{\Xi}} d\phi \right)^2 \\ & \left. + H^{-2} d\Upsilon_\nu^2 \right], \end{aligned} \quad (3.2.71)$$

where

$$\tilde{\Delta}_r = (r^2 + a^2) (1 - H^2 r^2) - 2Mr^{3+\nu}, \quad (3.2.72a)$$

$$\tilde{\Delta}_\theta = 1 + H^2 a^2 \cos^2 \theta, \quad (3.2.72b)$$

$$\tilde{\Xi} = 1 + H^2 a^2. \quad (3.2.72c)$$

One can see that this metric is singular near $\theta = \pi/2$, which is due to the fact that the compactified space (the ν' -sphere) has vanishing radius at that point, and thus gives a singular dilaton. Such singular dilatons have also been found in some cases of T-duality [99, 100]. Calculating, e. g., the Kretschmann scalar one finds, however, the completely regular result

$$R_{ABCD}R^{ABCD} = \frac{2(\nu + 3)(\nu + 4)}{l^4} + \mathcal{O}\left(\theta - \frac{\pi}{2}\right). \quad (3.2.73)$$

Since also for $a \rightarrow 0$ the metric does not reduce to the Schwarzschild-AdS black hole (3.2.67), it is thus possible that a suitable coordinate transformation exists which yields a manifestly regular metric also for $\theta = \pi/2$. We leave a detailed investigation for further study.

3.2.4 Discussion

In this section, we have presented a map between Einstein spaces of negative and positive curvature, including a scalar field. In order to obtain such a map via generalized dimensional reduction, these spaces need to have the form of a direct product between an extended spacetime (the bulk) and a compact subspace, whose curvature has the same sign as the total space. Especially, spacetimes which are asymptotically AdS, with the subspace being a compact hyperbolic space, are mapped to a spacetime which is asymptotically de Sitter (deep in the bulk), with the transverse subspace a sphere. This map is a generalization of the AdS/Ricci-flat correspondence [52, 53], and we expect it to generalize to the case of additional matter fields such as gauge fields. Furthermore, nondiagonal reductions are probably possible, as well as the study of moduli of the internal space (note, however, that compact hyperbolic spaces do not possess massless shape moduli by the Mostow rigidity theorem [87, 101]). In general, the mapping is between solutions with different compact dimensions, and the number of compact dimensions must be analytically continued after the map to a positive value. One must therefore know the solution for a general compact dimension ν , and it must be regular as $\nu \rightarrow 0$ for the continuation to be unambiguous. However, this does not seem to be a

strong restriction in practice, as exemplified by the application of the map to empty AdS/dS, black hole spacetimes and perturbations on top of AdS/dS.

A very direct application of the map is as a solution generator, mapping known solutions of positive and negative curvature to each other in nontrivial ways as exemplified by the asymptotically dS/AdS rotating black holes, where the AdS solution is most probably new. Other contexts of study suggest themselves: for example, the AdS/Ricci-flat map has been used to study hydrodynamics of black branes and the Gregory-Laflamme instability [1, 43, 52, 53]. Using the AdS/dS map derived in this section, these considerations could be extended also to de Sitter spacetime.

An important fact (which applies in the same way in the AdS/Ricci-flat correspondence) concerns the mapping of the AdS boundary, which is sent to a brane in the bulk of dS. This brane has itself an intrinsic de Sitter geometry, and supports a stress tensor which serves as the source of perturbations, and which is the negative of the Brown-York stress tensor in the perturbed AdS geometry. These perturbations are obtained by mapping perturbations near the boundary of AdS that encode holographic information from the AdS/CFT correspondence, and the stress tensor on the brane is compatible with what one would expect if the dual CFT at the AdS boundary can be consistently reduced over a compact hyperbolic space (for the AdS/Ricci-flat correspondence, the reduction over a torus is consistent [102, 103] and the corresponding statement can be made). This discovery suggests that a putative holographic dual to de Sitter space is not to be found at infinity in analogy with the AdS case, but instead on such a brane.

In the next chapter we come back to the study of black hole solutions and their relation with fluids. In this context the AdS/Ricci flat will give us a useful way to check our result in asymptotically flat space with known results in AdS.

Chapter 4

Kaluza-Klein reduction of relativistic fluids and their gravity duals

4.1 Introduction

Kaluza-Klein dimensional reduction is a well known method to obtain solutions to a gravitational theory coupled to a Maxwell field, plus a scalar (dilaton) field. Velocities (or momenta) along the compactified direction result in electric charges in the reduced theory [66]. Thus, if we take a neutral black string solution of the vacuum Einstein theory, perform a boost along the direction of the string and then dimensionally reduce in this direction, we obtain an electrically charged black hole of the Einstein-Maxwell-dilaton theory, for a particular value of the dilaton coupling [104].

It should be clear that this method is not exclusive to gravitational theories. The identification between momenta along the internal direction and conserved charges in the reduced theory is in fact generic. Note, however, that in a non-gravitational theory, one obtains charges of a global symmetry group — e.g., a global $U(1)$ for reduction in a circle — while in the gravitational case, since the relevant spacetime symmetries are gauged, they are charges of a gauge symmetry group.

In this chapter we are interested in applying the Kaluza-Klein procedure to relativistic hydrodynamics. That is, we begin with a relativistic fluid without any conserved particle number in p spatial dimensions, where $p - N$ of these are non-compact directions and N of them form an N -torus. We assume that none of the fluid variables depend on the internal directions, but the fluid can have non-trivial velocity along

them. These velocities give internal momenta that in the reduced theory appear as conserved global charges, i.e., particle numbers for N different species. For a perfect fluid, this reduction is a straightforward one. Of more interest is the reduction of the first-order dissipative terms. Viscosity of the higher-dimensional fluid in the internal directions gives rise not only to viscosities but also conductivities in the reduced theory.

We shall do our analysis for a generic relativistic fluid in p spatial dimensions with no conserved particle number, without assuming any specific equation of state nor constituent relation for its first-order transport coefficients. When applying our results to particular fluids, we will consider a class of recent interest in the context of dual relations between fluid dynamics and black brane dynamics. These are the fluids that correspond to neutral black p -branes of the vacuum Einstein theory, and which feature in the blackfold approach, presented in Sec.2.2, to black brane dynamics [41, 42]. Ref. [42] developed the dictionary between the spacetime fluctuations of these black branes and the fluctuations of specific fluids. Using this mapping, our results yield a mapping between the dynamics of charged black branes in Kaluza-Klein theory and the hydrodynamics of certain charged fluids. The map includes their fluid equation of state and first-order transport coefficients. Note that the Kaluza-Klein black brane solutions differ from other charged black branes in their coupling to the dilaton. While the dilaton plays no direct role in the dual fluid description, since it is not associated to any conserved quantity of the black brane, the value of its coupling affects the equation of state and constituent relations.

There have been some previous studies of Kaluza-Klein reduction in the context of fluid/gravity correspondences [54, 67, 68, 105, 106]. However, these have been restricted to the fluids that are dual to AdS black branes, and moreover they only work out explicitly the cases of circle [67] and 2-torus reduction [68]. The results of [67, 68] can be mapped, via the AdS/Ricci-flat connection of [52], to our results for circle reductions of a neutral vacuum black brane. Vice versa, our results can be readily translated into results for AdS black branes with N different charges using this mapping. The perfect fluid dynamics of asymptotically flat charged branes (with arbitrary dilaton coupling) was studied in [51, 107]. Dissipative effects of non-dilatonic asymptotically flat charged branes have been analyzed in [43]. The first-order hydrodynamics of asymptotically flat black D3-branes has been studied in [44], but the charge in this case can not be redistributed along the worldvolume and therefore the dynamics is qualitatively different. Moreover, in [46, 47] the Kaluza-Klein approach has been applied, in a slightly different manner, to obtain first-derivative corrections of charged black brane (extrinsic) dynamics.

In our opinion it is useful to treat the Kaluza-Klein reduction of fluids separately from any specific fluid/gravity dualities. First, this makes clear how the procedure stands on its own within the context of hydrodynamics without any reference to General Relativity. Second, by not tying the reduction to any particular fluid, we achieve a large degree of generality. Clearly, the method can be extended to the case in which the higher-dimensional fluid carries a particle number or some other property, but we will not pursue this in the present thesis.

4.2 Hydrodynamic Kaluza-Klein ansatz and reduction of the perfect fluid

Let us consider a neutral relativistic fluid in flat space-time in $p+1$ dimensions described by a stress energy tensor of the form in (2.1.3). The hydrodynamical behaviour of this fluid is governed by the stress energy tensor conservation equations $\partial_A T^{AB} = 0$. Its complete description requires the specification of the equation of state, namely the relation between P and ϱ , and of the viscosities. For the most part we will keep them general, and will only specify them in Sec. 4.4. Furthermore, we consider that the uncharged fluid is in the Landau frame where $u^A T_{AB}^{diss} = 0$.

We assume moreover that the spacetime in which the fluid moves contains N compact directions that form an N -torus

$$d\hat{s}^2 = \sum_{j=1}^N dy_j^2 + \eta_{ab} d\sigma^a d\sigma^b, \quad (4.2.1)$$

where the metric η_{ab} is the Minkowski metric in $p - N + 1$ spacetime dimensions and the coordinates y_j are identified with periodicity $2\pi R_j$. We take the fluid to move with non-zero velocity along the N compactified dimensions. On Kaluza-Klein reduction this will give rise to charges in the reduced fluid.

The Kaluza-Klein ansatz for the field requires that none of the fluid variables depend on the internal directions y_j . The velocity profile is

$$u_a = \hat{u}_a \prod_{i=1}^N \cosh \alpha_i, \quad u_{y_j} = \sinh \alpha_j \prod_{k=1}^{j-1} \cosh \alpha_k, \quad j = 1, \dots, N \quad (4.2.2)$$

where α_i are boost parameters characterizing the velocity along the compact directions and \hat{u}_a is the velocity in the reduced spacetime, which is unit-normalized with respect

to η_{ab} ,

$$\hat{u}^a \hat{u}^b \eta_{ab} = -1. \quad (4.2.3)$$

Note that it should be possible to formulate an ansatz for the velocity field where the different boosts enter in a manner that preserves the local symmetry $SO(N)$ that rotates them (this is broken globally by the compact size of the torus). The above ansatz does not show this, but it is a convenient one for our calculations.¹

Let us apply this Kaluza-Klein reduction ansatz to the perfect fluid stress energy tensor. Substituting (4.2.2) in (2.1.3) we obtain

$$\begin{aligned} T_{ab} &= V \left((\varrho + P) \hat{u}_a \hat{u}_b \prod_{i=1}^N \cosh^2 \alpha_i + P \eta_{ab} \right), \\ T_{ay_j} &= V (\varrho + P) \sinh \alpha_j \hat{u}_a \prod_{i=1}^N \cosh \alpha_i \prod_{k=1}^{j-1} \cosh \alpha_k, \\ T_{y_j y_{j'}} &= V \left((\varrho + P) \sinh \alpha_{j'} \sinh \alpha_j \prod_{k=1}^{j-1} \cosh \alpha_k \prod_{i=1}^{j'-1} \cosh \alpha_i + \eta_{jj'} P \right), \end{aligned} \quad (4.2.4)$$

where $V = \prod_{j=1}^N (2\pi R_j)$ is volume of the torus. The factor V appears because T_{AB} refers to densities so we have to include the internal volume we are going to integrate out. The form of the stress energy tensor in the reduced theory is

$$\hat{T}_{ab} = (\hat{\varrho} + \hat{P}) \hat{u}_a \hat{u}_b + \hat{P} \eta_{ab}, \quad \hat{T}_{ay_j} = u_a \hat{q}_j, \quad (4.2.5)$$

where the energy density, the pressure and a set of N charge densities \hat{q}_j (one for each boost parameter α_j) in the reduced theory, respectively, are given by

$$\begin{aligned} \hat{P} &= PV, \quad \hat{\varrho} = \hat{P} \left(-1 + \prod_{i=1}^N \cosh^2 \alpha_i \right) + \varrho V \prod_{m=1}^N \cosh^2 \alpha_m, \\ \hat{q}_j &= (\hat{P} + \hat{\varrho}) \frac{\sinh \alpha_j}{\prod_{i=j}^N \cosh \alpha_i}. \end{aligned} \quad (4.2.6)$$

The temperature associated to the reduced fluid becomes

$$\hat{\mathcal{T}} = \frac{\mathcal{T}}{\prod_{i=1}^N \cosh \alpha_i} \quad (4.2.7)$$

¹Our choice is in this sense analogous to choosing polar coordinates for a sphere, which allows easy explicit calculation but obscures the rotational symmetry.

due to the fact that we have changed the timelike Killing vector. From the conservation of the entropy current for the initial fluid, we can read off the reduced entropy density. We obtain

$$\hat{s} = sV \prod_{i=1}^N \cosh \alpha_i. \quad (4.2.8)$$

From the Euler relation

$$\hat{P} + \hat{\varrho} = \hat{\mathcal{T}}\hat{s} + \sum_{j=1}^N \hat{q}_j \hat{\mu}_j \quad (4.2.9)$$

the chemical potential for each charge takes the form

$$\hat{\mu}_j = \frac{\sinh \alpha_j}{\prod_{i=j}^N \cosh \alpha_i}. \quad (4.2.10)$$

Since we assume that the first law is satisfied for the initial neutral fluid, it is possible to verify that the same is true for the reduced fluid. The neutral fluid obeys the law

$$d\varrho = \mathcal{T}ds \quad (4.2.11)$$

from which it follows

$$d\hat{\varrho} = \hat{\mathcal{T}}d\hat{s} + \sum_{i=1}^N \hat{\mu}_i d\hat{q}_i \quad (4.2.12)$$

using

$$\begin{aligned} \hat{\varrho} + \hat{P} &= V(\varrho + P) \prod_{i=1}^N \cosh^2 \alpha_i && \text{from Eq.(4.2.6),} \\ d\alpha_{j+1} &= d\alpha_j \frac{\tanh \alpha_{j+1}}{\sinh \alpha_j \cosh \alpha_j} && \text{from Eq.(B.1.5)} \end{aligned} \quad (4.2.13)$$

and that $\varrho + P = \mathcal{T}s$.

4.3 Reduction of dissipative terms

The Kaluza-Klein reduction has given us a charged fluid. When including dissipative terms we expect the presence of another set of transport coefficients, namely a heat conductivity matrix. These coefficients measure the response of the charge current to changes in temperature and in chemical potential.

In order to reduce the first-derivative terms in the stress energy tensor, we need to express the expansion θ defined in Eq.(2.1.9) in terms of the new velocities. We find

that

$$\theta = \prod_{i=1}^N \cosh \alpha_i \left(\hat{\theta} + \sum_{k=1}^N \tanh \alpha_k \hat{u}_a \partial^a \alpha_k \right), \quad (4.3.1)$$

where $\hat{\theta} = \partial^a \hat{u}_a$.

The equation of conservation of the stress energy tensor relates the gradients of the rapidities to $\hat{\theta}$ as

$$\hat{u}_a \partial^a \alpha_j = \hat{\theta} \frac{\cosh \alpha_j \sinh \alpha_j \prod_{l=j+1}^N \cosh^2 \alpha_l}{1 + (-1 + \varrho') \prod_{i=1}^N \cosh^2 \alpha_i}, \quad (4.3.2)$$

where

$$\varrho' = c_s^{-2} = \frac{\partial \varrho}{\partial P}, \quad (4.3.3)$$

where c_s is the speed of sound. The explicit calculation can be found in the App. B.1. Substituting this result in Eq.(4.3.1) the expansion becomes

$$\theta = \hat{\theta} \frac{\varrho' \prod_{i=1}^N \cosh^3 \alpha_i}{1 + (-1 + \varrho') \prod_{i=1}^N \cosh^2 \alpha_i}. \quad (4.3.4)$$

The orthogonal projectors tensor in Eq.(2.1.9) is given by

$$\begin{aligned} P_{ab} &= \prod_{i=1}^N \cosh^2 \alpha_i \hat{u}_a \hat{u}_b + \eta_{ab}, \\ P_{ay_j} &= \hat{u}_a \sinh \alpha_j \prod_{i=1}^N \cosh \alpha_i \prod_{k=1}^{j-1} \cosh \alpha_k, \\ P_{y_j y_{j'}} &= \sinh \alpha_{j'} \sinh \alpha_j \prod_{k=1}^{j-1} \cosh \alpha_k \prod_{i=1}^{j'-1} \cosh \alpha_i + \eta_{jj'}. \end{aligned} \quad (4.3.5)$$

The shear viscosity tensor in Eq.(2.1.9) takes the form

$$\begin{aligned} \sigma_{ab} &= \sum_{i=1}^N P_{(a}^c P_{b)}^{y_i} \partial_c u_{y_i} + P_a^c P_b^d \partial_{(c} u_{d)} - \frac{P_{ab} \theta}{p}, \\ \sigma_{ay_j} &= P_a^c P_{y_j}^d \partial_{(c} u_{d)} + \sum_{i=1}^N P_{(a}^{y_i} P_{y_j)}^d \partial_d u_{y_i} - \frac{P_{ay_j} \theta}{p}, \\ \sigma_{y_j y_{j'}} &= P_{y_j}^c P_{y_{j'}}^d \partial_{(c} u_{d)} + \sum_{i=1}^N P_{(y_j}^{y_i} P_{y_{j'}})^d \partial_d u_{y_i} - \frac{P_{y_j y_{j'}} \theta}{p}. \end{aligned} \quad (4.3.6)$$

We have all the ingredients to compute the new transport coefficients. However, our reduced fluid is not in the Landau frame. Indeed, we find that $u^A T_{AB} = 0$ implies

$$u^a T_{ab}^{diss} + \sum_{j=1}^N u^{y_j} T_{y_j b}^{diss} = 0, \quad u^a T_{ay_j}^{diss} + \sum_{j'=1}^N u^{y_{j'}} T_{y_{j'} y_j}^{diss} = 0, \quad (4.3.7)$$

or using Eq.(4.2.2)

$$\hat{u}^a T_{ab}^{diss} = -\frac{\sum_{j=1}^N \sinh \alpha_j}{\prod_{i=j}^N \cosh \alpha_i} T_{y_j b}^{diss}, \quad \hat{u}^a T_{ay_j}^{diss} = -\frac{\sum_{j'=1}^N \sinh \alpha_{j'}}{\prod_{i=j'}^N \cosh \alpha_i} T_{y_{j'} y_j}^{diss}. \quad (4.3.8)$$

This means that we cannot directly extract the coefficients from the reduced stress energy tensor but we need to introduce some frame-invariant formulae. In [108] was proposed an efficient way to extract those coefficients based on a general dissipative correction to the stress energy tensor and the charge currents. In order to avoid unphysical solutions we require the semi-positivity of the divergence of local entropy current. Following the same procedure as in [108] and generalizing the result for N charges we construct frame invariant formulae

$$\begin{aligned} \hat{P}_c^a \hat{P}_d^b T_{ab}^{diss} - \frac{1}{p-N} \hat{P}_{cd} \hat{P}^{ab} T_{ab}^{diss} &= -2\hat{\eta} \hat{\sigma}_{cd}, \\ \hat{P}_a^b \left(T_{by_j}^{diss} + \frac{\hat{q}_j}{\hat{\rho} + \hat{P}} \hat{u}^c T_{cb}^{diss} \right) &= -\sum_{j'=1}^N \hat{\kappa}_{jj'} \hat{P}_a^b \partial_b \left(\frac{\hat{\mu}_{j'}}{\hat{\mathcal{T}}} \right), \\ \frac{\hat{P}^{ab} T_{ab}^{diss}}{p-N} - \frac{\partial \hat{P}}{\partial \hat{\rho}} \hat{u}^a \hat{u}^b T_{ab}^{diss} + \sum_{j=1}^N \frac{\partial \hat{P}}{\partial \hat{q}_j} \hat{u}^a T_{ay_j}^{diss} &= -\hat{\zeta} \hat{\theta}. \end{aligned} \quad (4.3.9)$$

Using these we can extract the viscosities $\hat{\eta}$, $\hat{\zeta}$ and the matrix of conductivities $\hat{\kappa}_{jj'}$. The derivative $\partial \hat{P} / \partial \hat{\rho}$ is evaluated at constant charges, while $\partial \hat{P} / \partial \hat{q}_j$ are evaluated keeping fixed the energy density and the other charges $q_{k \neq j}$.

We obtain

$$\begin{aligned} \hat{\eta} &= \eta V \prod_{i=1}^N \cosh \alpha_i, & \hat{\kappa}_{jj} &= \eta V \hat{\mathcal{T}} \left(1 - \frac{\sinh^2 \alpha_j}{\prod_{l=j}^N \cosh^2 \alpha_l} \right) \prod_{i=1}^N \cosh \alpha_i, \\ \hat{\kappa}_{jk} &= \hat{\kappa}_{kj} = -\eta V \hat{\mathcal{T}} \frac{\sinh \alpha_j \sinh \alpha_k}{\prod_{i=j}^N \cosh \alpha_i} \prod_{l=1}^{k-1} \cosh \alpha_l, & \text{with } k &\neq j, \end{aligned} \quad (4.3.10)$$

$$\hat{\zeta} = 2\eta V \prod_{i=1}^N \cosh \alpha_i \left[\frac{1}{p-N} + \frac{(-1 + \prod_{i=1}^N \cosh^2 \alpha_i) \sum_{l=1}^N \sinh^2 \alpha_l \prod_{m=l+1}^N \cosh^2 \alpha_m}{(1 + (-1 + \varrho') \prod_{i=1}^N \cosh^2 \alpha_i)^2} - \frac{\varrho'^2 \prod_{h=1}^N \cosh^4 \alpha_h}{p(1 + (-1 + \varrho') \prod_{i=1}^N \cosh^2 \alpha_i)^2} \right] + \zeta V \frac{\varrho'^2 \prod_{h=1}^N \cosh^5 \alpha_h}{(1 + (-1 + \varrho') \prod_{i=1}^N \cosh^2 \alpha_i)^2}. \quad (4.3.11)$$

These are the main results of this article.

The transport coefficients can be rewritten in terms of the independent thermodynamic variables of the reduced theory, the temperature and the chemical potentials, using Eq.(4.2.7) and Eq.(4.2.10) functions of the rapidities.

Observe that the viscosity to entropy density ratio remains constant under the reduction,

$$\frac{\hat{\eta}}{\hat{s}} = \frac{\eta}{s}. \quad (4.3.12)$$

Furthermore, since the entropy current for our charged fluid in a canonical form is

$$\hat{j}_s^a = \hat{s} \hat{u}^a - \frac{u_b T^{ab}}{\hat{\mathcal{T}}} - \frac{1}{\hat{\mathcal{T}}} \sum_{j=1}^N \mu_j T_{diss}^{aj} \quad (4.3.13)$$

using the relations in Eq.(4.3.8) and substituting the values of the chemical potentials Eq.(4.2.10), it is easy to see that

$$\hat{j}_s^a = \hat{s} \hat{u}^a. \quad (4.3.14)$$

Comparing this result with the entropy density of our neutral initial fluid

$$\hat{j}_s^A = s u^A \quad (4.3.15)$$

multiplied by the volume factor V , we recover the result obtain from the Euler relation in Eq.(4.2.8).

Finally, the speed of sound is given by

$$\hat{c}_s^2 = \frac{\partial \hat{P}}{\partial \hat{\rho}} = \frac{1}{1 + (-1 + \varrho') \prod_{i=1}^N \cosh^2 \alpha_i}, \quad (4.3.16)$$

where the derivative is considered at fixed \hat{s}/\hat{q}_j for every \hat{q}_j .

4.4 Charged black brane/fluid duals

The previous analysis can be applied to the case of the fluid dual to a black p -brane. Let us consider a black p -brane in $D = p + n + 3$ dimensions with $p + 1$ worldvolume coordinates of the p -brane and $n + 2$ coordinates in directions transverse to that. Since we perform a Kaluza Klein reduction exclusively on the worldvolume directions, we focus only on the $p + 1$ coordinates. This means that the p dimensions of the black p -brane can be seen as the p spatial dimensions of the previous fluid.

In [42] was shown that the long-wavelength dynamics of a neutral black brane in $D = p + n + 3$ dimensions can be described in terms of a fluid with equation of state

$$\varrho = -(n + 1)P, \quad (4.4.1)$$

and viscosities

$$\eta = \frac{s}{4\pi}, \quad \zeta = 2\eta \left(\frac{1}{p} + \frac{1}{n + 1} \right). \quad (4.4.2)$$

If we substitute these values in Eqs.(4.2.13), (4.3.10), we obtain the reduced thermodynamic quantities

$$\begin{aligned} \hat{P} &= PV, & \hat{\varrho} &= -\hat{P} \left(1 + n \prod_{i=1}^N \cosh^2 \alpha_i \right), \\ \hat{q}_j &= -\hat{P} n \sinh \alpha_j \prod_{i=1}^N \cosh \alpha_i \prod_{k=1}^{j-1} \cosh \alpha_k, \end{aligned} \quad (4.4.3)$$

and the transport coefficients of the charged fluid

$$\begin{aligned} \hat{\eta} &= \frac{\Omega_{n+1} V}{16\pi G} \left(\frac{4\pi \hat{T}}{n} \right)^{-n-1} \left(1 - \sum_{i=1}^N \mu_i^2 \right)^{\frac{n}{2}}, \\ \hat{\kappa}_{jj} &= \frac{\Omega_{n+1} V}{16\pi G} \left(\frac{4\pi}{n} \right)^{-n-1} \hat{T}^{-n} (1 - \mu_j^2) \left(1 - \sum_{i=1}^N \mu_i^2 \right)^{\frac{n}{2}}, \\ \hat{\kappa}_{jk} &= -\frac{\Omega_{n+1} V}{16\pi G} \left(\frac{4\pi}{n} \right)^{-n-1} \hat{T}^{-n} \mu_k \mu_j \left(1 - \sum_{i=1}^N \mu_i^2 \right)^{\frac{n}{2}}, \\ \hat{\zeta} &= 2\hat{\eta} \left[\frac{1}{p - N} - \frac{(-1 - n - (\sum_{i=1}^N \mu_i^2)^2)}{(-1 - n - \sum_{m=1}^N \mu_m^2)^2} \right], \end{aligned} \quad (4.4.4)$$

using the explicit values of the temperature and the shear viscosity in (2.2.7).

We can compare our results with those found in Eq.(3.4.17) and Eqs. (3.4.38)-(3.4.40) in [67] for $N = 1$ in AdS. This can be done using the AdS/Ricci flat map

in [52] which allows to relate the dynamics of Ricci-flat black p -branes in $n + p + 3$ dimensions to that of black d -branes in $\text{AdS}_{2\sigma+1}$, by identifying

$$-n \rightarrow 2\sigma, \quad p \rightarrow d. \quad (4.4.5)$$

If we apply this map to the equation of state and the transport coefficients that we obtain for $N = 1$, we find the same results as in [67] with

$$\alpha_i \rightarrow \omega_i \quad \text{and} \quad \frac{\Omega_{n+1}V}{16\pi G} \rightarrow -L. \quad (4.4.6)$$

where L is defined after Eq.(3.1.3) in [67]. For $N = 2$ the map to black d -branes in $\text{AdS}_{2\sigma+1}$ is

$$-n \rightarrow 2\sigma, \quad p \rightarrow d + 1. \quad (4.4.7)$$

In this case we recover the results of [68] in Eq.(3.1.18) and Eqs. (3.2.42)-(3.2.51) for the Kaluza-Klein Einstein-Maxwell-Dilaton theory containing two Maxwell fields, three neutral scalars and an axion in AdS, again using Eqs.(2.2.7). Note that the speed of sound and the other thermodynamic quantities as entropy, temperature and chemical potential agree too.

Finally, we study whether the bound

$$\frac{\hat{\zeta}}{\hat{\eta}} \geq 2 \left(\frac{1}{p - N} - \hat{c}_s^2 \right) \quad (4.4.8)$$

proposed in [109] is satisfied. The bulk viscosity for a charged black $(p - N)$ -brane takes the form

$$\hat{\zeta} = 2\eta V \prod_{i=1}^N \cosh \alpha_i \left(\frac{1}{p - N} - \frac{2 \prod_{i=1}^N \cosh^2 \alpha_i - (n + 2) \prod_{m=1}^N \cosh^4 \alpha_m - 1}{(1 - (n + 2) \prod_{i=1}^N \cosh^2 \alpha_i)^2} \right). \quad (4.4.9)$$

In terms of the speed of sound

$$\hat{c}_s^2 = \frac{1}{1 - (2 + n) \prod_{i=1}^N \cosh^2 \alpha_i}, \quad (4.4.10)$$

the bulk to shear viscosity ratio can be written as

$$\frac{\hat{\zeta}}{\hat{\eta}} = 2 \left(\frac{1}{p - N} - \hat{c}_s^2 \right) - 2\hat{c}_s^4 \left((n + 4) \prod_{i=1}^N \cosh^2 \alpha_i - (n + 2) \prod_{m=1}^N \cosh^4 \alpha_m - 2 \right). \quad (4.4.11)$$

The relation (4.4.8) requires that

$$n \geq -2 + \frac{2}{\prod_{i=1}^N \cosh^2 \alpha_i}, \quad (4.4.12)$$

which is satisfied for all $n \geq 0$. Thus the bound is always satisfied. In contrast, the bound is always violated in [67, 68] for the black d -branes with $\sigma > 1$, where $2\sigma + 1$ are the initial spacetime dimensions.

An alternative bound was proposed in [67],

$$\frac{\hat{\zeta}}{\hat{\eta}} \geq 2 \left(\frac{1}{p - N} - \hat{c}_q^2 \right) \quad (4.4.13)$$

in terms of the speed of sound at constant charge density

$$\hat{c}_q = \left. \frac{\partial \hat{P}}{\partial \hat{q}} \right|_{q_j} = \frac{2 \prod_{i=1}^N \cosh^2 \alpha_i - 1}{1 - (2 + n) \prod_{i=1}^N \cosh^2 \alpha_i}. \quad (4.4.14)$$

It is straightforward to show that in our case this bound is always violated. We obtain

$$\frac{\hat{\zeta}}{\hat{\eta}} = 2 \left(\frac{1}{p - N} - \hat{c}_q^2 \right) - 2\hat{c}_s^4 \left((2 + n) \prod_{i=1}^N \cosh^2 \alpha_i (-1 + \prod_{m=1}^N \cosh^2 \alpha_m) \right). \quad (4.4.15)$$

In order to satisfy the bound in (4.4.13) we would need $n \leq -2$. The inversion of the results regarding both bounds (4.4.8) and (4.4.13) as compared to [67] and [68] is expected from the mappings (4.4.5) and (4.4.7). On the other hand, for electrically charged, non-dilatonic asymptotically flat black brane solutions, ref. [43] finds that the bound (4.4.8) is satisfied only for small enough charge density, while the bound (4.4.13) is always violated.² Note Eq.(4.3.12) implies that the KSS bound [31, 110] is saturated.

²Jakob Gath informs us (private communication) that for sufficiently large values of the dilaton coupling these bounds are satisfied/violated in the same manner as we have found: (4.4.8) is always satisfied, and (4.4.13) is always violated, for all values of the charge density.

Chapter 5

Probing the Hydrodynamic Limit of (Super)gravity

5.1 Introduction

Remaining in the context of black hole hydrodynamics, in this chapter we shall be interested in the effective behavior of a quite general class of black brane solutions captured by the action (5.2.1) which will be introduced in Sec. 5.2. Although this action is rather general, we will restrict ourselves to the cases where the black p -branes source a $(p+1)$ -form *or* a 1-form gauge potential. In the following we will refer to these two types of brane charge as fundamental charge and Maxwell charge, respectively. In particular, the treatment of these two cases will allow us to capture the effective hydrodynamic descriptions of the NS and Dp -branes of type II supergravity along with the M2 and M5-branes of eleven dimensional supergravity. Moreover, our computation also captures the effective theory of $(p+1)$ -dimensional smeared brane configurations of D0 of type IIA supergravity. However, instead of fixing the value of the dilaton coupling and spacetime dimension to the ones relevant for the specific supergravities, we will keep these parameters free. This allows us to extract the dependence of these parameters in the hydrodynamic transport coefficients, which turns out to be quite useful for examining the general features of the hydrodynamics. We note that the part of the computation pertaining to Maxwell charge also provides the non-trivial dilatonic generalization of the results for the Reissner-Nordström black brane worked out in [43]. Moreover, we emphasize that in this work we do not consider asymptotically (co-dimension 1) AdS branes but rather asymptotically flat configurations of general co-dimension.

Considerable research has gone into understanding the stability properties of black branes carrying various types of smeared charges (the literature is extensive, for a review see e.g. [111]). Understanding these properties is interesting from a pure general relativistic point of view *viz.* the Gregory-Laflamme (GL) instability [21, 22], black hole phase transitions [112] etc., but also plays an important rôle for understanding aspects of the (un)stable vacua of string and M-theory. In general, having access to an effective fluid dynamic description naturally allows one to address questions regarding the stability properties of the system in question. For example, to leading order, i.e., at the perfect fluid level (equivalently; at the thermodynamic level), an imaginary speed of sound signifies a fundamental instability in the system. In the context of brane physics, this was noted in [41] where an instability in the sound mode of the effective fluid of the Schwarzschild black brane exactly was identified with the GL instability of the brane. A GL instability is naturally characterized by a dispersion relation which describes the “dispersion” of the instability on the worldvolume. Although the exact form of this relation is only accessible numerically many of its features can be understood from the hydrodynamic description. In particular, turning the picture around, the lack of unstable hydrodynamic modes in the effective theory (to a given order in the derivative expansion) is equivalent to the lack of a GL instability, at least to that given order.

One of the main results stressed in this chapter is that (to first order in the fluid derivative expansion) the stability properties of the fundamentally charged dilatonic black brane remains solely determined by the speed of sound. In this way, the system will exhibit a stable branch of configurations for sufficiently small values of the dilaton coupling. This includes the Dp -branes, $p < 5$, of type II supergravity along with the M2 and M5 branes of M-theory. However, it does *not* include the D5, D6 and NS5 brane. We note that a similar conclusion was reached in [107], but we refine the analysis to first order and use the correct value for the bulk viscosity. This result is furthermore in accordance with expectations from various numerical works [21, 22, 113]. On the other hand, we find that the dilatonic Maxwell charged black branes cannot be made stable for any value of the dilaton coupling or the charge. In particular, this includes the smeared D0 configurations of type IIA supergravity. Again, this is in accordance with general expectations [114, 115]. We note that, as in Ref. [43], this is a genuine first-order derivative effect, meaning that the instability is not visible to leading order.

Another interesting aspect of our computation relates to various proposed hydrodynamic bounds in gravity [31, 34, 109, 110, 116]. As mentioned above, we keep the dilaton coupling free in our computations. In addition to elucidating the (in)stability properties of the various branes this also provides us with an extra tunable parameter

to examine the possible violation of the hydrodynamic bounds. As expected, we find that the shear viscosity-to-entropy ratio bound $\eta/s \geq 1/4\pi$ is saturated for our entire class of gravitational solutions. In contrast we find that the (holographic) bulk viscosity “bound” is violated for the entire class of fundamentally charged branes thus providing a simple example of its violation.

Although the setup employed in this work is conceptually quite different from the hydrodynamic limit of AdS/CFT (the fluid/gravity correspondence), some of the results of the two approaches can nevertheless be related. This is perhaps not too surprising since the latter should in principle be obtainable from the former in the near-horizon limit. The precise connection between the effective fluid dynamic theory of the asymptotically flat (non-dilatonic) D3-brane and the fluid/gravity correspondence on AdS₅ was explored in Ref. [44]. Here the effective gravitational dynamics of the D3-brane subject to Dirichlet boundary conditions at an appropriate cutoff surface was considered along the lines of ideas introduced in the paper(s) [117, 118]. It was directly shown that the fluid/gravity correspondence and the hydrodynamic effective theory are obtained as the two (most interesting) extremes where the cutoff surface is taken to be located in the near-horizon throat region and at spatial infinity, respectively. Perhaps more surprisingly, the results of the fluid/gravity correspondence can also be related to the effective hydrodynamics of the (neutral) Schwarzschild black p -brane. This was shown in the paper(s) [52, 53] where the authors managed to derive a mapping from a certain class of asymptotically AdS solutions to asymptotically flat solutions and vice versa presented in detail in Sec. 3.1. This class of solutions (on each side of the mapping, respectively) exactly includes the Ricci-flat and the AdS Schwarzschild black branes, respectively. More technically, the mapping is established by noting that the hydrodynamic sector on either side (of the mapping) is completely included in a reduced lower dimensional theory. Solutions to these two reduced theories can then be related by a simple analytical continuation in the dimension of the particular space on which the reduction is performed (a sphere and a torus, respectively). In this way, solutions on one side can be reduced, analytically continued and consistently uplifted to the other side and vice versa. This, conceptually quite simple, procedure neatly allowed [52] to derive the second-order fluid dynamic transport coefficients of the asymptotically flat Schwarzschild black brane from the results of the (co-dimension one) AdS black brane in general dimensions [119]. In this chapter we will present a modified version of the mapping which allows us to include Maxwell charge.

This chapter is organized as follows. In the Sec. 5.2 we introduce the leading order (seed) geometries around which we will consider hydrodynamic perturbations. Before presenting the first-order results of the fundamentally charged black brane and analyzing their stability, we briefly review the associated thermodynamics and explain how the perturbative procedure is carried out. In Sec. 5.3 we turn our attention to Maxwell charged black branes and work out the first-order transport coefficients and discuss the associated hydrodynamic stability properties. We conclude the chapter by performing a non-trivial cross-check of our results with known results from AdS by introducing a modified version of the AdS/Ricci-flat correspondence.

5.2 Hydrodynamics of black p -branes

In this section we shall be interested in D dimensional p -brane solutions (i.e., solutions with horizon topology $\mathbf{R}^p \times S^{D-p-2}$) of the following action¹ [120, 121]

$$I = \int_D \left(R * 1 - 2 d\phi \wedge * d\phi - \frac{1}{2} \sum_{q \in \mathcal{I}} \mathcal{F}_{(q+2)} \wedge * \mathcal{F}_{(q+2)} \right). \quad (5.2.1)$$

Here $\mathcal{F}_{(q+2)} = e^{a_q \phi} dC_{(q+1)}$, $q \in \mathcal{I}$, are the dilaton weighted field strengths associated with the gauge potentials $C_{(q+1)}$ and \mathcal{I} denotes the collective set of gauge potentials in the theory. Notice that some of the forms can be of the same rank nonetheless they have different couplings a_q to the dilaton which distinguishes them. The action (5.2.1) is quite general, however, for specific choices of \mathcal{I} and dilaton couplings, it captures the (bosonic part of the) supergravity descriptions of type IIA/B (in the Einstein frame) and M-theory relevant for description of the D/NS/M-branes and their intersections. Notice that the aforementioned supergravity actions also contain a topological term needed to preserve supersymmetry of the full theory, however, this term does not play a rôle for obtaining the flat p -brane solutions [122]. The action (5.2.1) corresponds to IIA (IIB) supergravity for $D = 10$, $\mathcal{I}_{\text{RR}} = \{0, 2\}$ ($\mathcal{I}_{\text{RR}} = \{1, 3\}$) and $\mathcal{I}_{\text{NS}} = \{1\}$ [123–125] and eleven-dimensional supergravity for $D = 11$ and $\mathcal{I}_{\text{M}} = \{2\}$ [126]. In general, the D/NS/M-branes couple both electrically and magnetically to the above potentials. We unify the description in the standard way by writing the field strengths in the electric ansatz, where now the index q in the action (5.2.1) runs over the (allowed) spatial dimensions of the branes of the theory. Given a dilaton coupling a , it will be convenient

¹We work in units where $G_{\text{Newton}} = \frac{1}{16\pi}$.

to define a parameter N to further unify the description through the relation

$$a^2 = \frac{4}{N} - \frac{2(q+1)(D-q-3)}{D-2}. \quad (5.2.2)$$

The real positive parameter N (usually an integer for string/M-theory corresponding to the number of different types of branes in an intersection [127]) in general is preserved under dimensional reduction [51].² Also note that the parameter N mods out the \mathbf{Z}_2 reflection symmetry of the solution space $a \rightarrow -a$. For all the fundamental D/NS/M-branes of type II string theory and M-theory $N = 1$, and $a_{Dp} = (3-p)/2$ for the Dp -branes, while $a^2 = 1$ for the F1 ($a_{F1} = -1$) and NS5 brane ($a_{NS5} = 1$). Also notice that the dilaton coupling (5.2.2) vanishes for $D = 11$, $q = 2, 5$, consistent with the fact that M-theory contains no dilaton.

In the following we will consider singly fundamentally charged p -branes, i.e., $q = p$. We therefore (consistently) truncate the action (5.2.1) to $\mathcal{I} = \{p\}$. Moreover, we will keep the dilaton coupling $a \equiv a_p$ free. One easily works out the equations of motion,

$$\begin{aligned} \square\phi &= \frac{a}{4(p+2)!} \mathcal{F}^2, \quad d(e^{a\phi} * \mathcal{F}) = 0, \\ G^\nu{}_\mu &= \frac{1}{2(p+1)!} (\mathcal{F} \cdot \mathcal{F})^\nu{}_\mu + \left(2(\partial\phi)^2 - \frac{\mathcal{F}^2}{4(p+2)!} \right) \delta^\nu{}_\mu, \end{aligned} \quad (5.2.3)$$

where $G_{\mu\nu}$ denotes the Einstein tensor and μ, ν label the spacetime directions. As explained in Sec. 5.1, we are interested in p -brane solutions to the theory (5.2.1) characterized by horizon topology $\mathbf{R}^p \times S^{n+1}$, where we break the ∂_i symmetries on \mathbf{R}^p (and thus implicitly breaking ∂_t as well) perturbatively while maintaining the $SO(n+2)$ symmetry on the transverse sphere (note that the total spacetime dimension D is related to the positive integer parameter n according to $n = D - p - 3$). These perturbations exactly capture the hydrodynamic sector of the black brane as we review below.³ The family of leading order unperturbed (seed) p -branes solutions to the EOMs

²Since we require the dilaton to be physical (i.e., we require $a^2 \geq 0$), the parameter N is bounded from above $N \leq \frac{2(D-2)}{(D-q-3)(q+1)}$.

³Breaking the $SO(n+2)$ would roughly correspond to elastic perturbations, see [45] and related works.

(5.2.3) was worked out in Ref. [51] and takes the form

$$\begin{aligned} ds^2 &= h^{-\frac{Nn}{p+n+1}} \left(-f u_a u_b dx^a dx^b + \Delta_{ab} dx^a dx^b + h^N (f^{-1} dr^2 + r^2 d\Omega_{(n+1)}^2) \right), \\ \phi &= \frac{aN}{4} \log h, \quad A_{(p+1)} = -\sqrt{N \left(\frac{\gamma_0 + 1}{\gamma_0} \right)} (h^{-1} - 1) \star 1. \end{aligned} \quad (5.2.4)$$

Here we have applied a general boost u^a ($u_a u^a = -1$) to the solution in the $p + 1$ worldvolume directions labeled by $x^a = (t, x^i)$. The tensor $\Delta_{ab} = \eta_{ab} + u_a u_b$ is the projector onto the directions parallel to the brane but orthogonal to u^a , while $\star 1 = dx^0 \wedge \dots \wedge dx^p$ denotes the induced volume form on the brane geometry. The two functions f and h are given by,

$$f(r) \equiv 1 - \left(\frac{r_0}{r} \right)^n, \quad h(r) \equiv 1 + \gamma_0 \left(\frac{r_0}{r} \right)^n. \quad (5.2.5)$$

Here r_0 parametrizes the horizon radius and γ_0 parametrizes the charge of the solution.

According to fluid/gravity lore (review in Sec. 2.1) there is a one-to-one correspondence between the solutions to the EOMs (5.2.3) around the solution (5.2.4), and the relativistic Navier-Stokes equations,

$$\text{div} T = 0, \quad d \star j = 0. \quad (5.2.6)$$

Here $T = T^{ab}$ is the effective stress tensor and j is the effective current which are matched order by order in a relativistic fluid derivative expansion. The effective stress tensor and current encompass the asymptotic data of the perturbed solution and the correspondence allows one to reconstruct the full gravitational solution (to any given order in the derivatives) from these asymptotic tensor structures. At lowest order, i.e., no derivatives *and* flat intrinsic geometry, the correspondence is trivial as it is non-dynamical. Indeed, computing the asymptotic stress tensor and current of the solution (5.2.4), one obtains the stress tensor and current [107]

$$T_{ab} = \varrho u_a u_b + P \Delta_{ab}, \quad j = Q \star 1. \quad (5.2.7)$$

Here ϱ , P and Q denotes the energy (density), pressure and charge of the brane and can be computed from the Gibbs free energy G , which in turn is computed from the

on-shell action and takes the form

$$G = \text{Vol}(S^{n+1}) \left(\frac{n}{4\pi \mathcal{T}} \sqrt{\left(1 - \frac{\Phi^2}{N}\right)^N} \right)^n. \quad (5.2.8)$$

The temperature \mathcal{T} and the chemical potential Φ are the intensive thermodynamic variables which do not depend on Newton's constant and are easily written in terms of the parameters r_0 and γ_0 using standard methods,

$$\mathcal{T} = \frac{n}{4\pi r_0 \sqrt{(1 + \gamma_0)^N}}, \quad \Phi = \sqrt{\frac{N\gamma_0}{1 + \gamma_0}}. \quad (5.2.9)$$

Notice that the entropy s and charge Q are conjugate to \mathcal{T} and Φ and are computed from G in the usual way. The energy density ϱ and pressure P are then derived using the Gibbs-Duhem relation $w \equiv \varrho + P = \mathcal{T}s$ and the defining identity $G = -P - \Phi Q$. At lowest order and flat intrinsic geometry, the correspondence between fluid dynamics and gravity is therefore just a convenient repackaging of black hole thermodynamics in terms of a relativistic (perfect) fluid. However, note that if one abandons the requirement of flat intrinsic geometry, the statement becomes an equivalence between gravity and perfect fluid dynamics on a curved p -submanifold (known as *the blackfold approach*, see Sec.2.2 for a review), which is a non-trivial statement. In this work we keep the intrinsic geometry flat, or equivalently, we do not perturb the transverse sphere S^{n+1} .

5.2.1 The perturbative expansion

In order to carry out the perturbative procedure we proceed in the standard way. Here we will give a brief summary of the computation and refer to Appendix C for many of the details (also see the papers [32, 42, 43]). In order to ensure that the perturbative problem is well-posed, we need to cast the metric (5.2.4) into Eddington-Finkelstein (EF) form (i.e., a coordinate transformation $x^a \rightarrow \sigma^a(r)$ tailored so that $|dr| = 0$). In these coordinates the metric (5.2.4) takes the form

$$ds^2 = h^{-\frac{Nn}{p+n+1}} \left(\left(-f u_a u_b + \Delta_{ab} \right) d\sigma^a d\sigma^b - 2h^{\frac{N}{2}} u_a d\sigma^a dr + h^N r^2 d\Omega_{(n+1)}^2 \right). \quad (5.2.10)$$

Transforming the coordinates of course also induces a transformation of the gauge field, however, one can easily show that in the case of Schwarzschild \rightarrow EF coordinates the transformation of the gauge field can be undone by a suitable gauge transformation.

We therefore keep the form of the gauge field (5.2.4) consistent with our gauge choice introduced below. According to the ideas of fluid/gravity outlined above, the solution (5.2.10) (along with the associated matter fields) is part of a larger class of solutions ds_f^2 for which the parameters u^a , r_0 and γ_0 (collectively denoted by $\xi = (u^a, r_0, \gamma_0)$) are worldvolume fluctuating functions. This solution, which reduces to (5.2.10) for constant u^a , r_0 and γ_0 , is in general unknown, but can be probed perturbatively in a derivative expansion. Therefore for long-wavelength perturbations,

$$ds_f^2 = ds^2 + ds_\partial^2 + \mathcal{O}(\partial^2), \quad A_f = A + A_\partial + \mathcal{O}(\partial^2), \quad \phi_f = \phi + \phi_\partial + \mathcal{O}(\partial^2). \quad (5.2.11)$$

Here ds^2 is the geometry (5.2.10) expanded to first order in worldvolume derivatives and ds_∂^2 denotes the first-order correction coming from the full solution ds_f^2 (and similarly for the matter fields). The main purpose of this section is to compute the first-order expansion of the full solution and extract the first-order effective currents. The EOMs exhibit a large gauge redundancy. In order to simplify the computations it is convenient to choose a (consistent) gauge where the transverse components of (A_∂) are taken to zero and furthermore $(g_\partial)_{rr} = 0$, $(g_\partial)_{\Omega\Omega} = 0$. The latter gauge choice allows us to reduce over the transverse sphere S^{n+1} , effectively leaving us with a $p + 2$ dimensional problem. Notice that although the transverse S^{n+1} drops out of the problem, the parameter n still plays an important rôle as it will enter the various coefficients in the resulting set of equations. Choosing the appropriate ansatz for the perturbations (collectively denoted by $\psi_\partial = (g_\partial, A_\partial, \phi_\partial)$) and plugging them into the EOMs (5.2.3) produces two sets of qualitatively different equations, schematically of the form

$$\text{Constraint: } \mathbb{C}_\partial \partial\xi + \mathcal{O}(\partial^2) = 0, \quad \text{Dynamical: } \mathbb{L}_r^{(1)} \mathbb{L}_r^{(2)} \psi_\partial = s_\partial(r) + \mathcal{O}(\partial^2). \quad (5.2.12)$$

Here \mathbb{C}_∂ is an operator acting on the derivatives of the intrinsic fields ξ and $L_r^{(1)}$ and $L_r^{(2)}$ are two first-order linear differential operators acting on the perturbations ψ_∂ as a function of the radial coordinate r (and only r) and finally $s_\partial(r)$ is a source term (which is a rational function in r whose coefficients depend on $\partial\xi$). We note that in order to obtain the dynamical equations one has to explicitly use the constraint equations. The constraint equations are independent of the radial coordinate and, as the name suggests, put constraints on (i.e., relations between) the derivatives of the intrinsic fields. As expected, the constraint equations are found to be equivalent to the conservation equations of the leading order perfect fluid stress tensor and current (5.2.7). Notice that the conservation of j takes the form $\partial_a Q = 0$, which just expresses

that the charge Q is non-fluctuating along the worldvolume. Locally the inverses of the differential operators $\mathbb{L}_r^{(1)}$ and $\mathbb{L}_r^{(2)}$ exist and the formal solution to the dynamical equations reads

$$\psi_{\partial} = \left(\mathbb{L}_r^{(2)}\right)^{-1} \left(\mathbb{L}_r^{(1)}\right)^{-2} s_{\partial} + \left(\mathbb{L}_r^{(2)}\right)^{-1} h_1 + h_2 . \quad (5.2.13)$$

Here h_1 and h_2 denote functions in the kernel of $\mathbb{L}_r^{(1)}$ and $\mathbb{L}_r^{(2)}$, respectively. We note that the inverse operators of $\mathbb{L}_r^{(1)}$ and $\mathbb{L}_r^{(2)}$ in general involve various integrations which when evaluated on s_{∂} are quite complicated leading to various types of hypergeometric functions. The local decomposition (5.2.13) is of course not unique, however, if we require the inverse of $\mathbb{L}_r^{(1)}$ to exist globally (in particular at $r = r_0$) or equivalently require horizon regularity, the homogeneous solution h_1 is forced to vanish leaving only h_2 , which is then fixed by the boundary conditions and choice of fluid frame. Indeed, a subset of the freedom in the homogeneous solution h_2 comes directly from the seed solution (5.2.10) and can be generated by $\mathcal{O}(\partial)$ shifts $r_0 \rightarrow r_0 + \delta r_0$, $\gamma_0 \rightarrow \gamma_0 + \delta \gamma_0$ and $u^a \rightarrow u^a + \delta u^a$ (along with gauge transformations of A_f). Such shifts of course map to new (regular) asymptotically flat solutions which differ from (5.2.10) by $\mathcal{O}(\partial)$. From a relativistic fluid point of view, this freedom is expected and corresponds to $\mathcal{O}(\partial)$ redefinitions of the temperature, chemical potential and fluid velocity. In order to fix the gauge (the fluid frame), we require that the first-order solution reduces to (5.2.10) when the fluctuations vanish, which in turn corresponds to choosing the Landau frame on the fluid side. The remaining freedom in h_2 parameterizes non-renormalizable modes which we require to vanish by virtue of asymptotic flatness.⁴ In this way the freedom in the homogeneous solution h_2 can be completely removed and we obtain the full solution to first order in the derivative expansion.

5.2.2 Transport coefficients

Having obtained the first-order regular asymptotically flat corrected solution and reexpressing it in Schwarzschild coordinates, it is straightforward to compute the induced effective stress tensor using familiar techniques and extract the first-order transport coefficients. By direct computation we obtain the following effective stress tensor

$$T_{ab} = \varrho u_a u_b + P \Delta_{ab} + \Pi_{ab}^{(1)} + \mathcal{O}(\partial^2) \quad \text{with} \quad \Pi_{ab}^{(1)} = -2\eta\sigma_{ab} - \zeta\vartheta\Delta_{ab} . \quad (5.2.14)$$

⁴For $n = 1$ one needs to fix some additional gauge freedom in $g_{\partial r i}$ in order to ensure asymptotically flatness.

Here σ_{ab} and ϑ are the (fluid) shear and expansion of the congruences u^a , respectively, and the coefficients η and ζ are the corresponding shear and bulk viscosity.⁵ They explicitly evaluate to

$$\eta = \frac{s}{4\pi}, \quad \frac{\zeta}{\eta} = 2 \left(\frac{1}{p} + \frac{C - 2n}{n + 1 + C\gamma_0} \gamma_0 + \frac{(n + 1)(1 + (C - 2n)\gamma_0)}{(n + 1 + C\gamma_0)^2} \right), \quad (5.2.15)$$

where we have defined the constant $C \equiv 2 - n(N - 2)$. For fixed r_0 , the viscosities are parametrized by the charge parameter γ_0 and the parameter N . The neutral limit can be obtained independently by taking either of the parameters to zero. Indeed, for large values of the dilaton coupling the dynamics of the brane effectively reduces to that of the neutral black p -brane (we have checked that our results reduce to those obtained in the neutral limit [42]). We note that the shear viscosity increases with the charge while bulk-to-shear viscosity ratio decreases as charge is added to the brane (for fixed r_0). As expected the gravitational solution saturates the hydrodynamic bound $\eta/s \geq 1/4\pi$ [110, 116]. We also note that the charge current $j = Q \star 1$ does not receive any first-order contribution. This is of course just a reflection of current conservation in the effective theory. Finally, we have checked that our results agree with those obtained for the D3-brane in Ref. [44] (here $p = 3$, $D = n + p + 3 = 10$, $a = 0$).⁶

5.2.3 Dynamical stability

With the fluid transport determined, we can now address the stability properties of fundamentally charged branes by analyzing the response of their corresponding effective fluids under small long-wavelength perturbations. The dynamics of a charged fluid is governed by the worldvolume conservation equations given by Eq. (5.2.6). Here, we are interested in the case where the stress tensor T takes the form of a general dissipative fluid to first order (5.2.14). For the sound mode(s) we write the dispersion relation, valid up to second order in the wave vector $k = \sqrt{k_i k^i}$,⁷ as

$$\omega(k) = \pm c_s k + i \mathbf{a}_s k^2. \quad (5.2.16)$$

Here c_s is the speed of sound given by $c_s^2 = \partial P / \partial \rho$, where the thermodynamical quantity kept fixed when taking the derivative depends on the specific type of charged fluid in

⁵Notice that for $p = 1$ the shear tensor vanishes.

⁶One has to employ the limit $R_c \rightarrow 1$ and make use of the identifications $r_-^4 = r_0^4 \gamma_0$, $r_+^4 = r_0^4 (1 + \gamma_0)$ and $\gamma_0 = (1 - \delta_\epsilon) / \delta_\epsilon$.

⁷Here the relativistic wave vector is $k^a = \{\omega, k^i\}$.

question. The attenuation coefficient \mathbf{a}_s controls the dampening of the longitudinal sound mode and is determined by the first-order transport coefficients (5.2.15). In order for the fluid to be dynamically stable we must require that the speed of sound squared c_s^2 and the attenuation coefficient \mathbf{a}_s are both positive. In addition to the sound mode, the fluid also exhibits a transverse shear mode,

$$\omega(k) = \frac{i\eta}{w} k^2 \quad , \quad (5.2.17)$$

which is stable provided that $\eta > 0$.

Now, for fundamentally charged p -branes the charge is not allowed to redistribute itself on the worldvolume of the brane, since it is conserved along all directions as noted previously. This means that the dynamics of the effective fluid will be reminiscent of that of a neutral brane, since the charge only plays a rôle in the equation of state. In particular, the leading order stability is solely determined by the sound mode (5.2.16). The system will therefore be stable to linear order in k as long as the speed of sound squared,

$$c_s^2 = \left(\frac{\partial P}{\partial \varrho} \right)_{Q_p} = - \frac{1 + (2 - nN)\gamma_0}{n + 1 + C\gamma_0} \quad , \quad (5.2.18)$$

is positive. We note that in the limit of vanishing charge ($\gamma_0 \rightarrow 0$) we recover $c_s^2 = -1/(n+1)$ [42] signifying that the neutral brane exhibits a Gregory-Laflamme (GL) instability [21, 22]. However, for finite γ_0 we find, as in Ref. [107], that there exists a threshold,

$$\bar{\gamma}_0 = \frac{1}{nN - 2} \quad , \quad (5.2.19)$$

above which the black brane is stable under long-wavelength perturbations to linear order. For fixed temperature, the threshold value $\bar{\gamma}_0$ is precisely where the brane configuration reaches its maximal charge. As illustrated in Fig. 5.1, this point exactly corresponds to a transition point between an unstable branch and a stable branch of configurations with the neutral brane configuration located at the endpoint $\gamma_0 \rightarrow 0$ of the unstable branch. For sufficiently large dilaton coupling all fundamentally charged p -branes are therefore unstable, since they approximate the neutral brane. On the other hand, the stable branch connects with the extremal limit and since γ_0 measures the ratio between local electrostatic energy and thermal energy of the fluid, the stable regime is where the electrostatic energy is dominant. Notice that the limit $\gamma_0 \rightarrow \infty$ corresponds to flat space. However, it is not entirely clear if any of the hydrodynamic interpretation survives in the strict limit. The threshold value does not exist in instances

Brane	a	$\bar{\gamma}_0$	c_s^2	$w\mathbf{a}_s/\eta$
Dp	$\frac{3-p}{2}$	$\frac{1}{5-p}$	$\frac{(5-p)\gamma_0-1}{8-p+(9-p)\gamma_0}$	$\frac{72-17p+p^2+8(8-p)\gamma_0+4(9-p)\gamma_0^2}{(8-p+(9-p)\gamma_0)^2}$
M2	0	$\frac{1}{4}$	$\frac{4\gamma_0-1}{7+8\gamma_0}$	$\frac{1}{2} \left(1 + \frac{63}{(7+8\gamma_0)^2} \right)$
M5	0	1	$\frac{\gamma_0-1}{4+5\gamma_0}$	$\frac{4}{5} \left(1 + \frac{9}{(4+5\gamma_0)^2} \right)$

Table 5.1 The expansion coefficients of the sound mode (5.2.16) for the p -branes of ten and eleven dimensional supergravity ($N = 1$). For a sufficiently large value of γ_0 the threshold value $\bar{\gamma}_0$ is exceeded and the fundamentally charged branes are stable. We note that the threshold value in ten dimensional supergravity increases with the spatial dimension and that black NS/Dp-branes are always unstable for $p \geq 5$. It is also worth noting that the values for the D1 and D4 are equivalent to those of the M2 and M5, respectively, due to Type II A \leftrightarrow M-theory relation. Finally, the values for the fundamental string and NS5 are equivalent to those of the D1 and D5, respectively, as N is invariant under $a \rightarrow -a$.

where $nN < 2$, since γ_0 is a non-negative parameter. In those cases, the speed of sound is imaginary for all values of γ_0 . Finally, for the branes in ten and eleven dimensional supergravity we have listed several values of interest in Table 5.1. In particular, we note that the threshold $\bar{\gamma}_0$ does not exist for $p = 5, 6$ in $D = 10$. This is in agreement with the expectation that the supergravity descriptions of D/NS/M-branes are stable with the exception of the D5, D6 and NS5 brane [21, 22, 107, 113].

We can now proceed by refining the analysis to quadratic order in k by including the second-order term in the sound mode. As explained, in the absence of charge diffusion, the attenuation coefficient will take the exact same form as a neutral fluid, hence

$$\mathbf{a}_s = \frac{1}{w} \left(\left(1 - \frac{1}{p} \right) \eta + \frac{\zeta}{2} \right) . \quad (5.2.20)$$

The effects of the fluid carrying charge therefore only appears through the explicit dependence on Q in the shear and bulk viscosities given by Eq. (5.2.15). When the threshold (5.2.19) exists, we find, as shown in Fig. 5.1, that the attenuation coefficient is positive for both branches of configurations. The stability is therefore fully determined by the linear order, i.e., by the speed of sound. This is in contrast to configurations with smeared charges where the attenuation coefficient plays an important rôle for the stability properties of the effective fluid as we shall see in Sec. 5.3.2. When the

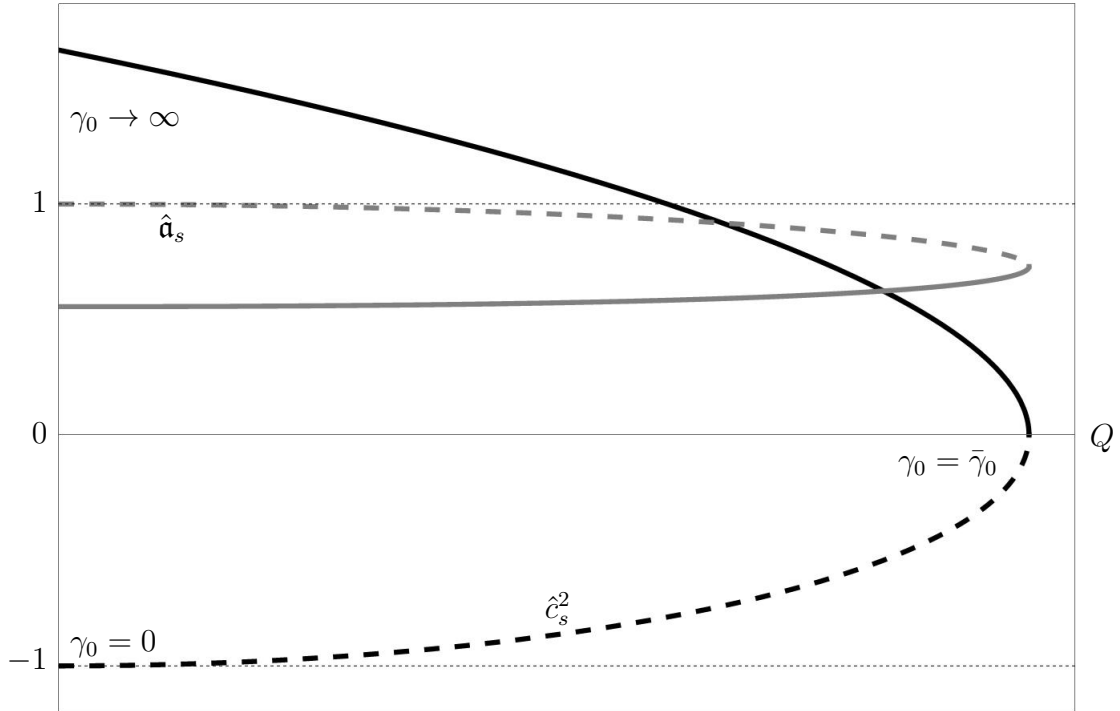


Fig. 5.1 The qualitative behavior of the coefficients of the sound mode given by Eq. (5.2.16) as a function of the charge Q for a fixed temperature \mathcal{T} . The quantities \hat{c}_s^2 and \hat{a}_s correspond to the speed of sound squared and the attenuation coefficient normalized with respect to their neutral values, respectively. There is one unstable branch connected to the neutral limit ($\gamma_0 \rightarrow 0$) plotted with dashed lines and one stable branch connected to the extremal limit where both coefficients are positive. The stable branch is reached exactly when the charge parameter γ_0 exceeds the threshold $\bar{\gamma}_0$ given by Eq. (5.2.19). This point $\bar{\gamma}_0$ corresponds to the maximal charge of the brane configuration for a given fixed temperature.

threshold exists, the fundamentally charged p -brane is therefore dynamically stable for sufficiently large charge parameter γ_0 at least to next-to-leading order.

An occurrence of a dynamical GL-like instability is conjectured to be intercorrelated with a thermodynamical stability [113, 128, 129] *viz.* the correlated stability conjecture. It is therefore interesting to relate the above dynamical analysis to the thermodynamic properties of the effective fluid. The condition for thermodynamic stability is computed in the canonical ensemble, since the charge is fixed in the system and thus only requires positivity of the specific heat c_{Q_p} . Using the thermodynamic quantities (5.2.9) and the expression for the speed of sound (5.2.18) one can show that the point where the specific heat becomes positive overlaps precisely with the threshold value given by Eq. (5.2.19), *i.e.*, the configuration with the maximally allowed charge (for a given

temperature). Indeed, as pointed out in Ref. [107], there is a direct relation between the speed of sound and the specific heat c_{Q_p} at fixed charge given by

$$c_s^2 = \left(\frac{\partial P}{\partial \varrho} \right)_{Q_p} = s \left(\frac{\partial \mathcal{T}}{\partial \varrho} \right)_{Q_p} = \frac{s}{c_{Q_p}} . \quad (5.2.21)$$

For this system, we therefore find that the dynamical stability is in agreement with the correlated stability conjecture. Although, our results are only valid to first order we expect the statement to hold to all orders.

5.3 Hydrodynamics of dilatonic Maxwell charged branes

In this section, we write down the first-order effective hydrodynamic expansion for the p -branes of the theory (5.2.1) with $q = 0$ (Einstein-Maxwell-Dilaton (EMD) theory). These results provide the dilaton generalization of the results originally presented in Ref. [43]. In terms of the parameter N , the dilaton coupling a now takes the form,

$$a^2 = \frac{4}{N} - 2 \left(\frac{D-3}{D-2} \right) . \quad (5.3.1)$$

In particular, for the parameters relevant for type IIA supergravity, we have $a = 3/2$, and the action (5.2.1) is that appropriate for describing smeared configurations of D0-branes. The leading order solution is given by

$$\begin{aligned} ds^2 &= h^{-\left(\frac{n+p}{n+p+1}\right)N} \left(-f u_a u_b dx^a dx^b + h^N \left(\Delta_{ab} dx^a dx^b + f^{-1} dr^2 + r^2 d\Omega_{(n+1)}^2 \right) \right) , \\ \phi &= \frac{aN}{4} \log h , \quad A_{(1)} = \sqrt{N \left(\frac{\gamma_0 + 1}{\gamma_0} \right)} \left(h^{-1} - 1 \right) u_a dx^a . \end{aligned} \quad (5.3.2)$$

The effective stress tensor and Maxwell current are computed from the asymptotics of the solution and take the perfect fluid form,

$$T_{ab} = \varrho u_a u_b + P \Delta_{ab} , \quad j_a = \mathcal{Q} u_a . \quad (5.3.3)$$

Here the energy density ϱ , pressure P and charge density \mathcal{Q} are obtained from the free energy in the usual way. Direct computation of the on-shell action reveals that the free

energy G again takes the form (5.2.8). Moreover, the two parameters r_0 and γ_0 are related to the temperature \mathcal{T} and chemical potential Φ as in Eq. (5.2.9). However, the Gibbs-Duhem relation now takes the form $w \equiv \varrho + P = \mathcal{T}s + \Phi\mathcal{Q}$. Here we have used a calligraphed \mathcal{Q} to denote the monopole charge density in order to distinguish it from the fundamental dipole type charge Q considered in the previous section.

5.3.1 Transport coefficients

Carrying out the perturbative computation of the first-order corrected fields and the corresponding effective currents follows the procedure explained in Sec. 5.2 (see App. C for many of the details and e.g. Ref. [43]). The most important difference between the two computations consists of the existence of an additional $\text{SO}(p)$ vector (dynamical) equation in the Maxwell case. This is in accordance with the fact that a worldvolume one-form potential contains p more degrees of freedom than a top-form potential. The constraint equations coming from Einstein's equations take the same form as before but the constraint equation deriving from the Maxwell equation is shown to be equivalent to current conservation, $\partial_a j^a = 0$. This allows for fluid dynamical fluctuations in the charge density \mathcal{Q} , which in turn shows up as a new charge diffusion transport coefficient in the effective theory. The most general first-order derivative corrected effective current, consistent with the second law of thermodynamics, takes the form (here written in the Landau frame)

$$j^a = \mathcal{Q}u^a + \Upsilon_{(1)}^a + \mathcal{O}(\partial^2) \quad \text{with} \quad \Upsilon_{(1)}^a = -\mathfrak{D} \left(\frac{\mathcal{Q}\mathcal{T}}{w} \right)^2 \Delta^{ab} \partial_a \left(\frac{\Phi}{\mathcal{T}} \right). \quad (5.3.4)$$

Here \mathfrak{D} is the transport coefficient associated with diffusion (appropriately normalized).

Without further ado, we now present our results for the transport coefficients. The shear and bulk viscosities are given by

$$\eta = \frac{s}{4\pi}, \quad \frac{\zeta}{\eta} = \frac{2}{p} + \frac{2}{C} \left(2 - N + \frac{(n+1)N}{(n+1+C\gamma_0)^2} \right), \quad (5.3.5)$$

here C is the constant introduced below Eq. (5.2.15). Again, for fixed r_0 , the viscosities are parametrized by γ_0 and N and they reduce to the values of the neutral limit if either of the parameters are taken to zero. As expected, the shear viscosity saturates the bound $\eta/s \geq 1/4\pi$. The diffusion constant \mathfrak{D} , associated with the effective current

(Eq. (5.3.4)), is determined to

$$\frac{\mathfrak{D}}{\eta} = \frac{4\pi r_0(1 + \gamma_0)}{nN\gamma_0\sqrt{(1 + \gamma_0)^N}} \quad , \quad (5.3.6)$$

As is straightforward to check, these results agree with those of [43] in the limit where the dilaton coupling goes to zero, or equivalently, $N \rightarrow \frac{2(D-2)}{D-3}$.

5.3.2 Dynamical stability

We now analyze the dispersion relations of the fluid associated to the Maxwell charged branes. In contrast to the fundamentally charged branes, discussed previously, the Maxwell charged branes exhibit charge diffusion which significantly changes the effective dynamics. Most notably, since the charge density can redistribute over the worldvolume, this gives rise to an additional longitudinal mode with the following dispersion relation,

$$\omega(k) = i\mathfrak{a}_{\mathfrak{D}}k^2 \quad . \quad (5.3.7)$$

This mode is associated to the attenuation of the (long-wavelength) diffusion of charge and is a first-order derivative effect. The existence of this charge diffusion mode explicitly means that the stability of the system to second order in k is not only determined by the attenuation coefficient \mathfrak{a}_s of the sound mode (5.2.16), but also by the attenuation coefficient $\mathfrak{a}_{\mathfrak{D}}$. In order for the system to be stable to second order one must therefore require both to be positive. As before this system also exhibits a transverse shear mode given by Eq. (5.2.17). However, since the shear viscosity is positive, this mode does not play any rôle for the stability properties of the fluid.

To linear order in k , the stability of the Maxwell system is, similarly to the fundamentally charged brane, solely determined by the sound mode. More precisely, it is dictated by the speed of sound squared which for the Maxwell system is given by

$$c_s^2 = \left(\frac{\partial P}{\partial \varrho} \right)_{\frac{s}{\mathfrak{D}}} = - \frac{1 + (2 - N)\gamma_0}{(1 + \gamma_0 N)(n + 1 + C\gamma_0)} \quad . \quad (5.3.8)$$

In the limit of vanishing charge ($\gamma_0 \rightarrow 0$) we again recover the neutral value for the speed of sound. For finite γ_0 we find the threshold,

$$\bar{\gamma}_0 = \frac{1}{N - 2} \quad , \quad (5.3.9)$$

Brane	a	$\bar{\gamma}_0$	c_s^2	$w\mathbf{a}_s/\eta$	$w\mathbf{a}_\mathfrak{D}/\eta$
D0	$\frac{3}{2}$	-1	$-\frac{1}{8-p+(9-p)\gamma_0}$	$(9-p)(8-p)(\gamma_0+1)^2 c_s^4$	1

Table 5.2 Coefficients of the longitudinal sound and diffusion mode for the black D0-brane smeared in $p \geq 1$ directions. Note that the first-order coefficient (speed of sound squared) is negative whereas both of the second-order attenuation coefficients are positive.

above which the Maxwell charged black brane is stable to leading order. Note that the threshold only exists for $N > 2$, or equivalently, when the dilaton coupling a is sufficiently small.⁸ The qualitative behavior of the speed of sound (for $N > 2$) is illustrated in Fig. 5.2. In particular, we find that there exist two branches of brane configurations for the same charge density; an unstable branch ($\gamma_0 < \bar{\gamma}_0$) connected to the neutral brane configuration and a stable branch ($\gamma_0 > \bar{\gamma}_0$) connected to the extremal brane configuration. However, in contrast to the fundamentally charged brane, the merging point (defined by $\bar{\gamma}_0$) does not coincide with the maximal charge configuration. On the other hand, if the threshold does not exist, i.e., $N < 2$, the speed of sound is imaginary for all charge densities. The system is thus unstable independent of the charge. This instability is in accordance with the one observed for configurations of smeared D0-branes ($N = 1$) [114, 115]. In Table 5.2, we list the values of interest connected to this special case.

We now address the stability to quadratic order in k . We therefore consider the two attenuation coefficients \mathbf{a}_s and $\mathbf{a}_\mathfrak{D}$ associated to the sound and diffusion mode, respectively. For the sound mode we find, in contrast to Eq. (5.2.20), the following modification due to the presence of charge diffusion,

$$\mathbf{a}_s = \frac{1}{w} \left(\left(1 - \frac{1}{p}\right) \eta + \frac{\zeta}{2} + \frac{2}{\mathcal{T}} \frac{\mathcal{Q}^2}{c_s^2} \left(\frac{\mathcal{Q}^2}{w\Phi} \frac{c}{C_\mathcal{Q}} \right)^2 \mathfrak{D} \right), \quad (5.3.10)$$

where we have introduced the specific heat capacity $C_\mathcal{Q}$ and the (inverse) isothermal permittivity c given in Eq. (5.3.12). For the diffusion mode (5.3.7), we find

$$\mathbf{a}_\mathfrak{D} = \frac{\mathcal{Q}^2}{c_s^2 w} \frac{c}{C_\mathcal{Q}} \mathfrak{D}. \quad (5.3.11)$$

⁸Explicitly the dilaton coupling squared has to be smaller than $\bar{a}^2 = \frac{2}{n+p+1}$.

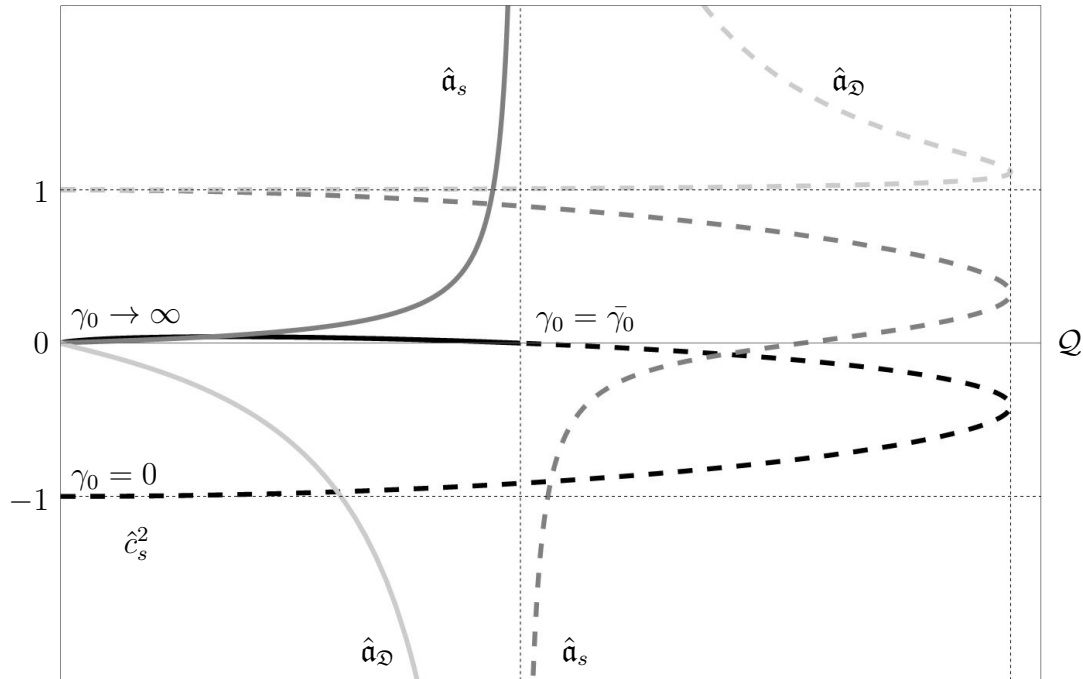


Fig. 5.2 The qualitative behavior of the coefficients of the longitudinal modes given by Eq. (5.2.16) and Eq. (5.3.7) as a function of the charge density \mathcal{Q} for fixed local temperature \mathcal{T} . The quantities \hat{c}_s^2 , $\hat{\mathbf{a}}_s$ and $\hat{\mathbf{a}}_{\mathcal{D}}$ are given by the Eqs. (5.3.8), (5.3.10) and (5.3.11) normalized with respect to their individual neutral values. Dashed lines are for $\gamma_0 < \bar{\gamma}_0$ while filled lines are for $\gamma_0 > \bar{\gamma}_0$. We observe that no region exists where all three quantities are positive at the same charge density \mathcal{Q} . Furthermore, the attenuation coefficients both show a hyperbolic behavior at the threshold $\bar{\gamma}_0$ indicated by a vertical dashed line. Note that due to the choice of normalization of the diffusion coefficient in Eq. (5.3.4), the attenuation coefficient $\bar{\mathbf{a}}_{\mathcal{D}}$ takes a fictitious finite value in the neutral limit.

Assuming that $N > 2$, the attenuation coefficients exhibit a hyperbolic divergence around $\bar{\gamma}_0$. We refer to Fig. 5.2, where we have plotted a generic case of the two longitudinal modes. This divergent behavior at $\bar{\gamma}_0$ is very different compared to the continuous behavior observed for \mathbf{a}_s in Sec. 5.2.3 (see Fig. 5.1). Indeed, it seems that the linearized analysis breaks down at the threshold $\bar{\gamma}_0$. However, besides this new feature we still find that both the speed of sound squared and the attenuation coefficient \mathbf{a}_s are positive when γ_0 surpasses the threshold. The stability of the sound mode is therefore, similarly to the fundamentally charged branes, solely dictated by the speed of sound. In contrast to the attenuation coefficient of the sound mode, it is quite apparent from Eq. (5.3.11), that the hyperbolic feature of the diffusion attenuation coefficient

is simply dictated by the inverse speed of sound. We therefore find that the diffusion mode has exactly the complementary behavior of the sound mode, that is, when the sound mode is stable the charge diffusion mode is unstable and vice versa. The Maxwell charged brane configurations therefore suffer a GL instability for all charge densities.

Finally, we check whether the dynamical GL-like instability observed above is connected with the thermodynamic stability of the system as predicted by the correlated stability conjecture. The conditions for thermodynamic stability of the Maxwell black brane are computed in the grand canonical ensemble since charge is allowed to redistribute itself in the directions of the brane. This exactly leads to the requirement of positive specific heat capacity and positive (inverse) isothermal permittivity [130, 131],

$$\begin{aligned} C_{\mathcal{Q}} &= \left(\frac{\partial \varrho}{\partial \mathcal{T}} \right)_{\mathcal{Q}} = \left(\frac{n+1+C\gamma_0}{(nN-2)\gamma_0-1} \right) s \quad , \\ c &= \left(\frac{\partial \Phi}{\partial \mathcal{Q}} \right)_{\mathcal{T}} = \left(\frac{1}{(\gamma_0+1)(1-(nN-2)\gamma_0)} \right) \frac{1}{s\mathcal{T}} \quad . \end{aligned} \tag{5.3.12}$$

It is straightforward to see that these two conditions $C_{\mathcal{Q}} > 0$ and $c > 0$ are complementary and can never be satisfied. Indeed, the two quantities exchange signs at $\gamma_0 = 1/(nN-2)$. Comparing with the dynamical analysis above, we observe that it is not sufficient to consider the dispersion relations to leading order, i.e., only considering the speed of sound c_s , since it predicts the system to be stable above the threshold (5.3.9). However, when we include first-order corrections (the attenuation terms \mathbf{a}_s and $\mathbf{a}_{\mathcal{Q}}$), we exactly identify a similar complementary behavior between the sound mode and the diffusion mode. We therefore find that the dynamical and thermodynamical analysis predict a similar behavior for the system, but point out that while the threshold value for the above thermodynamic quantities exactly corresponds to the point where the configuration obtains maximal charge density, the threshold (5.3.9) for the dynamical stability corresponds to a smaller charge density as noted above (with the coincidentally exception of $n = 1$). A similar effect was also observed in [43]. This can seem puzzling at first, but we emphasize that it is *not* in contradiction with the correlated stability conjecture.

5.3.3 A check: Mapping to AdS

In the previous section we have analyzed the hydrodynamic behavior of dilatonic Maxwell charged brane solutions. In this section, we present a non-trivial check of our results with Ref. [67] using a modified version of the AdS/Ricci-flat correspondence [52,

53] which in its original form provides a map relating a certain class of asymptotically locally AdS solutions to Ricci-flat solutions. Starting with pure Einstein gravity, we modify the map by performing a Kaluza-Klein (KK) reduction. This gives us the possibility to connect with EMD theory, which is a subset of the class of theories (5.2.1). From this starting point, we continue as Ref. [52, 53] by performing a diagonal reduction and connect the reduced theory (after an appropriate analytic continuation) to theories which admit asymptotically local AdS solutions. With this modification in hand, we can map the first-order corrected solutions of the previous section to their corresponding class of asymptotically locally AdS spacetimes obtained in Ref. [67].

We begin by performing a KK reduction of the Einstein-Hilbert action. This takes us to EMD theory and connects with the action (5.2.1) in $(n + p + 3)$ -dimensions with $q = 0$ and fixes the coupling constant a to

$$a^2 = \frac{2(\alpha + 1)}{\alpha} , \quad (5.3.13)$$

with $\alpha \equiv n + p + 1$. We then perform a diagonal reduction (over the sphere S^{n+1}) with metric ansatz

$$ds^2 = e^{\frac{2}{\alpha}\chi(x,r)} \left(ds_{p+2}^2(x,r) + d\Omega_{(n+1)}^2 \right) , \quad (5.3.14)$$

where the $(p + 2)$ -dimensional reduced metric, the Maxwell field, the dilaton field, and the scalar field χ are independent of the $(n + 1)$ -directions of sphere. Note that this ansatz includes the solutions given by Eq. (5.3.2). The action of the lower dimensional theory takes the form

$$\begin{aligned} \mathcal{I} = \text{Vol}(S^{n+1}) \int_{p+2} e^\chi & \left(\mathcal{R} \star 1 + \star n(n+1) - \frac{1}{\alpha(\alpha+1)} d\phi \wedge \star d\phi \right. \\ & \left. + \left(\frac{\alpha+1}{\alpha} \right) d\chi \wedge \star d\chi - \frac{1}{2} e^{-\frac{2}{\alpha}(\chi+\phi)} F_2 \wedge \star F_2 \right) , \end{aligned} \quad (5.3.15)$$

where \mathcal{R} is the $(p + 2)$ -dimensional Ricci scalar and F_2 is the field strength of the KK gauge field. Note that the second term comes from the integration over the sphere and that we have performed a suitable Weyl rescaling

$$\phi^2 \rightarrow \frac{1}{2\alpha(\alpha+1)} \phi^2 . \quad (5.3.16)$$

To establish the map, we now consider Einstein gravity with a negative cosmological constant $\Lambda = -d(d-1)/2$ in $(d+1)$ -dimensions,⁹

$$I_\Lambda = \int_{d+1} \left(R_\Lambda - 2\Lambda \right) * 1 \quad . \quad (5.3.17)$$

We compactify the theory on a $\beta \equiv (d-p-1)$ -dimensional torus using the following ansatz

$$ds_\Lambda^2 = ds_{p+2}^2(x, r) + e^{2\frac{\phi(x,r)+\chi(x,r)}{\beta}} \left(dy - A_a(x, r) dx^a \right)^2 + e^{\frac{2}{\beta}(\chi(x,r) - \frac{\phi(x,r)}{\beta-1})} d\ell_{\beta-1}^2 \quad . \quad (5.3.18)$$

Here y is a distinguished direction along the torus \mathbb{T}^β and $d\ell_{\beta-1}^2$ denotes the line element of the remaining part of the torus. Using the reduction ansatz (5.3.18), the reduced action is (dropping a total derivative)

$$\begin{aligned} \mathcal{I}_\Lambda = \text{Vol}(\mathbb{T}^\beta) \int_{p+2} e^\chi \left(\mathcal{R} * 1 + *d(d-1) - \frac{1}{\beta(\beta-1)} d\phi \wedge *d\phi \right. \\ \left. + \left(\frac{\beta-1}{\beta} \right) d\chi \wedge *d\chi - \frac{1}{2} e^{2\frac{\phi+\chi}{\beta}} F_2 \wedge *F_2 \right) \quad , \quad (5.3.19) \end{aligned}$$

with $F_2 = dA$. Suppose that we now have access to closed analytic expressions of solutions to the reduced action (5.3.19) for any positive integer d . It then makes sense to extend the domain via an analytic continuation [54] of the parameter d . In this way, we can view solutions as a function of d which now can take any real value. In particular, it makes sense to consider solutions for negative values of d . The same reasoning can be applied to the action (5.3.15) where the solutions are viewed as functions of n . Direct inspection of the two actions (5.3.19) and (5.3.15) shows that they are proportional under the analytic continuation $d \leftrightarrow -n$,

$$\text{Vol}(S^{n+1}) \mathcal{I}_\Lambda \leftrightarrow \text{Vol}(\mathbb{T}^\beta) \mathcal{I} \quad . \quad (5.3.20)$$

This implies that we can obtain solutions to the reduced theory (5.3.15) by a simple reflection of the dimensionality parameter starting from the reduced theory (5.3.19) and vice versa. In this way, knowing solutions of the form (5.3.14) of the higher dimensional theory (for any $n \in \mathbb{N}$) allows us to consistently uplift to solutions of the form (5.3.18) (for any $d-1 \in \mathbb{N}$) using the connection between the two reduced theories (5.3.20) and vice versa.

⁹Working in units where the AdS radius is set to unity.

Now, with the modified version of the mapping in hand, we can relate brane solutions of EMD theory + hydro to those of AdS_{d+1} compactified on $(d - p - 1)$ flat directions.¹⁰ The effective hydrodynamics of branes in AdS_{d+1} compactified on a torus (as described above) was worked out in the Ref. [67] directly from the AdS results in general $(d + 1)$ dimensions [119]. We can thus map the solutions of the reduced AdS theory to solutions of EMD considered in this work and in turn compare the transport coefficients. This provides us with a non-trivial cross-check of our results for the particular value (5.3.13) of the dilaton coupling. Going through this exercise, we find a perfect agreement between the transport coefficients (Eqs. (5.3.5)-(5.3.6) and Eqs. (3.4.38)-(3.4.40) of [67], respectively.¹¹

Finally, we can in a similar way as in Sec. 5.3.2 check the dynamical features of the asymptotically local AdS solutions explicitly by computing the dispersion relations of the associated fluid. In contrast to the asymptotically flat solutions one finds that all the coefficients of both the sound mode (5.2.16) and the diffusion mode (5.3.7) are continuous and positive for all values of the charge density. We therefore find that no threshold value exists for the particular dilaton coupling (5.3.13) and furthermore that the hyperbolic behavior has been resolved through the analytic continuation (compare e.g. with Fig. 5.2). The solutions are thus stable to first order which is perhaps not too surprising, since they originate from stable neutral AdS branes [132] through consistent reductions. In addition, one can easily check that they are also thermodynamically stable by computing the specific heat and isothermal permittivity (see Eq. (5.3.12)) and checking explicitly that they are positive for all values of the charge.

5.4 Discussion

We have performed the perturbative procedure which captures the hydrodynamic sector of fundamentally charged (dilaton) black branes and branes with Maxwell charge smeared over their worldvolume. The main result of this section are the first-order transport coefficients that determine the dissipative behavior of the effective fluids. They are listed in Eq. (5.2.15) and Eqs. (5.3.5)-(5.3.6). Furthermore, for each class of branes we have obtained the dispersion relations of the effective fluids for which we refer to Fig. 5.1 and 5.2. As explained in the main text, many of our results apply to

¹⁰We note that care must be taken for fixing $n = 1$ after the analytic continuation, since while this might still be some perturbed solution it will not correspond to the asymptotically flat perturbed solution that we have been considering. In a similar way one should take care from the reversed perspective if fixing $d = 2$.

¹¹Note, that [67] uses a different normalization of the diffusion coefficient.

brane descriptions arising in string and M-theory. We have highlighted the interesting values in Table 5.1 and 5.2.

We have computed the shear and bulk viscosities and in particular found their dependence on the (local) charge and dilaton coupling. We find that both classes of black branes have a shear viscosity satisfying $\eta/s = 1/4\pi$ thus saturating the universality KSS bound [110, 116]. It is reasonable to expect that this result holds for any kind of smeared brane solution of the action (5.2.1). Even though there, at least to our knowledge, does not exist a universal bound on the bulk-to-shear viscosity ratio, it is nevertheless still interesting to test our result against the well-known (holographic) “bound” proposed by Buchel [109]. We find that the ratio for fundamentally charged branes always violates this bound for all non-zero values of the charge and only saturates it in the neutral limit. In contrast, we find that branes with smeared charge continue to satisfy the bound for small charge parameter, but break the bound for sufficiently large values of the charge parameter. Although violations of the Buchel bound already exist in the literature [133], our setup thus provides two additional and physically simple examples. In Ref. [67] a different inequality and potential bound was proposed for Maxwell charged AdS branes, but it is always violated for our asymptotically flat branes. This was also observed in [1]. Indeed, if a universal bound on the shear-to-bulk exists, it would need a rather a non-trivial modification, it seems. Finally, the presence of smeared charge on the worldvolume gives rise to an additional hydrodynamic diffusion mode. We have determined the value of the transport coefficient \mathfrak{D} associated with charge diffusion and explicitly found its dependence on the dilaton coupling. In fact, we note that even though it generalizes the result for zero dilaton coupling in [43], it takes exactly the same form in terms of the parameter N . We note that all the transport coefficients are positive as required by thermodynamic consistency (the second law of thermodynamics).

We have analyzed the dynamical stability of both classes of charged black branes by considering the response of their corresponding effective fluids to small long-wavelength perturbations. To leading order, both systems have a branch of configurations that suffers from a GL instability in the sound mode [21, 22]. This branch connects naturally with the neutral brane configuration which is indeed known to be unstable [42]. However, for a certain regime of the solution parameters, both systems also have a branch of stable configurations for a given charge connecting with the extremal limit. When taking first-order effects into account, this seemingly similar behavior of the two systems breaks down. For the system with fundamental charge we find that the attenuation coefficient of the sound mode is positive for all values of the charge and thus the

stability is fully determined by the leading order i.e. by the speed of sound. In contrast, an additional longitudinal diffusion mode plays a crucial rôle for the Maxwell system which in turn leads to a complementary behavior between the stability of the sound and diffusion mode. The Maxwell black brane therefore suffers from a GL instability for all values of the charge. This complementary behavior is similar to the behavior of thermodynamic stability under change of charge and hence our result is in accordance with the correlated stability conjecture [128, 129]. We note that this was also observed for the Reissner-Nordström black brane considered in [43] and that similar observations have been done for other smeared branes, see e.g. [130, 134] for the case of smeared D p -branes.

In Sec. 5.3.3, we presented a cross-check of the transport coefficients associated with the fluid dynamics of the Maxwell charged branes utilizing a modified version of the “AdS/Ricci flat correspondence” [52, 53]. Although, it would be interesting to obtain a deeper understanding of whether any physics can be attributed to the existence of such a mapping, we can at least here comment with a partial answer with respect to its possible generalizations. In our endeavors trying to relate generic theories with an action of the type (5.2.1) to theories with a cosmological constant, we found that mappings of this kind are indeed possible. Unfortunately, despite allowing for a substantial amount of freedom between the field contents of the theories one in general ends up with pathological theories containing a scalar field having a kinetic term with the “wrong” sign. This is mainly due to severe restrictions arising from the requirements of consistent dimensional reductions. However, it is worth mentioning an interesting application of the current map (as it is presented in Sec. 5.3.3), namely, that it provides us with a tool for working out the second-order corrected charged solutions by starting directly from the known second-order results in AdS [32, 119]. We leave this exercise for the future. Before ending this paragraph, it is also interesting to note that since part of our computation is connected to the fluid description of the near horizon throat geometry (AdS) of stacks of D/M-branes, there are two, seemingly unrelated, schemes relating the results of the fluid/gravity correspondence to those of the asymptotically flat branes (and vice versa). It is therefore tempting to think that the two approaches are related although the precise connection still remains unclear. Hopefully our results will help shed some light over these unresolved issues. In this regard it is also interesting to note that the hydrodynamic regimes of the spinning black D3-brane was recently considered in [135] extending the work of [44]. Here, the theory naturally includes a U(1) gauge field. In the light of our results for the Maxwell black

brane it would be of considerable interest to review whether they can be related (for specific parameters) to at least a subsector of the hydrodynamic limit of the spinning D3.

Chapter 6

Conclusions

In this thesis we have made progress on the study of higher dimensional gravity by focusing on the properties of black holes and branes and their dynamics. We have developed two main projects:

- we have provided several maps between different dynamical spacetimes,
- we have determined the hydrodynamical behaviour of fluids dual to some classes of black holes.

Detailed discussions about the results obtained, and about future directions, can be found at the end of each chapter. Here we give a brief summary of the new, original results presented in this thesis.

In the first part of the thesis we have developed an extension of the AdS/Ricci flat correspondence to spacetimes with positive cosmological constant, including scalar matter, and found a new Kerr/AdS solution with hyperbolic horizon from a known Kerr/dS solution using this map. The AdS/dS correspondence may help understanding how to set up holography in dS space.

Another line of research was the study of fluids using the KK dimensional reduction. Choosing a generic relativistic fluid, without assuming any specific equation of state nor constituent relation, performing a boost in N internal dimensions, compactifying them and reducing on a N dimensional torus, we have obtained a charged fluid with N charges. Momenta in the compactified directions are interpreted as charges in the reduced theory. We were able to compute the transport coefficients of this charged fluid as the shear viscosity, bulk viscosity and the thermal conductivity. The same analysis has been applied to a particular fluid: the fluid dual to a black p -brane. We have obtained the shear viscosity, bulk viscosity and thermal conductivity matrix for a black p -brane with N charges in the compact directions. This method is particularly interesting since it allows to study the hydrodynamics of charged objects without

performing a perturbative analysis. Indeed, the results were obtained algebraically from those of a neutral brane by simply applying dimensional reduction techniques.

In the last part of the thesis we have investigated the hydrodynamics properties of fundamentally charged (dilaton) black branes and branes with Maxwell charge smeared over their worldvolume. We have determined the dissipative behavior of the effective fluids associated to those branes and analysed their dynamical stability. We have moreover modified the AdS/Ricci flat correspondence to include charged cases using a non diagonal KK reduction. This generalized map has been used to give a non trivial check of our results which indeed agree with the mapped coefficients in [67].

To conclude, in this thesis we have shown how higher dimensional gravity is surprisingly rich of new phenomena. Playing with spacetime dimension and mapping apparently unrelated theories living in different number of dimensions has revealed various successful predictions and results. This work improves the current comprehension of GR in spacetimes with general dimension and gives hints to holography in spacetimes with asymptotics different than AdS.

Chapter 7

Resumen en castellano

La teoría de la Relatividad General (RG) en más de cuatro dimensiones es especialmente interesante. Añadir dimensiones extra genera una multitud de nuevos fenómenos que nos dan indicios para entender mejor e investigar la naturaleza de esta teoría de la gravitación. Los agujeros negros son nuestra mejor herramienta para estudiar la GR en dimensiones superiores. Si tratamos la dimensión del espaciotiempo como un parámetro libre de la teoría, sorprendentemente emergen agujeros negros con topología del horizonte no esférica y con una estructura de fase mucho más rica. Además estos agujeros negros no siempre son soluciones estables y pueden manifestar inestabilidades. Investigar estas nuevas características y propiedades contribuye a comprender el por qué GR en cuatro dimensiones es tan peculiar.

Una de las principales razones para estudiar la gravedad en más dimensiones se debe a la teoría de cuerdas. Esta teoría es nuestro candidato más prometedor para resolver el problema de la inadecuada descripción cuántica de la gravedad. Lo sorprendente es que para ser consistente la teoría de cuerdas necesita dimensiones extra (10 dimensiones o 11 para M-theory). Probablemente el mayor éxito en el contexto de teoría de cuerdas es el descubrimiento de la dualidad entre teorías cuánticas de campo (QFT) y gravedad. Más precisamente, existe una equivalencia entre la física cuántica de sistemas fuertemente acoplados y la dinámica clásica de teorías de gravedad en una dimensión más alta. Denominada “Correspondencia AdS/CFT”, en su forma original relaciona una teoría de gravedad en espacio anti-de Sitter (AdS) con una teoría de campo conforme (CFT) que vive en su frontera. Curiosamente las dos teorías duales viven en un número diferentes de dimensiones. Por esto se dice que la correspondencia AdS/CFT es holográfica. Particularmente interesante es el límite hidrodinámico de la correspondencia, la “dualidad fluido/gravedad”. Cuando la teoría cuántica de campo se encuentra en un estado de equilibrio local está correctamente

descrita por la hidrodinámica. Esto se traduce en perturbaciones de longitud de onda larga en la teoría dual de gravedad. En cierto régimen, las ecuaciones de Einstein en D dimensiones son equivalentes a las ecuaciones de Navier-Stokes en $D - 1$ dimensiones. Esto permite describir la dinámica de agujeros negros en termino del fluido dual que vive en la frontera de su espaciotiempo.

Esta tesis se desarrolla en este contexto teórico centrándose principalmente en el estudio de la gravedad en dimensiones superiores con un enfoque en las relaciones entre diferentes tipos de espaciotiempo y el análisis y caracterización de agujeros negros. Para este último objetivo hemos desarrollado y adaptado teorías efectivas que nos permiten estudiar la dinámica de agujeros negros en ciertos regímenes. La relación entre gravedad y fluido, introducida anteriormente en espacio AdS, es una de ellas. Otro método aproximado para el estudio de agujeros negros es enfoque de “blackfold”. Esta teoría efectiva describe la dinámica de agujeros negros en un espaciotiempo genérico en el régimen en que la longitud de onda λ de la perturbaciones considerada es mucho mayor que el radio del horizonte. También en este caso el agujero negro admite una descripción hidrodinámica. Ambas teorías efectivas permiten calcular entonces el tensor energía-impulso asociado al fluido dual al agujero negro y es posible extraer los coeficientes de transporte al primer orden en derivadas. Los detalles de estos dos métodos utilizados se han presentado en el Capítulo 2.

Otra línea de estudio analizada es el desarrollo de mapas entre espaciotiempos diferentes. El primer ejemplo de este relación es la correspondencia AdS/Ricci-plano que hemos presentado en el Capítulo 3. Tomando como punto de partida la teoría Einstein y utilizando reducciones dimensionales sobre toros y sobre esferas es posible encontrar una serie de relaciones entre soluciones de las teorías reducidas. Específicamente, reduciendo la acción en AdS sobre un toro y en un espacio Ricci-plano sobre una esfera, hemos encontrado una correspondencia que permite relacionar una con otra mediante una correspondencia en el número de dimensiones. La utilidad de este mapa está en el poder predecir resultados en espaciotiempos Ricci-planos partiendo de AdS sin necesidad de resolver separadamente las ecuaciones en cada caso.

En esta tesis hemos conseguido desarrollar una extensión de el mapa anterior para espacios de Einstein con curvatura positiva y negativa. A partir de un espacio de curvatura positiva compactificando algunas dimensiones sobre una esfera y continuando analíticamente en el número de dimensiones compactas se obtiene un espacio de curvatura negativa con un subespacio hiperbólico compacto, y viceversa. Una vez derivado el mapa, lo hemos aplicado a espacios de Sitter (dS) y AdS y a agujeros negros de Schwarzschild-dS/AdS. Además, hemos estudiado perturbaciones en la frontera de

AdS, que a través del mapa nos dan sugerencias sobre una posible construcción de holografía en espacio de dS. De hecho, la frontera de un espacio asintóticamente AdS se mapea en una brana en el centro de dS y las perturbaciones cerca de la frontera tienen como fuente un tensor energía-impulso confinado en esta brana. Este tensor resulta ser igual al negativo del tensor de Brown-York para la métrica perturbada de AdS. Interesante es el uso del mapa como generador de soluciones. A partir de una solución en un determinado espaciotiempo el mapa genera directamente la correspondiente solución en el otro espaciotiempo sin necesidad de resolver ninguna ecuación. Utilizando el mapa para el agujero negro de Kerr/dS hemos obtenido entonces una nueva solución de Kerr/AdS con horizonte hiperbólico.

En el Capítulo 4 hemos estudiado la hidrodinámica de fluidos utilizando la reducción dimensional de Kaluza Klein (KK). Escogiendo un fluido relativista, sin fijar ecuaciones de estado o relaciones constituyentes, haciendo un boost en N dimensiones internas, compactificándolas y reduciendo sobre un toro N dimensional obtendremos un fluido cargado con N cargas. Los momentos en las direcciones compactificadas se interpretan como cargas en la teoría reducida. Por lo tanto, en este contexto hemos investigado cómo varían los coeficientes de transporte de la teoría inicial como la “shear and bulk viscosity” y además hemos conseguido calcular la conductividad térmica. Presentamos los resultados obtenidos en (4.3.10).

El mismo estudio ha sido también aplicado a un fluido específico: el fluido dual a una p -brana negra. Como hemos mencionado antes, dada la correspondencia entre gravedad y fluidos podemos describir branas negras como fluidos y calcular los coeficientes de transporte. Utilizando la reducción dimensional de KK a partir de una p -brana negra neutra en D dimensiones en un espacio asintóticamente plano, hemos conseguido calcular la viscosidad de shear, la viscosidad de bulk y la matriz de conductividad térmica de una p -brana negra con N cargas en las direcciones compactas. Este resultado es muy interesante porque permite estudiar la hidrodinámica de objetos cargados sin necesidad de rehacer el análisis de perturbaciones de la brana: los resultados se obtienen algebraicamente a partir de los de una brana neutra, mediante la técnica de reducción dimensional. Además utilizando la correspondencia AdS/Ricci-plano hemos podido mapear los coeficientes obtenidos y compararlos con los resultados conocidos para branas negras cargadas en Anti-deSitter presentados en [67, 68]. Hemos podido verificar así que los coeficientes de transporte obtenidos con ambos métodos coinciden.

En el Capítulo 5 hemos extendiendo el estudio de las propiedades hidrodinámicas de branas negras a los casos en que las branas llevan cargas de diferentes tipos. Hemos

analizado la hidrodinámica del fluido dual en dos clases generales de branas negras cargadas y con acoplo dilatónico incluyendo D/NS/M branas en supergravedad en once y diez dimensiones. En particular, consideramos los casos en que la brana negra está acoplada a un potencial de $(p + 1)$ -forma, que llamamos brana con carga fundamental, y brana acoplada a un campo de Maxwell. En ambos casos el acoplo dilatónico y la dimensión de la brana son arbitrarios. Estudiando perturbaciones de estas soluciones en régimen hidrodinámico hemos derivado los coeficientes de transporte (5.2.15) y (5.3.5)-(5.3.6) al primer orden en derivadas.

También hemos investigado las propiedades de estabilidad de estos sistemas hidrodinámicos analizando la respuesta a pequeñas perturbaciones de longitud de onda larga. En el caso de branas con carga fundamental hemos encontrado que existe una rama de configuraciones cargadas estables por un determinado régimen del espacio de parámetros. Esto confirma que D/NS/M-branas tienen configuraciones estables, excepto las D5, D6, y NS5, como es de esperar por argumentos termodinámicos. En contraste, las branas con carga de Maxwell presentan inestabilidad de Gregory-Laflamme independientemente del valor de su carga. Esto verifica el resultado de que las configuraciones de D0-branas son inestables.

Hemos además extendido la correspondencia AdS/Ricci-plano, que relaciona soluciones de Einstein sin y con constante cosmológica negativa, utilizando reducciones dimensionales de Kaluza-Klein no diagonales y una continuación analítica en el número de dimensiones. Esta modificación del mapa permite conectar soluciones cargadas y con acoplo dilatónico de AdS a espacios asintóticamente planos. Hemos utilizado esta extensión y mapeado los coeficientes de transporte encontrados. Esto nos ha permitido comprobar que nuestros resultados coinciden con los coeficientes de transporte calculados anteriormente en AdS en [67].

Acabamos la tesis con una discusión en el Capítulo 6 sobre los resultados obtenidos y proponemos posibles proyectos para el futuro. Detalles técnicos de nuestros cálculos se pueden encontrar en los apéndices que siguen a la conclusión.

Appendix A

Curvature tensor from dimensional reduction

In this appendix we explicitly give the equations obtained from a diagonal dimensional reduction for a given metric ansatz. In particular we compute the curvature tensors in the two cases presented in Chapt.3.

A.1 Curvature tensors for a product metric

For the product space metric (3.2.3), one easily calculates the Christoffel symbols directly from the definition

$$\bar{\Gamma}_{bc}^a = \Gamma_{bc}^a + \alpha (\delta_c^a \nabla_b + \delta_b^a \nabla_c - g_{bc} \nabla^a) \phi, \quad (\text{A.1.1a})$$

$$\bar{\Gamma}_{b\gamma}^a = 0, \quad (\text{A.1.1b})$$

$$\bar{\Gamma}_{\beta\gamma}^a = -\beta e^{2(\beta-\alpha)\phi} \gamma_{\beta\gamma} \nabla^a \phi, \quad (\text{A.1.1c})$$

$$\bar{\Gamma}_{bc}^\alpha = 0, \quad (\text{A.1.1d})$$

$$\bar{\Gamma}_{b\gamma}^\alpha = \beta \delta_\gamma^\alpha \partial_b \phi, \quad (\text{A.1.1e})$$

$$\bar{\Gamma}_{\beta\gamma}^\alpha = \Gamma_{\beta\gamma}^\alpha [\gamma]. \quad (\text{A.1.1f})$$

The curvature tensors follow as

$$\begin{aligned} \bar{R}_{mn} = & R_{mn} - [(n-2)\alpha + \nu\beta] \nabla_m \nabla_n \phi \\ & + [(n-2)\alpha^2 + 2\nu\alpha\beta - \nu\beta^2] \nabla_m \phi \nabla_n \phi \\ & - \alpha g_{mn} \left[\nabla^a \nabla_a \phi + [(n-2)\alpha + \nu\beta] \nabla^a \phi \nabla_a \phi \right], \end{aligned} \quad (\text{A.1.2a})$$

$$\bar{R}_{m\nu} = \bar{R}_{\mu n} = 0, \quad (\text{A.1.2b})$$

$$\begin{aligned} \bar{R}_{\mu\nu} &= R_{\mu\nu} - \beta e^{2(\beta-\alpha)\phi} \gamma_{\mu\nu} \nabla^a \nabla_a \phi \\ &\quad - \beta e^{2(\beta-\alpha)\phi} \gamma_{\mu\nu} [(n-2)\alpha + \nu\beta] \nabla^a \phi \nabla_a \phi, \end{aligned} \quad (\text{A.1.2c})$$

$$\begin{aligned} e^{2\alpha\phi} \bar{R} &= R + e^{2(\alpha-\beta)\phi} R[\gamma] - 2[(n-1)\alpha + \nu\beta] \nabla^a \nabla_a \phi \\ &\quad - \left[(n-1)(n-2)\alpha^2 + 2(n-2)\nu\alpha\beta \right. \\ &\quad \left. + \nu(\nu+1)\beta^2 \right] \nabla^a \phi \nabla_a \phi. \end{aligned} \quad (\text{A.1.2d})$$

If we put an additional stress tensor on the right-hand side of (3.2.14), which only has components in the extended directions T_{mn} , the reduced equations of motion (3.2.15) have the form

$$\begin{aligned} R_{mn} &- \lambda(n+\nu-1)/\ell^2 e^{2\alpha\phi} g_{mn} - \alpha g_{mn} \nabla^a \nabla_a \phi \\ &- [(n-2)\alpha + \nu\beta] \nabla_m \nabla_n \phi \\ &+ [(n-2)\alpha^2 + 2\nu\alpha\beta - \nu\beta^2] \nabla_m \phi \nabla_n \phi \\ &- \alpha [(n-2)\alpha + \nu\beta] g_{mn} \nabla^a \phi \nabla_a \phi \end{aligned} \quad (\text{A.1.3a})$$

$$\begin{aligned} &= 8\pi G_N^{n+\nu} \left(T_{mn} - \frac{1}{(n+\nu-2)} g_{mn} T \right), \\ &\beta \left[\nabla^a \nabla_a \phi + [(n-2)\alpha + \nu\beta] \nabla^a \phi \nabla_a \phi \right] \\ &\quad + \left[\lambda(n+\nu-1)/\ell^2 - k(\nu-1)H^2 e^{-2\beta\phi} \right] e^{2\alpha\phi} \\ &= \frac{8\pi}{(n+\nu-2)} G_N^{n+\nu} T, \end{aligned} \quad (\text{A.1.3b})$$

where the trace is defined by $T = g^{mn} T_{mn}$.

A.2 Curvature tensors for asymptotically AdS with a CHS

For the metric (3.2.42) at $r = \text{const}$, we calculate to leading order in h_{ab} and ψ

$$\Gamma_{bc}^a = \frac{1}{2} (\partial_b h_c^a + \partial_c h_b^a - \partial^a h_{bc}), \quad (\text{A.2.1a})$$

$$\Gamma_{b\gamma}^a = 0, \quad (\text{A.2.1b})$$

$$\Gamma_{\beta\gamma}^a = \gamma_{\beta\gamma}^{(-1)} \eta (\delta_0^a - \eta \partial^a \psi + 2\delta_0^a \psi + h^{a0}), \quad (\text{A.2.1c})$$

$$\Gamma_{bc}^\alpha = 0, \quad (\text{A.2.1d})$$

$$\Gamma_{b\gamma}^\alpha = \left(\eta^{-1} \delta_b^0 + \partial_b \psi \right) \delta_\gamma^\alpha, \quad (\text{A.2.1e})$$

$$\Gamma_{\beta\gamma}^\alpha = \Gamma_{\beta\gamma}^\alpha \left[\gamma^{(-1)} \right]. \quad (\text{A.2.1f})$$

From this we obtain the Ricci tensor and scalar (using that the compact space is Einstein)

$$\begin{aligned} \mathcal{R}_{bd} &= \partial^a \partial_{(b} h_{d)a} - \frac{1}{2} \partial^2 h_{bd} - \frac{1}{2} \partial_b \partial_d (h + 2\nu\psi) \\ &\quad - \frac{\nu}{\eta} \left[\partial_{(b} h_{d)0} - \frac{1}{2} \partial_\eta h_{bd} + 2\delta_{(b}^0 \partial_{d)} \psi \right], \end{aligned} \quad (\text{A.2.2a})$$

$$\mathcal{R}_{b\delta} = 0, \quad (\text{A.2.2b})$$

$$\begin{aligned} \mathcal{R}_{\beta\delta} &= \gamma_{\beta\delta}^{(-1)} \left[-\eta^2 \partial^2 \psi - \eta \partial^m h_{m0} + \frac{1}{2} \eta \partial_\eta (h + 4\nu\psi) \right. \\ &\quad \left. + (\nu - 1) (2\psi + h_{00}) \right], \end{aligned} \quad (\text{A.2.2c})$$

$$\begin{aligned} \mathcal{R} &= \frac{r^2}{\ell^2} \left[\partial^m \partial^n h_{mn} - \partial^2 (h + 2\nu\psi) - \frac{2\nu}{\eta} \partial^m h_{m0} \right. \\ &\quad \left. + \frac{\nu}{\eta} \partial_\eta (h + 4\nu\psi) + \frac{\nu(\nu - 1)}{\eta^2} (2\psi + h_{00}) \right]. \end{aligned} \quad (\text{A.2.2d})$$

Appendix B

Extracting transport coefficients

In this appendix we compute the equations of motion of the N -charge hydrodynamic system presented in Chapt. 4 from energy momentum conservation relations. We then show how to extract the transport coefficients for the reduced theory making use of the frame-independent method introduced in [108].

B.1 Equations of motion for the reduced theory

The perfect fluid part of the reduced stress energy tensor in (4.2.4) satisfies the following conservation equations

$$\partial^a T_{ab} = 0 = (1 + \varrho') \hat{u}_a \hat{u}_b \prod_{i=1}^N \cosh^2 \alpha_i \partial^a \hat{P} + \partial_b \hat{P} \quad (\text{B.1.1})$$

$$+ (\varrho V + \hat{P}) \prod_{i=1}^N \cosh^2 \alpha_i \left(2 \hat{u}_a \hat{u}_b \sum_{k=1}^N \tanh \alpha_k \partial^a \alpha_k + \hat{\theta} \hat{u}_b + \hat{u}_a \partial^a \hat{u}_b \right),$$

$$\partial^a T_{ay_j} = 0 = \left[(1 + \varrho') \hat{u}_a \partial^a \hat{P} + (\varrho V + \hat{P}) \left(\sum_{i=1}^N \tanh \alpha_i \hat{u}_a \partial^a \alpha_i \right. \quad (\text{B.1.2}) \right.$$

$$\left. + \sum_{l=1}^{j-1} \tanh \alpha_l \hat{u}_a \partial^a \alpha_l + \coth \alpha_j \hat{u}_a \partial^a \alpha_j + \hat{\theta} \right] \sinh \alpha_j$$

$$\prod_{i=1}^N \cosh \alpha_i \prod_{k=1}^{j-1} \cosh \alpha_k$$

where

$$\varrho' = \frac{\partial \varrho}{\partial P} \quad \text{and} \quad \frac{\partial \varrho}{\partial \hat{P}} = \varrho' \frac{1}{V}.$$

If we contract the Eq. (B.1.1) with \hat{u}^b we find

$$\hat{u}_a \partial^a \log \hat{P} = -\frac{(\varrho V + \hat{P})}{\hat{P}} \prod_{i=1}^N \cosh^2 \alpha_i \frac{2 \sum_{k=1}^N \tanh \alpha_k \hat{u}_a \partial^a \alpha_k + \hat{\theta}}{(1 + \varrho') \prod_{i=1}^N \cosh^2 \alpha_i - 1}. \quad (\text{B.1.3})$$

In addition, Eq. (B.1.2) can be rewritten as

$$\begin{aligned} \hat{u}_a \partial^a \log \hat{P} = & -\frac{(\varrho V + \hat{P})}{\hat{P}(1 + \varrho')} \left(\sum_{i=1}^N \tanh \alpha_i \hat{u}_a \partial^a \alpha_i + \sum_{l=1}^{j-1} \tanh \alpha_l \hat{u}_a \partial^a \alpha_l \right. \\ & \left. + \coth \alpha_j \hat{u}_a \partial^a \alpha_j + \hat{\theta} \right). \end{aligned} \quad (\text{B.1.4})$$

If we take the latter relation for two different indices, j and k with $j \neq k$ (corresponding to the conservation of two different components of the stress energy tensor) and we subtract them, we obtain

$$\sum_{i=k}^{j-1} \tanh \alpha_i \hat{u}_a \partial^a \alpha_i = \coth \alpha_k \hat{u}_a \partial^a \alpha_k - \coth \alpha_j \hat{u}_a \partial^a \alpha_j, \quad j > k \quad (\text{B.1.5})$$

or equivalently

$$\hat{u}_a \partial^a \alpha_{i+1} = \hat{u}_a \partial^a \alpha_i \frac{\tanh \alpha_{i+1}}{\sinh \alpha_i \cosh \alpha_i}. \quad (\text{B.1.6})$$

Now, let us compare Eq. (B.1.3) and Eq. (B.1.4). This gives

$$\begin{aligned} & -\frac{2 \sum_{k=1}^N \tanh \alpha_k \hat{u}_a \partial^a \alpha_k + \hat{\theta}}{(1 + \varrho') \prod_{i=1}^N \cosh^2 \alpha_i - 1} \prod_{i=1}^N \cosh^2 \alpha_i = \\ & -\frac{1}{(1 + \varrho')} \left(\sum_{i=1}^N \tanh \alpha_i \hat{u}_a \partial^a \alpha_i + \sum_{l=1}^{j-1} \tanh \alpha_l \hat{u}_a \partial^a \alpha_l + \coth \alpha_j \hat{u}_a \partial^a \alpha_j + \hat{\theta} \right) \end{aligned} \quad (\text{B.1.7})$$

Since we want the relation between the reduced expansion and a derivatives of specific rapidity α_j , we replace in Eq. (B.1.7) the other derivatives of the remaining rapidities in term of the one chosen using Eq. (B.1.5). This gives

$$\hat{u}_a \partial^a \alpha_j = -\hat{\theta} \frac{\prod_{i=1}^{j-1} \text{sech}^2 \alpha_i \tanh \alpha_j}{1 - \varrho' + \prod_{l=1}^N \text{sech}^2 \alpha_l} \quad (\text{B.1.8})$$

that can be rewritten as

$$\hat{u}_a \partial^a \alpha_j = \hat{\theta} \frac{\cosh \alpha_j \sinh \alpha_j \prod_{l=j+1}^N \cosh^2 \alpha_l}{1 + (-1 + \varrho') \prod_{i=1}^N \cosh^2 \alpha_i}. \quad (\text{B.1.9})$$

The Eq. (B.1.3) in terms of $\hat{u}_a \partial^a \alpha_j$ only is given by

$$\hat{u}_a \partial^a \log \hat{P} = -\frac{\varrho V + \hat{P}}{\hat{P}} \coth \alpha_j \prod_{i=1}^{j-1} \cosh^2 \alpha_i \hat{u}_a \partial^a \alpha_j \quad (\text{B.1.10})$$

using the result in Eq. (B.1.9).

The reduced acceleration is obtain from Eq. (B.1.1)

$$\begin{aligned} \hat{u}_a \partial^a \hat{u}_b = & -\frac{\partial_b \log \hat{P}}{\left(1 + \frac{\varrho V}{\hat{P}}\right) \prod_{i=1}^N \cosh^2 \alpha_i} - \frac{\hat{P}(1 + \varrho')}{\hat{P} + \varrho V} \hat{u}_b \hat{u}_a \partial^a \log \hat{P} \\ & - 2\hat{u}_a \hat{u}_b \sum_{k=1}^N \tanh \alpha_k \partial^a \alpha_k - \hat{u}_b \hat{\theta}. \end{aligned} \quad (\text{B.1.11})$$

Using Eqs. (B.1.5), (B.1.9), and (B.1.10), this becomes

$$\hat{u}_a \partial^a \hat{u}_b = -\frac{\partial_b \log \hat{P}}{\left(1 + \frac{\varrho V}{\hat{P}}\right) \prod_{i=1}^N \cosh^2 \alpha_i} + \frac{\hat{u}_a \hat{u}_b \partial^a \alpha_j}{\cosh \alpha_j \sinh \alpha_j \prod_{i=j+1}^N \cosh^2 \alpha_i}. \quad (\text{B.1.12})$$

B.2 Dissipative transport coefficients

Shear viscosity

The first term in Eq. (4.3.9) is given by

$$\hat{P}_c^a \hat{P}_d^b T_{ab}^{diss} = -V \hat{P}_c^a \hat{P}_d^b \left(2\eta \left(\sum_{i=1}^N P_{(a}^l P_{b)}^{yi} \partial_l u_{y_i} + P_a^l P_b^m \partial_l u_m \right) - \frac{P_{ab} \theta}{p} \right) + \zeta P_{ab} \theta. \quad (\text{B.2.1})$$

Taking into account that

$$\hat{P}_c^a \hat{P}_d^b P_a^l P_b^m = \hat{P}_c^l \hat{P}_d^m, \quad \hat{P}_c^l \hat{P}_d^m \partial_l \hat{u}_m = 0, \quad \hat{P}_c^a P_a^{yj} = 0 \quad (\text{B.2.2})$$

the Eq. (B.2.1) becomes

$$\hat{P}_c^a \hat{P}_d^b T_{ab}^{diss} = -V \left(2\eta \left(\prod_{i=1}^N \cosh \alpha_i \hat{P}_c^l \hat{P}_d^m \partial_l \hat{u}_m \right) - \frac{\hat{P}_{cd} \theta}{p} \right) + \zeta \hat{P}_{cd} \theta. \quad (\text{B.2.3})$$

For what concerns the second term in Eq. (4.3.9) we get

$$\frac{1}{p-N} \hat{P}_{cd} \hat{P}^{ab} T_{ab}^{diss} = -V \left(2\eta \left(\frac{1}{p-N} \prod_{i=1}^N \cosh \alpha_i \hat{P}_{cd} \hat{P}^{ab} \partial_{(a} \hat{u}_{b)} - \frac{\hat{P}_{cd}}{p} \theta \right) + \zeta \hat{P}_{cd} \theta \right)$$

considering that

$$\hat{P}^{ab} P_{ab} = p - N, \quad \hat{P}^{cd} \partial_{(c} \alpha_i \hat{u}_{d)} = 0, \quad \hat{P}^{ab} P_{(a}^c P_{b)}^{yi} = 0. \quad (\text{B.2.4})$$

If now we subtract (B.2.4) with (B.2.3) we are able to extract the shear viscosity. In fact

$$\begin{aligned} & -2V\eta \prod_{i=1}^N \cosh \alpha_i \left(\hat{P}_c^l \hat{P}_d^m \partial_{(l} \hat{u}_{m)} - \frac{1}{p-N} \hat{P}_{cd} \hat{P}^{ab} \partial_{(a} \hat{u}_{b)} \right) \\ & = -2V\eta \prod_{i=1}^N \cosh \alpha_i \left(\hat{P}_c^l \hat{P}_d^m \partial_{(l} \hat{u}_{m)} - \frac{1}{p-N} \hat{P}_{cd} \hat{\theta} \right) = -2\hat{\eta} \hat{\sigma}_{cd}, \end{aligned}$$

where $\hat{P}^{ab} \partial_{(a} \hat{u}_{b)} = \hat{\theta}$ and $\hat{\sigma}_{cd}$ is defined as

$$\hat{\sigma}_{cd} = \hat{P}_c^a \hat{P}_d^b \partial_{(a} \hat{u}_{b)} - \frac{1}{p-N} \hat{\theta} \hat{P}_{cd}. \quad (\text{B.2.5})$$

We recover the result anticipated in Eq. (4.3.10), that is

$$\hat{\eta} = \eta V \prod_{i=1}^N \cosh \alpha_i. \quad (\text{B.2.6})$$

Heat conductivity matrix

We now compute the heat conductivity matrix elements. The second equation in (4.3.10) can be simplified substituting the Eqs. (4.3.8) that leads to

$$\hat{P}_a^b \left(T_{by_j}^{diss} - \frac{\sinh \alpha_j}{\prod_{i=j}^N \cosh \alpha_i} \sum_{j'=1}^N \frac{\sinh \alpha_{j'}}{\prod_{i'=j'}^N \cosh \alpha_{i'}} T_{by_{j'}}^{diss} \right) \quad (\text{B.2.7})$$

where we have also replaced the values of the reduced density charge, pressure and energy density from (4.2.6). It is convenient to split the above expression into two parts: one with index $j' = j$ and the other with different indices $k \neq j$ as

$$\hat{P}_a^b T_{by_j}^{diss} \left(1 - \frac{\sinh^2 \alpha_j}{\prod_{i=j}^N \cosh \alpha_i^2} \right) - \hat{P}_a^b \frac{\sinh \alpha_j}{\prod_{i=j}^N \cosh \alpha_i} \sum_{k=1}^N \frac{\sinh \alpha_k}{\prod_{i'=k}^N \cosh \alpha_{i'}} T_{by_k}^{diss}. \quad (\text{B.2.8})$$

So, we extract the heat conductivity coefficients from the relations

$$\hat{P}_a^b T_{by_j}^{diss} \left(1 - \frac{\sinh^2 \alpha_j}{\prod_{i=j}^N \cosh \alpha_i^2} \right) = -\hat{\kappa}_{jj} \hat{P}_a^b \partial_b \left(\frac{\hat{\mu}_j}{\hat{\mathcal{T}}} \right), \quad (\text{B.2.9})$$

$$-\hat{P}_a^b \frac{\sinh \alpha_j}{\prod_{i=j}^N \cosh \alpha_i} \sum_{k=1}^N \frac{\sinh \alpha_k}{\prod_{i'=k}^N \cosh \alpha_{i'}} T_{by_k}^{diss} = -\sum_{k=1}^N \hat{\kappa}_{jk} \hat{P}_a^b \partial_b \left(\frac{\hat{\mu}_k}{\hat{\mathcal{T}}} \right). \quad (\text{B.2.10})$$

The $\hat{P}_a^b T_{by_j}^{diss}$ term is given by

$$\begin{aligned} \hat{P}_a^b T_{by_j}^{diss} = & -\eta V \hat{P}_a^c \left(\sinh \alpha_j \prod_{l=1}^{j-1} \cosh \alpha_l \prod_{l'=1}^N \cosh \alpha_{l'} \right. \\ & \left. (-\partial_c \prod_{i'=1}^N \cosh \alpha_{i'} + \prod_{i=1}^N \cosh \alpha_i \hat{u}_b \partial^b \hat{u}_c) + \sum_{j'=1}^N P_{y_j}^{y_{j'}} \partial_c u_{y_{j'}} \right). \end{aligned} \quad (\text{B.2.11})$$

Using the expression (B.1.12) for the acceleration, and the fact that $\hat{P}^{ab} u_b = 0$, this becomes

$$\begin{aligned} & -\eta V \hat{P}_a^c \left[\sinh \alpha_j \prod_{l=1}^{j-1} \cosh \alpha_l \prod_{l'=1}^N \cosh \alpha_{l'} \left(-\partial_c \prod_{i'=1}^N \cosh \alpha_{i'} - \frac{\partial_c \log \hat{P}}{(1 + \frac{eV}{\hat{P}}) \prod_{i=1}^N \cosh \alpha_i} \right) \right. \\ & \left. + \sum_{j'=1}^N P_{y_j}^{y_{j'}} \partial_c u_{y_{j'}} \right] \end{aligned} \quad (\text{B.2.12})$$

Making explicit the value of $P_{y_j}^{y_i}$ and simplifying we obtain

$$\hat{P}_a^b T_{by_j}^{diss} = -\eta V \hat{P}_a^c \sinh \alpha_j \prod_{l=1}^{j-1} \cosh \alpha_l \left(\sum_{l'=1}^{j-1} \tanh \alpha_{l'} \partial_c \alpha_{l'} + \coth \alpha_j \partial_c \alpha_j - \frac{\partial_c \log \hat{P}}{1 + \frac{eV}{\hat{P}}} \right). \quad (\text{B.2.13})$$

For what concerns the right part of the formula (B.2.9), if we substitute the values (4.2.7) and (4.2.10) we find

$$\begin{aligned} \hat{P}_a^b \partial_b \left(\frac{\hat{\mu}_j}{\hat{\mathcal{T}}} \right) &= \hat{P}_a^b \partial_b \left(\frac{\sinh \alpha_j \prod_{i=1}^{j-1} \cosh \alpha_i}{\hat{\mathcal{T}}} \right) \\ &= \frac{\hat{P}_a^b}{\hat{\mathcal{T}}} \frac{\sinh \alpha_j}{\prod_{i=j}^N \cosh \alpha_i} \left(\coth \alpha_j \partial_b \alpha_j + \sum_{l=1}^{j-1} \tanh \alpha_l \partial_b \alpha_l - \frac{\partial_b \log \hat{P}}{1 + \frac{eV}{\hat{P}}} \right). \end{aligned} \quad (\text{B.2.14})$$

Now we are able to extract the elements of the heat conductivity metric from Eq. (B.2.9) only replacing the result obtained in Eq. (B.2.13) and (B.2.14). This leads to

$$\begin{aligned} & -\eta V \hat{P}_a^c \sinh \alpha_j \prod_{l=1}^{j-1} \cosh \alpha_l \left(1 - \frac{\sinh^2 \alpha_j}{\prod_{i=j}^N \cosh \alpha_i^2}\right) \left(\sum_{l'=1}^{j-1} \tanh \alpha_{l'} \partial_c \alpha_{l'} + \coth \alpha_j \partial_c \alpha_j\right. \\ & \left. - \frac{\partial_c \log \hat{P}}{1 + \frac{\varrho V}{\hat{P}}}\right) = -\hat{\kappa}_{jj} \frac{\hat{P}_a^c}{\hat{\mathcal{T}}} \frac{\sinh \alpha_j}{\prod_{i=j}^N \cosh \alpha_i} \left(\coth \alpha_j \partial_c \alpha_j + \sum_{l=1}^{j-1} \tanh \alpha_l \partial_c \alpha_l - \frac{\partial_c \log \hat{P}}{1 + \frac{\varrho V}{\hat{P}}}\right). \end{aligned}$$

So, the diagonal elements are

$$\hat{\kappa}_{jj} = \eta V \hat{\mathcal{T}} \prod_{i=1}^N \cosh \alpha_i \left(1 - \frac{\sinh^2 \alpha_j}{\prod_{i=j}^N \cosh \alpha_i^2}\right), \quad (\text{B.2.15})$$

as already shown in Eq. (4.3.10).

The same procedure is performed for the Eq. (B.2.10). We find that

$$\begin{aligned} & -\hat{P}_a^b T_{byk}^{diss} \frac{\sinh \alpha_j}{\prod_{i=j}^N \cosh \alpha_i} \sum_{k=1}^N \frac{\sinh \alpha_k}{\prod_{i'=k}^N \cosh \alpha_{i'}} \quad (\text{B.2.16}) \\ & = -\sum_{k=1}^N \hat{\kappa}_{jk} \frac{\hat{P}_a^c}{\hat{\mathcal{T}}} \frac{\sinh \alpha_k}{\prod_{i=k}^N \cosh \alpha_i} \left(\coth \alpha_k \partial_c \alpha_k + \sum_{l=1}^{k-1} \tanh \alpha_l \partial_c \alpha_l - \frac{\partial_c \log \hat{P}}{1 + \frac{\varrho V}{\hat{P}}}\right). \end{aligned}$$

Comparing the last two equations, term by term, in the sum it is easy to find that

$$\hat{\kappa}_{jk} = -\eta V \hat{\mathcal{T}} \frac{\sinh \alpha_j \sinh \alpha_k}{\prod_{i=j}^N \cosh \alpha_i} \prod_{l=1}^{k-1} \cosh \alpha_l. \quad (\text{B.2.17})$$

Bulk viscosity

First of all, we need to compute the derivatives of the pressure with respect to energy density and the charges. Due to the fact that $\partial \hat{P} / \partial \hat{\varrho}$ is calculated with constant charges \hat{q}_j and $\partial \hat{P} / \partial \hat{q}_j$ keeping fixed the energy density and the remaining $q_{k \neq j}$ charges, we need to use

$$d\hat{\varrho} = 0 \Rightarrow d \log \hat{P} = -2 \frac{(\hat{P} + \varrho V)}{\hat{P}} \frac{\prod_{m=1}^N \cosh^2 \alpha_m \sum_{l=1}^N \tanh \alpha_l}{[-1 + (\varrho' + 1) \prod_{k=1}^N \cosh^2 \alpha_k]} d\alpha_l \quad (\text{B.2.18})$$

$$\begin{aligned} d\hat{q}_j = 0 \Rightarrow d \log \hat{P} &= -\frac{(\hat{P} + \varrho V)}{\hat{P}(1 + \varrho')} \left[\sum_{l=1}^N \tanh \alpha_l d\alpha_l + \coth \alpha_j d\alpha_j \right. \\ & \left. + \sum_{k=1}^{j-1} \tanh \alpha_k d\alpha_k \right]. \quad (\text{B.2.19}) \end{aligned}$$

The considered derivatives are given by

$$\begin{aligned}\frac{\partial \hat{P}}{\partial \hat{\varrho}} &= \frac{1}{\left[-1 + (1 + \varrho') \prod_{l=1}^N \cosh^2 \alpha_l\right] + 2 \frac{\hat{P} + \varrho V}{\hat{P}} \prod_{i=1}^N \cosh \alpha_i^2 \sum_{l=1}^N \tanh \alpha_l \frac{\partial \alpha_l}{\partial \log \hat{P}}}, \\ \frac{\partial \hat{P}}{\partial \hat{q}_j} &= \frac{1}{(1 + \varrho') A + \frac{\hat{P} + \varrho V}{\hat{P}} AB},\end{aligned}\tag{B.2.20}$$

with

$$\begin{aligned}A &= \sinh \alpha_j \prod_{i=1}^N \cosh \alpha_i \prod_{k=1}^{j-1} \cosh \alpha_k \\ B &= \sum_{l=1}^N \tanh \alpha_l \frac{\partial \alpha_l}{\partial \log \hat{P}} + \sum_{k=1}^{j-1} \tanh \alpha_k \frac{\partial \alpha_k}{\partial \log \hat{P}} + \coth \alpha_j \frac{\partial \alpha_j}{\partial \log \hat{P}}\end{aligned}\tag{B.2.21}$$

Combining conveniently Eqs. (B.2.18) and (B.2.19) in Eqs. (B.2.20) we obtain that

$$\begin{aligned}\frac{\partial \hat{P}}{\partial \hat{\varrho}} &= \frac{2 \prod_{i=1}^N \cosh^2 \alpha_i - 1}{1 + (-1 + \varrho') \prod_{l=1}^N \cosh^2 \alpha_l}, \\ \frac{\partial \hat{P}}{\partial \hat{q}_j} &= \frac{-2 \sinh \alpha_j \prod_{i=1}^N \cosh \alpha_i \prod_{m=1}^{j-1} \cosh \alpha_m}{1 + (-1 + \varrho') \prod_{l=1}^N \cosh^2 \alpha_l}.\end{aligned}\tag{B.2.22}$$

Let now evaluate the first term in Eq. (4.3.9). We find that

$$\frac{\hat{P}^{ab} T_{ab}^{diss}}{p - N} = -\hat{\theta} V \prod_{l=1}^N \cosh \alpha_l \left(\frac{2\eta}{p - N} + \left(\frac{-2\eta}{p} + \zeta \right) \frac{\varrho' \prod_{m=1}^N \cosh^2 \alpha_m}{1 + (-1 + \varrho') \prod_{i=1}^N \cosh^2 \alpha_i} \right).\tag{B.2.23}$$

The remaining terms can be simplified considering the Eqs. (4.3.8). These become

$$-\sum_{j'=1}^N \frac{\sinh \alpha_{j'}}{\prod_{m=j'}^N \cosh \alpha_m} \left(\frac{\partial \hat{P}}{\partial \hat{\varrho}} \sum_{j=1}^N \frac{\sinh \alpha_j}{\prod_{i=j}^N \cosh \alpha_i} + \sum_{j=1}^N \frac{\partial \hat{P}}{\partial \hat{q}_j} \right) T_{y_j y_{j'}}^{diss}\tag{B.2.24}$$

Using the Eqs. (B.1.9), (B.1.5), (B.2.22) and replacing the components of the stress energy tensor $T_{y_j y_{j'}}^{diss}$ we find

$$\begin{aligned}-\hat{\zeta} \hat{\theta} &= -2\eta \hat{\theta} V \prod_{i=1}^N \cosh \alpha_i \left[\frac{1}{p - N} - \frac{\varrho'^2 \prod_{h=1}^N \cosh^4 \alpha_h}{p(1 + (-1 + \varrho') \prod_{i=1}^N \cosh^2 \alpha_i)^2} \right. \\ &\quad \left. + \frac{(-1 + \prod_{i=1}^N \cosh^2 \alpha_i) \sum_{l=1}^N \sinh \alpha_l^2 \prod_{m=l+1}^N \cosh^2 \alpha_m}{[1 + (-1 + \varrho') \prod_{i=1}^N \cosh^2 \alpha_i]^2} \right]\end{aligned}$$

$$- \zeta \hat{\theta} V \frac{\varrho'^2 \prod_{h=1}^N \cosh^5 \alpha_h}{(1 + (-1 + \varrho') \prod_{i=1}^N \cosh^2 \alpha_i)^2}.$$

in terms of $\hat{\theta}$ only. Remember that for the initial expansion we use the values found in the Eq.(4.3.4) . It is straightforward to read now the bulk viscosity as already presented in Eq.(4.3.10).

Appendix C

Details on the perturbative computation for Chapter 5

In this appendix we provide some of the details on our perturbative computation outlined in Sec. 5.2.1. When solving the perturbative equations we focus on the Maxwell charged case as it is in many regards the most intricate due to extra dynamical freedom in the vector sector. In section C.3 we provide the most relevant equations (and differences) pertaining to the fundamentally charged case.

C.1 Setting up the perturbative problem

As explained in Sec. 5.2.1, in order for the perturbative problem to be well-posed, we need to cast the fields into (ingoing) Eddington-Finkelstein (EF) form $(x^a, r, \Omega) \rightarrow (\sigma^a, r, \Omega)$ with $\sigma^a = (v, \sigma^i)$, defined in the usual way, i.e., so that $|dr|^2 = 0$. It is not difficult to verify that the coordinates,

$$\sigma^a = x^a + u^a r_\star, \quad r_\star(r) = r + \int_r^\infty dr \left(\frac{f - h^{N/2}}{f} \right), \quad (\text{C.1.1})$$

will do the job for both brane solutions (5.2.4) and (5.3.2). Note that we have chosen the integration constant appearing in r_\star so that $r_\star \rightarrow r$ for large r . In this way the EF coordinates reduce to ordinary Schwarzschild light cone coordinates far from the horizon. Notice that it is possible to write down a closed form expression for r_\star in

terms of the hypergeometric Appell function F_1 ,

$$r_\star(r) = r F_1 \left(-\frac{1}{n}; -\frac{N}{2}, 1; 1 - \frac{1}{n}; 1 - h, 1 - f \right) \approx r \left(1 - \frac{1}{n-1} \frac{r_0^n}{r^n} \left(1 + \frac{N\gamma_0}{2} \right) \right), \quad (\text{C.1.2})$$

where the last equality applies for large r and is valid up to $\mathcal{O}\left(\frac{1}{r^{2n-1}}\right)$. With this definition of r_\star , we will limit our analysis to the case where $n \geq 2$ (the analysis for $n = 1$ needs some modifications, however, at the end of the day, the results for the transport coefficients can be obtained by setting $n = 1$ in the results derived below).

In EF coordinates (C.1.1), the metric (5.2.4) for the fundamentally charged brane takes the form

$$ds^2 = h^{-\frac{Nn}{p+n+1}} \left(\left(-f u_a u_b + \Delta_{ab} \right) d\sigma^a d\sigma^b - 2h^{\frac{N}{2}} u_a d\sigma^a dr + h^N r^2 d\Omega_{(n+1)}^2 \right). \quad (\text{C.1.3})$$

Similarly, the Maxwell charged brane (5.3.2) takes the form

$$ds^2 = h^{-\left(\frac{n+p}{n+p+1}\right)N} \left(\left(-f u_a u_b + h^N \Delta_{ab} \right) d\sigma^a d\sigma^b - 2h^{\frac{N}{2}} u_a d\sigma^a dr + h^N r^2 d\Omega_{(n+1)}^2 \right). \quad (\text{C.1.4})$$

Transforming to the coordinates (C.1.1) introduces non-zero radial components to the two gauge fields. This transformation can, however, be undone by a suitable gauge transformation and the EF form of the gauge fields and in this particular gauge read

$$A = -\frac{1}{h} \left(\frac{r_0}{r} \right)^n \sqrt{N\gamma_0(\gamma_0 + 1)} \star 1 \quad \text{and} \quad A = \frac{1}{h} \left(\frac{r_0}{r} \right)^n \sqrt{N\gamma_0(\gamma_0 + 1)} u_a d\sigma^a, \quad (\text{C.1.5})$$

for the fundamentally and Maxwell charged branes, respectively. In particular, the two gauge fields only have components in the brane directions. Also note that the dilaton remains invariant under the coordinate transformation as it is independent of the brane directions.

We now promote the parameters u^a , r_0 and γ_0 to *slowly* varying worldvolume fields and look for the corrections ds_∂^2 , A_∂ , ϕ_∂ , so that ds_f^2 , A_f , ϕ_f solve the full set of EOMs to first order in the derivatives (cf. Eq. (5.2.11)). In order to do this, we first need to expand the leading order seed solutions (C.1.3)-(C.1.5) to first order in the derivatives. Carrying out this expansion is of course straightforward, however, the resulting expressions are rather lengthy and not very illuminating and therefore we omit them here. Moreover, in the following we employ the inherent Lorentz symmetry of the background to work in the rest frame in the point \mathcal{P} around which we consider hydrodynamic fluctuations

(in the ultra-local sense). We therefore take $u^a(\sigma^a)|_{\mathcal{P}} = (1, \mathbf{0})$. Moreover, we define $r_0(\sigma^a)|_{\mathcal{P}} \equiv r_0$ and $\gamma_0(\sigma^a)|_{\mathcal{P}} \equiv \gamma_0$. Similarly, all the (worldvolume) derivatives are understood to be evaluated at \mathcal{P} . For example, $\partial_a r_0(\sigma^a)|_{\mathcal{P}} \equiv \partial_a r_0$ and so forth.

The rest frame has a residual $\text{SO}(p)$ invariance which we use to split the resulting equations up into different sectors characterized according to their transformation under $\text{SO}(p)$. For the fundamentally charged black brane the scalar sector contains five scalars, the vector sector contains two vectors and the tensor sector contains one tensor. We parameterize the $\text{SO}(p)$ perturbations according to

$$\begin{aligned}
\text{Scalar: } (A_\partial)_{vi_1\dots i_p} &= -\sqrt{N\gamma_0(1+\gamma_0)} \frac{r_0^n}{r^n} h^{-1} a_{vi_1\dots i_p}, \quad (g_\partial)_{vr} = h^{N(\frac{1}{2}-\frac{n}{n+p+1})} f_{vr}, \\
(g_\partial)_{vv} &= h^{1-\frac{Nn}{n+p+1}} f_{vv}, \quad \text{Tr}(g_\partial)_{ij} = h^{-\frac{Nn}{n+p+1}} \text{Tr} f_{ij}, \quad \phi_\partial = f_\phi, \\
\text{Vector: } (g_\partial)_{vi} &= h^{-\frac{Nn}{n+p+1}} f_{vi}, \quad (g_\partial)_{ri} = h^{N(\frac{1}{2}-\frac{n}{n+p+1})} f_{ri}, \\
\text{Tensor: } (\bar{g}_\partial)_{ij} &= h^{-\frac{Nn}{n+p+1}} \bar{f}_{ij},
\end{aligned} \tag{C.1.6}$$

where $(\bar{g}_\partial)_{ij} \equiv (g_\partial)_{ij} - \frac{1}{p}(\text{Tr}(g_\partial)_{kl})\delta_{ij}$, i.e., the traceless part of $(g_\partial)_{ij}$ and $\bar{f}_{ij} \equiv f_{ij} - \frac{1}{p}(\text{Tr} f_{kl})\delta_{ij}$. Similarly, the scalar sector of the Maxwell charged system contains five scalars while the vector and tensor sector contain three vectors and one tensor, respectively. Here we parameterize the $\text{SO}(p)$ perturbations in the three sectors according to

$$\begin{aligned}
\text{Scalar: } (A_\partial)_v &= -\sqrt{N\gamma_0(1+\gamma_0)} \frac{r_0^n}{r^n} h^{-1} a_v, \quad (g_\partial)_{vr} = h^{N(-\frac{1}{2}+\frac{1}{n+p+1})} f_{vr}, \\
(g_\partial)_{vv} &= h^{1-N(\frac{n+p}{n+p+1})} f_{vv}, \quad \text{Tr}(g_\partial)_{ij} = h^{\frac{N}{n+p+1}} \text{Tr} f_{ij}, \quad \phi_\partial = f_\phi, \\
\text{Vector: } (A_\partial)_i &= -\sqrt{N\gamma_0(1+\gamma_0)} a_i, \quad (g_\partial)_{vi} = h^{\frac{N}{n+p+1}} f_{vi}, \\
(g_\partial)_{ri} &= h^{N(-\frac{1}{2}+\frac{1}{n+p+1})} f_{ri}, \\
\text{Tensor: } (\bar{g}_\partial)_{ij} &= h^{\frac{N}{n+p+1}} \bar{f}_{ij}.
\end{aligned} \tag{C.1.7}$$

As explained in the outline of Sec. 5.2.1, we will work in a gauge where all the rest of the components of ds_∂^2 and A_∂ are taken to be zero. The consistency of this gauge choice can be checked a posteriori. We now proceed with solving the resulting EOMs to first order in the derivatives. The EOMs (from the action (5.2.1)) take the form,

$$\begin{aligned}
R_{\mu\nu} - 2\nabla_\mu\phi\nabla_\nu\phi - S_{\mu\nu} &\equiv \mathcal{E}_{\mu\nu} + \mathcal{O}(\partial^2) = 0, \\
\nabla_\mu \left(e^{a\phi} \mathcal{F}^\mu_{\rho_0\dots\rho_q} \right) &\equiv \mathcal{M}_{\rho_0\dots\rho_q} + \mathcal{O}(\partial^2) = 0, \\
g^{\mu\nu}\nabla_\mu\nabla_\nu\phi + \frac{a}{4(q+2)!} \mathcal{F}^2 &\equiv \mathcal{E}_{(\phi)} + \mathcal{O}(\partial^2) = 0.
\end{aligned} \tag{C.1.8}$$

Here $q = 0$ for the Maxwell system and $q = p$ for the fundamentally charged system and \mathcal{F} denotes the dilaton-weighted field strength $\mathcal{F} = e^{a\phi}dA$. Moreover, we have defined

$$S_{\mu\nu} = \frac{1}{2(q+1)!} \left(\mathcal{F}_{\mu\rho_0\dots\rho_q} \mathcal{F}_\nu{}^{\rho_0\dots\rho_q} - \frac{q+1}{(D-2)(q+2)} \mathcal{F}^2 g_{\mu\nu} \right). \quad (\text{C.1.9})$$

Notice that the right-hand sides of the EOMs (C.1.8), $\mathcal{E}_{\mu\nu}$, $\mathcal{M}_{\rho_0\dots\rho_q}$ and $\mathcal{E}_{(\phi)}$ are all $\mathcal{O}(\partial)$. The parameterization of the ansätze (C.1.6) and (C.1.7) are exactly chosen in such a way that the resulting equations only contain derivatives of f_{ab} , $a_{0\dots q}$ and f_ϕ and will thus be directly integrable as explained below Eq. (5.2.13). In the two subsequent sections we provide the most important details for solving the two systems.

C.2 Solving the Maxwell system

In this section we give some of the details for solving the three $\text{SO}(p)$ sectors for the Maxwell charged system.

Scalars of $\text{SO}(p)$

The scalar sector consists of eight independent equations which correspond to the vanishing of the components: \mathcal{E}_{vv} , \mathcal{E}_{rv} , \mathcal{E}_{rr} , $\text{Tr}\mathcal{E}_{ij}$, $\mathcal{E}_{\Omega\Omega}$, $\mathcal{E}_{(\phi)}$, \mathcal{M}_v and \mathcal{M}_r (cf. Eq. (C.1.8)).

Constraint equations: There are two constraint equations; $\mathcal{E}_v^r = 0$ and $\mathcal{M}_r = 0$. The two equations are solved consistently by

$$\partial_v r_0 = -\frac{r_0(1 - (N-2)\gamma_0)}{n+1 + (2-n(N-2))\gamma_0} \partial_i u^i, \quad \partial_v \gamma_0 = -\frac{2\gamma_0(1 + \gamma_0)}{n+1 + (2-n(N-2))\gamma_0} \partial_i u^i. \quad (\text{C.2.1})$$

The first equation corresponds to conservation of energy while the second equation can be interpreted as current conservation. These are equivalent to the scalar conservation equations given by (5.2.6) in the rest frame. Under the assumption that the fluid configuration satisfies the above constraints one is left with six dynamical equations with five unknowns.

Dynamical equations: The coupled system constituted by the dynamical equations is quite intractable. One approach to obtaining the solution to the system is to decouple the trace function $\text{Tr}f_{ij}$. Once $\text{Tr}f_{ij}$ is known, it turns out, as will be presented below,

that all the other functions can be obtained while ensuring that they are regular on the horizon. It is possible to obtain a 3rd order ODE for $\text{Tr}f_{ij}$ by decoupling it through a number of steps. However, first it is useful to note that the particular combination of $\text{Tr}\mathcal{E}_{ij}$ and $\mathcal{E}_{(\phi)}$ leads to the equation

$$\frac{d}{dr} \left[r^{n+1} f(r) T'(r) \right] = -(\partial_i u^i) r^n \left(2(n+1) + C \frac{r_0^n}{r^n} \gamma_0 \right) h(r)^{\frac{N}{2}-1} , \quad (\text{C.2.2})$$

where we have defined the constant $C \equiv 2 - n(N - 2)$ and

$$T(r) = \text{Tr}f_{ij}(r) + \frac{4p}{(n+p+1)a} f_\phi(r) . \quad (\text{C.2.3})$$

As we shall see this equation is very reminiscent of the equations for the tensor perturbations for which we know the solution to be

$$T(r) = c_T^{(1)} - 2(\partial_i u^i) \left(r_\star - \frac{r_0}{n} (1 + \gamma_0)^{\frac{N}{2}} \log f(r) \right) . \quad (\text{C.2.4})$$

Here we have imposed horizon regularity, since $\text{Tr}f_{ij}$ and f_ϕ are individually regular on the horizon. Once f_ϕ is known in terms of $\text{Tr}f_{ij}$ we can use \mathcal{E}_{rr} to eliminate f'_{rv} and then take linear combinations of the remaining equations. The resulting combinations can then be used to eliminate f'_{vv} and f''_{vv} such that one is left with two equations in terms of a_v and $\text{Tr}f_{ij}$ which can then be decoupled by standard means. The resulting equation is schematically of the form

$$H_3^{(n,p)}(r) [\text{Tr}f_{ij}]'''(r) + H_2^{(n,p)}(r) [\text{Tr}f_{ij}]''(r) + H_1^{(n,p)}(r) [\text{Tr}f_{ij}]'(r) = S_{\text{Tr}}(r) , \quad (\text{C.2.5})$$

where H_1, H_2 and H_3 do not depend on the sources (world-volume derivatives) and the source term S_{Tr} only depends on the scalar $\partial_i u^i$. The expressions for these functions are however very long and have therefore been omitted. After some work, one finds that the equation is solved by

$$\text{Tr}f_{ij}(r) = c_{\text{Tr}}^{(1)} + \gamma_0 c_{\text{Tr}}^{(2)} G(r) - 2(\partial_i u^i) \text{Tr}f_{ij}^{(s)}(r) , \quad (\text{C.2.6})$$

where the terms containing the two integration constants $c_{\text{Tr}}^{(1)}$ and $c_{\text{Tr}}^{(2)}$ correspond to the homogeneous solution. The entire family of homogeneous solutions to equation (C.2.5) of course has an additional one-parameter freedom which has been absorbed in

the particular solution $\text{Tr} f_{ij}^{(s)}(r)$ and been used to ensure horizon regularity.¹ With the introduction of $c_{\text{Tr}}^{(1)}$ we can safely take $c_T^{(1)} = 0$. The function G is given by

$$G(r) = -\frac{N}{n+p+1} \frac{r_0^n}{r^n} \left(2 + \left(2 - \frac{Nn}{n+p+1} \right) \frac{r_0^n}{r^n} \gamma_0 \right)^{-1}, \quad (\text{C.2.7})$$

and has an intricate relation to the gauge choice $(g_\partial)_{\Omega\Omega} = 0$ as we shall see later. The particular solution which is regular on the horizon is given by

$$\text{Tr} f_{ij}^{(s)}(r) = \frac{r_0}{n} (1 + \gamma_0)^{\frac{N}{2}} \alpha \gamma_0 G(r) + \left(r_\star - \frac{r_0}{n} (1 + \gamma_0)^{\frac{N}{2}} \log f(r) \right) (1 + \beta \gamma_0 G(r)), \quad (\text{C.2.8})$$

with the coefficients

$$\alpha = 2p \left(\frac{2(n+1) + C\gamma_0}{(n+1)^2 + C\gamma_0(2(n+1) + C\gamma_0)} \right) \quad \text{and} \quad \beta = p \left(\frac{n+2 + C\gamma_0}{n+1 + C\gamma_0} \right). \quad (\text{C.2.9})$$

With $\text{Tr} f_{ij}$ (and f_ϕ) given, the equation $\mathcal{E}_{rr} = 0$ will provide the derivative of f_{rv} ,

$$f'_{rv}(r) = \frac{r}{\left(2(n+1) + C \frac{r_0^n}{r^n} \gamma_0 \right) h(r)^{\frac{N}{2}-1}} \left(\frac{d}{dr} \left[h(r)^{\frac{N}{2}} [\text{Tr} f_{ij}]'(r) \right] - 4a \frac{d}{dr} \left[h(r)^{\frac{N}{2}} \right] f'_\phi(r) \right). \quad (\text{C.2.10})$$

Since this equation is a 1st order ODE, the regularity of the horizon is ensured by $\text{Tr} f_{ij}$. Note that it is possible to perform integration by parts and use that the derivative of r_\star takes a simpler form. One can thereafter obtain an analytical expression for the resulting integral. This expression is, however, quite cumbersome and we therefore only provide its large r asymptotics

$$f_{rv}(r) \approx f_{rv}^{(h)}(r) + (\partial_i u^i) \sum_{k=1}^{\infty} \frac{r_0^{nk}}{r^{nk}} \left[\alpha_{rv}^{(k)} r + \beta_{rv}^{(k)} r_0 \right]. \quad (\text{C.2.11})$$

Here the homogeneous solution takes the form

$$f_{rv}^{(h)}(r) = c_{rv} + \gamma_0 N c_{\text{Tr}}^{(2)} \frac{r_0^n}{r^n} \left(\frac{2p(n+p+1) + (n+p)(2p+C) \frac{r_0^n}{r^n} \gamma_0}{2p \left(2(n+p+1) + (2p+C) \frac{r_0^n}{r^n} \gamma_0 \right)^2} \right), \quad (\text{C.2.12})$$

¹Note that equation (C.2.5) has been derived under the assumption that $\partial_i u^i \neq 0$. This especially means that when there are no sources the one-parameter freedom disappears in accordance with (C.2.6).

and the particular solution is given in terms of the coefficients $\alpha_{rv}^{(k)}$ and $\beta_{rv}^{(k)}$ which depend on n, p, a , and γ_0 . These coefficients are in general very long and their expressions are therefore omitted.

Using the expression for f'_{rv} in terms of $\text{Tr}f_{ij}$, the Maxwell equation $\mathcal{M}_v = 0$ becomes a 2nd order ODE for the gauge field perturbation,

$$\frac{d}{dr} \left[\frac{1}{r^{n-1}} a'_v(r) \right] = \frac{nr^2}{\left(2(n+1) + C \frac{r_0^n}{r^n} \gamma_0\right)} \frac{d}{dr} \left[\frac{1}{r^{n+1}} [\text{Tr}f_{ij}]'(r) + 4a \frac{(n+1)}{r^{n+2}} f'_\phi(r) \right] . \quad (\text{C.2.13})$$

This equation is solved by a double integration. The inner integral is manifestly regular at the horizon, one can therefore work directly with the asymptotic behavior of the right-hand side before performing the integrations. The large r behavior of the perturbation function is thus found to be

$$a_v(r) \approx a_v^{(h)}(r) + (\partial_i u^i) \left(-\frac{n}{n-1} r + \sum_{k=1}^{\infty} \frac{r_0^{nk}}{r^{nk}} \left[\alpha_v^{(k)} r + \beta_v^{(k)} r_0 \right] \right) , \quad (\text{C.2.14})$$

where the first term constitute the homogeneous solution,

$$a_v^{(h)}(r) = c_v^{(1)} r^n + c_v^{(2)} - \gamma_0 c_{\text{Tr}}^{(2)} \frac{r_0^n}{r^n} \left(\frac{2p + C}{2p \left(2(n+p+1) + (2p+C) \frac{r_0^n}{r^n} \gamma_0\right)} \right) , \quad (\text{C.2.15})$$

and the particular solution is given in terms of the coefficients $\alpha_v^{(k)}$ and $\beta_v^{(k)}$ depending on n, p, a , and γ_0 .

The last perturbation function f_{vv} can be obtained from $\text{Tr}\mathcal{E}_{ij} = 0$ which provides a 1st order ODE for the perturbation. Horizon regularity is therefore ensured by the horizon regularity of $\text{Tr}f_{ij}$. Using the expression for f'_{rv} in terms of $\text{Tr}f_{ij}$ the equation is schematically of the form

$$f'_{vv}(r) = G_1 [\text{Tr}f_{ij}(r)] + G_2 [a_v(r)] + G_3 [f_\phi(r)] + S_{ii}(r) , \quad (\text{C.2.16})$$

where G_1, G_2, G_3 are differential operators and the source S_{ii} depends on $\partial_i u^i$. Again, the full expressions have been omitted and we only provide the large r behavior,

$$f_{vv}(r) \approx f_{vv}^{(h)}(r) + (\partial_i u^i) \sum_{k=1}^{\infty} \frac{r_0^{nk}}{r^{nk}} \left[\alpha_{vv}^{(k)} r + \beta_{vv}^{(k)} r_0 \right] , \quad (\text{C.2.17})$$

with the homogeneous part given by

$$f_{vv}^{(h)}(r) = c_{vv}^{(1)} + \frac{r_0^n}{r^n} \frac{1}{h(r)} \left(-2(1 + \gamma_0)(c_v^{(2)} - c_v^{(1)} r_0^n \gamma_0) + c_{\text{Tr}}^{(1)} \frac{(n + p + 1)(1 + \gamma_0)a^2}{2p} \right. \\ \left. + \left(\frac{(n + p + 1 + (2p + C)\gamma_0)h(r) - p\gamma_0 N f(r)}{p(2(n + p + 1) + (2p + C)\frac{r_0^n}{r^n}\gamma_0)} \right) c_{\text{Tr}}^{(2)} \right), \quad (\text{C.2.18})$$

and where the coefficients $\alpha_{vv}^{(k)}$ and $\beta_{vv}^{(k)}$ again depend on n, p, a , and γ_0 .

Finally, one must ensure that the remaining equations coming from \mathcal{E}_{vv} and the angular directions ($\mathcal{E}_{\Omega\Omega} = 0$) are satisfied. This will require the following relation

$$c_{vv}^{(1)} = -2c_{rv}. \quad (\text{C.2.19})$$

This completes the analysis of the scalar sector. The remaining undetermined integration constants are thus: $c_{\text{Tr}}^{(1)}, c_{\text{Tr}}^{(2)}, c_{rv}, c_v^{(1)}, c_v^{(2)}$. Note that the above functions reproduce the neutral case as $\gamma_0 \rightarrow 0$.

Vectors of $\text{SO}(p)$

The vector sector consists of $3p$ independent equations which correspond to the vanishing of the components: $\mathcal{E}_{ri}, \mathcal{E}_{vi}$ and \mathcal{M}_i .

Constraint equations: The constraint equations are given by the Einstein equations $\mathcal{E}^r_i = 0$ and are solved by

$$\partial_i r_0 = r_0(1 + N\gamma_0)\partial_v u_i, \quad (\text{C.2.20})$$

which are equivalent to conservation of stress-momentum. These are part of the conservation equations given by (5.2.6) in the rest frame. Similar to above we now proceed solving for the first-order corrections to the metric and gauge field under the assumption that the fluid profile satisfies the above constraint (C.2.20).

Dynamical equations: The remaining equations consist of p pairs of one Einstein equation $\mathcal{E}_{vi} = 0$ and one Maxwell equation $\mathcal{M}_i = 0$. The structure of these equations is the same as in the scalar sector. The Einstein equation $\mathcal{E}_{vi} = 0$ is schematically of

the form,

$$L_3^{(n,p)}(r)f_{vi}''(r) + L_2^{(n,p)}(r)f_{vi}'(r) + L_1^{(n,p)}(r)a_i'(r) = S_{vi}(r) \quad , \quad (\text{C.2.21})$$

while the Maxwell equation $\mathcal{M}_i = 0$ is,

$$M_3^{(n,p)}(r)a_i''(r) + M_2^{(n,p)}(r)a_i'(r) + M_1^{(n,p)}(r)f_{vi}'(r) = S_i(r) \quad . \quad (\text{C.2.22})$$

We omit the expressions for the functions L_k and M_k , $k = 1, \dots, 3$.

To decouple the system we differentiate \mathcal{E}_{vi} once and eliminate all $a_i(r)$ terms in \mathcal{M}_i . Doing so, one obtains a 3rd order ODE for $f_{vi}(r)$ which can be written on the form

$$\frac{d}{dr} \left[\frac{r^{n+1}f(r)}{h^N} \left(1 - c_1 \frac{r_0^n}{r^n} \right)^2 \frac{d}{dr} \left[\frac{r^{n+1}h^{N+1}}{\left(1 - c_1 \frac{r_0^n}{r^n} \right)} f_{vi}'(r) \right] \right] = S_{vi}(r) \quad , \quad c_1 \equiv \frac{N-1}{1+N\gamma_0} \gamma_0 \quad . \quad (\text{C.2.23})$$

It is possible to perform the first two integrations analytically and ensure regularity at the horizon. The first integration is straightforward while the second involves several non-trivial functions. The large r behavior of the f_{vi} function is found to be

$$f_{vi}(r) \approx c_{vi}^{(1)} - \left(1 - \frac{f(r)}{h(r)^N} \right) c_{vi}^{(2)} - (\partial_v u_i)r + \sum_{k=1}^{\infty} \frac{r_0^{nk}}{r^{nk}} \left[\alpha_{vi}^{(k)} r + \beta_{vi}^{(k)} r_0 \right] \quad , \quad (\text{C.2.24})$$

where the first two terms constitute the homogeneous solution and we find, in particular, that in order to ensure horizon regularity one must have

$$\beta_{vi}^{(2)} = -\frac{N}{4n} \left(\frac{2\gamma_0(1+\gamma_0)(\partial_v u_i) + (\partial_i \gamma_0)}{(1+\gamma_0)^{\frac{N}{2}-1}(1+N\gamma_0)} \right) \quad . \quad (\text{C.2.25})$$

The remaining set of coefficients $\alpha_{vi}^{(k)}$ and $\beta_{vi}^{(k)}$ are in general complicated expressions depending on the parameters in the problem. We therefore omit them as they provide no insight. Also, we notice that the sum in the function (C.2.24) vanishes in the neutral limit.

Once the solution of f_{vi} is given we can use \mathcal{E}_{vi} to determine a_i ,

$$a_i(r) \approx c_i^{(1)} + \frac{r_0^n}{r^n} \frac{1}{h(r)} c_{vi}^{(2)} + \sum_{k=1}^{\infty} \frac{r_0^{nk}}{r^{nk}} \left[\alpha_i^{(k)} r + \beta_i^{(k)} r_0 \right] \quad , \quad (\text{C.2.26})$$

where the first two terms correspond to the homogeneous solution. Again, we choose to omit the coefficients $\alpha_i^{(k)}$ and $\beta_i^{(k)}$. The remaining undetermined integration constants are thus: $c_i^{(1)}$, $c_{vi}^{(1)}$, and $c_{vi}^{(2)}$.

Tensors of $\text{SO}(p)$

There are no constraint equations in the tensor sector which consists of $p(p+1)/2 - 1$ dynamical equations given by

$$\mathcal{E}_{ij} - \frac{\delta_{ij}}{p} \text{Tr}(\mathcal{E}_{ij}) = 0 \quad . \quad (\text{C.2.27})$$

This gives an equation for each component of the traceless symmetric perturbation functions \bar{f}_{ij} ,

$$\frac{d}{dr} \left[r^{n+1} f(r) \bar{f}'_{ij}(r) \right] = -\sigma_{ij} r^n \left(2(n+1) + C \frac{r_0^n}{r^n} \gamma_0 \right) h(r)^{\frac{N}{2}-1} \quad , \quad (\text{C.2.28})$$

with the same structure as Eq. C.2.2. The spatial part of the shear tensor is

$$\sigma_{ij} = \partial_{(i} u_{j)} - \frac{1}{p} \delta_{ij} \partial_k u^k \quad . \quad (\text{C.2.29})$$

The solution is given by,

$$\bar{f}_{ij}(r) = \bar{c}_{ij} - 2\sigma_{ij} \left(r_\star - \frac{r_0}{n} (1 + \gamma_0)^{\frac{N}{2}} \log f(r) \right) \quad , \quad (\text{C.2.30})$$

where horizon regularity has been imposed and the integration constant(s) \bar{c}_{ij} is symmetric and traceless.

C.3 Solving the fundamentally charged system

As already explained, many of the differential equations appearing in fundamentally charged system are similar to the ones appearing for the Maxwell system. Instead of repeating these, in this section we provide the most important differences.

Scalars of $SO(p)$

The scalar sector consists of eight independent equations which correspond to the vanishing of the components: $\mathcal{E}_{vv}, \mathcal{E}_{rv}, \mathcal{E}_{rr}, \text{Tr}\mathcal{E}_{ij}, \mathcal{E}_{\Omega\Omega}, \mathcal{E}_{(\phi)}, \mathcal{M}_{a_1\dots a_{p+1}}$ and $\mathcal{M}_{r_{i_1}\dots i_p}$ with $i \in \{\sigma^i\}$.

Constraint equations: There are two constraint equations; $\mathcal{E}_v^r = 0$ and $\mathcal{M}_{r_{i_1}\dots i_p} = 0$ with $i \in \{\sigma^i\}$. The two equations are solved consistently by

$$\partial_v r_0 = -\frac{r_0(1+2\gamma_0)}{n+1+(2-n(N-2))\gamma_0}\partial_i u^i, \quad \partial_v \gamma_0 = -\frac{2n\gamma_0(1+\gamma_0)}{n+1+(2-n(N-2))\gamma_0}\partial_i u^i. \quad (\text{C.3.1})$$

The first equation corresponds to conservation of energy while the second equation can be interpreted as the charge density being constant in time.

Dynamical equations: After the constraint Eqs. (C.3.1) have been imposed one is left with a system very similar to the one obtained in the presence of Maxwell charge ($q = 0$). It consists of the six equations given by the components: $\mathcal{E}_{vv}, \mathcal{E}_{rr}, \text{Tr}\mathcal{E}_{ij}, \mathcal{E}_{\Omega\Omega}, \mathcal{E}_{(\phi)}$, and $\mathcal{M}_{a_1\dots a_{p+1}}$.

The particular combination of $\text{Tr}\mathcal{E}_{ij}$ and $\mathcal{E}_{(\phi)}$ gives Eq. (C.2.2), but now with the relation

$$T(r) = \text{Tr}f_{ij}(r) - \frac{4np}{(n+p+1)a}f_\phi(r), \quad (\text{C.3.2})$$

and is solved by the same expression given by Eq. (C.2.4). The equation for the trace $\text{Tr}f_{ij}$ is again similar to the $q = 0$ case and the solution can be put on the form given by (C.2.6) with (C.2.8), but where

$$G(r) = -\frac{N(p+1)r_0^n}{n+p+1r^n} \left(2 + \left(2 - \frac{Nn(p+1)}{n+p+1} \right) \frac{r_0^n}{r^n} \gamma_0 \right)^{-1}, \quad (\text{C.3.3})$$

and the coefficients are given by the expressions

$$\alpha = \frac{2pn^2}{p+1} \left(\frac{2(n+1) + C\gamma_0}{(n+1)^2 + C\gamma_0(2(n+1) + C\gamma_0)} \right) \quad \text{and} \quad \beta = \frac{p}{p+1} \left(\frac{n^2}{n+1 + C\gamma_0} \right). \quad (\text{C.3.4})$$

The solution of $\text{Tr}f_{ij}$ dictates the perturbation of the dilaton field through Eq. (C.3.2). With $\text{Tr}f_{ij}$ determined, one can find the remaining perturbation functions as follows: f_{rv} from \mathcal{E}_{rr} and f_{vv} from $\text{Tr}\mathcal{E}_{ij}$ by a single integration while the gauge field perturbation

$a_{vi_1\dots i_p}$ can be obtained from $\mathcal{M}_{va_1\dots a_p}$ by a double integration. Finally, we note that remaining undetermined integration constants are equivalent to the $q = 0$ case.

Vectors of $\text{SO}(p)$

The vector sector consists of $3p$ independent equations which correspond to the vanishing of the components: \mathcal{E}_{ri} , \mathcal{E}_{vi} and $\mathcal{M}_{vrj_1\dots j_{p-1}}$ with $j \neq i$.

Constraint equations: The constraint equations are given by the Einstein equations $\mathcal{E}_i^r = 0$ and $\mathcal{M}_{vrj_1\dots j_{p-1}} = 0$ with $j \neq i$. For each spatial index i one has a pair of equations that are solved by

$$\partial_i r_0 = \frac{r_0(1 + 2\gamma_0)}{1 - (nN - 2)\gamma_0} \partial_v u_i, \quad \partial_i \gamma_0 = -\frac{2n\gamma_0(1 + \gamma_0)}{1 - (nN - 2)\gamma_0} \partial_v u_i. \quad (\text{C.3.5})$$

The first equation corresponds to conservation of stress-momentum while the second equation censure that the charge density does not have any spatial gradients over the world-volume. We see that the current is more constrained compared to the case with Maxwell charge which is tied to the fact that the p -brane charge is not able to redistribute itself.

Dynamical Equations: After the constraint Eqs. (C.3.5) have been imposed the remaining p equations consist of 2nd order differential equations $\mathcal{E}_{vi} = 0$ of the form

$$\frac{d}{dr} \left[r^{n+1} f'_{vi}(r) \right] = S_{vi}(r). \quad (\text{C.3.6})$$

Each equation can be integrated analytically in order to obtain the perturbation functions f_{vi} . Horizon regularity is ensured due to the form of the differential operator. We note that the homogeneous solution gives rise to two integration constants: $c_{vi}^{(1)}$ and $c_{vi}^{(2)}$.

Tensors of $\text{SO}(p)$

It turns out that with the parametrization given by Eq. (C.1.6), the equations for the tensor perturbations take the exact same form as found for the Maxwell charge given by the form (C.2.28). The solution is therefore,

$$\bar{f}_{ij}(r) = \bar{c}_{ij} - 2\sigma_{ij} \left(r_* - \frac{r_0}{n} (1 + \gamma_0)^{\frac{N}{2}} \log f(r) \right), \quad (\text{C.3.7})$$

with σ_{ij} given by Eq. (C.2.29) and regularity of the horizon has been imposed. The constant \bar{c}_{ij} is again symmetric and traceless. Because of this closed-form expression, the shear viscosity will take the same form as found for the system with Maxwell charge.

C.4 Fixing the integration constants

We have determined the first-order derivative corrected solution for both types of branes. Both solutions are completely determined up to a set of integration constants, $c_{\text{Tr}}^{(1)}$, $c_{\text{Tr}}^{(2)}$, $c_v^{(1)}$, $c_v^{(2)}$, $c_{vi}^{(1)}$, $c_{vi}^{(2)}$, c_{rv} , \bar{c}_{ij} (and $c_i^{(1)}$ for $q = 0$). As explained in Sec. 5.2.1, these constants are fixed by virtue of asymptotic flatness and choice of fluid frame (gauge). The latter freedom exactly corresponds to constant $\mathcal{O}(\partial)$ shifts of the parameters of the $\mathcal{O}(\partial^0)$ fields, i.e., it parameterizes the homogeneous solution to the above differential equations. Indeed, for the zeroth order Maxwell solution (C.1.4), consider order $\mathcal{O}(\partial)$ constant shifts $r_0 \rightarrow r_0 + \delta r_0$, $\gamma_0 \rightarrow \gamma_0 + \delta \gamma_0$ and a constant gauge shift $a_v \rightarrow a_v + \delta a_v$. Moreover, by redefining the r coordinate as,

$$r \rightarrow r (1 + \gamma_0(n\delta \log r_0 + \delta \log \gamma_0)G(r)) \quad , \quad (\text{C.4.1})$$

with $G(r)$ given by (C.2.7), the angular directions do not receive first-order contributions in accordance with the gauge choice $(g_\partial)_{\Omega\Omega} = 0$. The resulting expressions after the shifts and coordinate transformation are of course still solutions and the overall change exactly corresponds to the homogeneous solution to the above differential equations in the scalar sector. More precisely, one can relate the integration constants to the shifts by,

$$\begin{aligned} c_{\text{Tr}}^{(2)} &= -2p(n\delta \log r_0 + \delta \log \gamma_0) \quad , \quad c_v^{(1)} = -\frac{\delta a_v}{r_0^n \sqrt{N\gamma_0(1+\gamma_0)}} \quad , \\ c_v^{(2)} &= -n\delta \log r_0 - \frac{1+2\gamma_0}{2(1+\gamma_0)}\delta \log \gamma_0 - \frac{\gamma_0}{\sqrt{N\gamma_0(1+\gamma_0)}}\delta a_v \quad . \end{aligned} \quad (\text{C.4.2})$$

For the vector sector one finds that the homogeneous part of the above solution corresponds to global constant shift of the boost $u_i \rightarrow u_i + \delta u_i$ and in the gauge $a_i \rightarrow a_i + \delta a_i$. With the same choice of radial coordinate, one has

$$c_{vi}^{(2)} = \delta u_i \quad , \quad c_i^{(1)} = -\frac{\delta a_i}{\sqrt{N\gamma_0(1+\gamma_0)}} \quad . \quad (\text{C.4.3})$$

Similar expressions relating the shifts to the integration constants can be derived for the fundamentally charged solution. In the following we require all the $\mathcal{O}(\partial)$ shifts to vanish. In the effective fluid description this exactly corresponds to choosing the Landau frame. This fixes the integration constants, $c_{\text{Tr}}^{(2)} = c_v^{(1)} = c_v^{(2)} = c_{vi}^{(2)} = 0$ (and $c_i^{(1)} = 0$ for $q = 0$).

To fix the remaining integration constants, we now impose asymptotic flatness to $\mathcal{O}(\partial)$. In order to do so, we must first transform our results back into Schwarzschild form. In addition to making the asymptotics more transparent, this is also needed for extracting the effective hydrodynamic currents. In order to change coordinates, we use the inverse of the transformation stated in equation (C.1.1) to $\mathcal{O}(\partial)$. The inverse transformation is worked out iteratively order by order. To first order, the transformation from EF to Schwarzschild coordinates is found to be,

$$\begin{aligned} v &= t + r_\star + \left[(t + r_\star) (\partial_{r_0} r_\star \partial_t r_0 + \partial_{\gamma_0} r_\star \partial_t \gamma_0) + x^i (\partial_{r_0} r_\star \partial_i r_0 + \partial_{\gamma_0} r_\star \partial_i \gamma_0) \right] + \mathcal{O}(\partial^2) \ , \\ \sigma^i &= x^i + \left[(t + r_\star) \partial_t u^i + \sigma^j \partial_j u^i \right] r_\star + \mathcal{O}(\partial^2) \ . \end{aligned} \quad (\text{C.4.4})$$

It is now possible to express all the fields in Schwarzschild coordinates and impose asymptotic flatness. This leads to

$$c_{rv} = 0 \ , \quad c_{vi}^{(1)} = 0 \ , \quad c_{\text{Tr}}^{(1)} = 0 \ , \quad \bar{c}_{ij} = 0 \ , \quad (\text{C.4.5})$$

for both types of branes. Having obtained the full first-order derivative corrected asymptotically flat solutions for both the Maxwell and fundamentally charged brane, it is now possible to read off the effective hydrodynamic currents using standard methods (see also [43]). Our results for the transport coefficients are presented in Sec. 5.2.2 and 5.3.1.

References

- [1] A. Di Dato, “Kaluza-Klein reduction of relativistic fluids and their gravity duals,” *JHEP* **1312** (2013) 087, [arXiv:1307.8365 \[hep-th\]](#).
- [2] A. Di Dato and M. B. Fröb, “Mapping AdS to dS spaces and back,” *Phys.Rev.* **D91** (2015) no. 6, 064028, [arXiv:1404.2785 \[hep-th\]](#).
- [3] A. Di Dato, J. Gath, and A. V. Pedersen, “Probing the Hydrodynamic Limit of (Super)gravity,” *JHEP* **1504** (2015) 171, [arXiv:1501.05441 \[hep-th\]](#).
- [4] C. Misner, K. Thorne, and J. Wheeler, *Gravitation*. W. H. Freeman, San Francisco, 1973.
- [5] R. M. Wald, *General Relativity*. The University of Chicago Press, 1984.
- [6] W. Israel, “Event horizons in static vacuum space-times,” *Phys. Rev.* **164** (Dec, 1967) 1776–1779.
- [7] D. C. Robinson, “Uniqueness of the kerr black hole,” *Phys. Rev. Lett.* **34** (Apr, 1975) 905–906.
- [8] J. D. Bekenstein, “Black holes and entropy,” *Phys. Rev. D* **7** (Apr, 1973) 2333–2346.
- [9] S. Hawking, “Particle Creation by Black Holes,” *Commun.Math.Phys.* **43** (1975) 199–220.
- [10] J. Bardeen, B. Carter, and S. Hawking, “The four laws of black hole mechanics,” *Communications in Mathematical Physics* **31** (1973) no. 2, 161–170.
- [11] S. Hawking, “Breakdown of Predictability in Gravitational Collapse,” *Phys.Rev.* **D14** (1976) 2460–2473.
- [12] S. D. Mathur, “What Exactly is the Information Paradox?,” *Lect.Notes Phys.* **769** (2009) 3–48, [arXiv:0803.2030 \[hep-th\]](#).
- [13] J. Polchinski, “What is String Theory?,” [arXiv:9411028 \[hep-th\]](#).
- [14] R. Emparan and H. S. Reall, “Black Holes in Higher Dimensions,” *Living Rev.Rel.* **11** (2008) 6, [arXiv:0801.3471 \[hep-th\]](#).
- [15] S. Hollands and A. Ishibashi, “Black hole uniqueness theorems in higher dimensional spacetimes,” *Class.Quant.Grav.* **29** (2012) 163001, [arXiv:1206.1164 \[gr-qc\]](#).

-
- [16] O. J. Dias, P. Figueras, R. Monteiro, J. E. Santos, and R. Emparan, “Instability and new phases of higher-dimensional rotating black holes,” *Phys.Rev.* **D80** (2009) 111701, [arXiv:0907.2248 \[hep-th\]](#).
- [17] C. Helfgott, Y. Oz, and Y. Yanay, “On the topology of black hole event horizons in higher dimensions,” *JHEP* **0602** (2006) 025, [arXiv:hep-th/0509013 \[hep-th\]](#).
- [18] R. Emparan and H. S. Reall, “Black Rings,” *Class.Quant.Grav.* **23** (2006) R169, [arXiv:hep-th/0608012 \[hep-th\]](#).
- [19] G. T. Horowitz and A. Strominger, “Black strings and P-branes,” *Nucl.Phys.* **B360** (1991) 197–209.
- [20] V. Niarchos, “Phases of Higher Dimensional Black Holes,” *Mod.Phys.Lett.* **A23** (2008) 2625–2643, [arXiv:0808.2776 \[hep-th\]](#).
- [21] R. Gregory and R. Laflamme, “Black strings and p-branes are unstable,” *Phys.Rev.Lett.* **70** (1993) 2837–2840, [arXiv:hep-th/9301052 \[hep-th\]](#).
- [22] R. Gregory and R. Laflamme, “The Instability of charged black strings and p-branes,” *Nucl.Phys.* **B428** (1994) 399–434, [arXiv:hep-th/9404071 \[hep-th\]](#).
- [23] R. Emparan and R. C. Myers, “Instability of ultra-spinning black holes,” *JHEP* **0309** (2003) 025, [arXiv:hep-th/0308056 \[hep-th\]](#).
- [24] J. C. V., “D-Brane Primer,” [arXiv:hep-th/0007170 \[hep-th\]](#).
- [25] J. M. Maldacena, “The Large N limit of superconformal field theories and supergravity,” *Int.J.Theor.Phys.* **38** (1999) 1113–1133, [arXiv:hep-th/9711200 \[hep-th\]](#).
- [26] E. Witten, “Anti-de Sitter space and holography,” *Adv.Theor.Math.Phys.* **2** (1998) 253–291, [arXiv:hep-th/9802150 \[hep-th\]](#).
- [27] O. Aharony, S. S. Gubser, J. M. Maldacena, H. Ooguri, and Y. Oz, “Large N field theories, string theory and gravity,” *Phys.Rept.* **323** (2000) 183–386, [arXiv:hep-th/9905111 \[hep-th\]](#).
- [28] L. Susskind, “The World as a hologram,” *J.Math.Phys.* **36** (1995) 6377–6396, [arXiv:hep-th/9409089 \[hep-th\]](#).
- [29] S. A. Hartnoll, “Lectures on holographic methods for condensed matter physics,” *Class.Quant.Grav.* **26** (2009) 224002, [arXiv:0903.3246 \[hep-th\]](#).
- [30] D. Mateos, “String Theory and Quantum Chromodynamics,” *Class.Quant.Grav.* **24** (2007) S713–S740, [arXiv:0709.1523 \[hep-th\]](#).
- [31] P. Kovtun, D. T. Son, and A. O. Starinets, “Viscosity in strongly interacting quantum field theories from black hole physics,” *Phys.Rev.Lett.* **94** (2005) 111601, [arXiv:hep-th/0405231 \[hep-th\]](#).

- [32] S. Bhattacharyya, V. E. Hubeny, S. Minwalla, and M. Rangamani, “Nonlinear Fluid Dynamics from Gravity,” *JHEP* **0802** (2008) 045, [arXiv:0712.2456 \[hep-th\]](#).
- [33] L. D. Landau and E. M. Lifshitz, *Fluid mechanics. Course of Theoretical Physics, Vol. 6*. 1987.
- [34] G. Policastro, D. T. Son, and A. O. Starinets, “The Shear viscosity of strongly coupled N=4 supersymmetric Yang-Mills plasma,” *Phys.Rev.Lett.* **87** (2001) 081601, [arXiv:hep-th/0104066 \[hep-th\]](#).
- [35] K. Maeda, M. Natsuume, and T. Okamura, “Viscosity of gauge theory plasma with a chemical potential from AdS/CFT,” *Phys.Rev.* **D73** (2006) 066013, [arXiv:hep-th/0602010 \[hep-th\]](#).
- [36] D. T. Son and A. O. Starinets, “Hydrodynamics of r-charged black holes,” *JHEP* **0603** (2006) 052, [arXiv:hep-th/0601157 \[hep-th\]](#).
- [37] N. Banerjee, J. Bhattacharya, S. Bhattacharyya, S. Dutta, R. Loganayagam, *et al.*, “Hydrodynamics from charged black branes,” *JHEP* **1101** (2011) 094, [arXiv:0809.2596 \[hep-th\]](#).
- [38] J. Erdmenger, M. Haack, M. Kaminski, and A. Yarom, “Fluid dynamics of R-charged black holes,” *JHEP* **0901** (2009) 055, [arXiv:0809.2488 \[hep-th\]](#).
- [39] S. Bhattacharyya, R. Loganayagam, S. Minwalla, S. Nampuri, S. P. Trivedi, *et al.*, “Forced Fluid Dynamics from Gravity,” *JHEP* **0902** (2009) 018, [arXiv:0806.0006 \[hep-th\]](#).
- [40] R. Emparan, T. Harmark, V. Niarchos, and N. A. Obers, “World-Volume Effective Theory for Higher-Dimensional Black Holes,” *Phys.Rev.Lett.* **102** (2009) 191301, [arXiv:0902.0427 \[hep-th\]](#).
- [41] R. Emparan, T. Harmark, V. Niarchos, and N. A. Obers, “Essentials of Blackfold Dynamics,” *JHEP* **1003** (2010) 063, [arXiv:0910.1601 \[hep-th\]](#).
- [42] J. Camps, R. Emparan, and N. Haddad, “Black Brane Viscosity and the Gregory-Laflamme Instability,” *JHEP* **1005** (2010) 042, [arXiv:1003.3636 \[hep-th\]](#).
- [43] J. Gath and A. V. Pedersen, “Viscous asymptotically flat Reissner-Nordström black branes,” *JHEP* **1403** (2014) 059, [arXiv:1302.5480 \[hep-th\]](#).
- [44] R. Emparan, V. E. Hubeny, and M. Rangamani, “Effective hydrodynamics of black D3-branes,” *JHEP* **1306** (2013) 035, [arXiv:1303.3563 \[hep-th\]](#).
- [45] J. Armas, J. Camps, T. Harmark, and N. A. Obers, “The Young Modulus of Black Strings and the Fine Structure of Blackfolds,” *JHEP* **1202** (2012) 110, [arXiv:1110.4835 \[hep-th\]](#).
- [46] J. Armas, J. Gath, and N. A. Obers, “Black Branes as Piezoelectrics,” *Phys.Rev.Lett.* **109** (2012) 241101, [arXiv:1209.2127 \[hep-th\]](#).

- [47] J. Armas, J. Gath, and N. A. Obers, “Electroelasticity of Charged Black Branes,” *JHEP* **1310** (2013) 035, [arXiv:1307.0504 \[hep-th\]](#).
- [48] R. Emparan, T. Harmark, V. Niarchos, N. A. Obers, and M. J. Rodriguez, “The Phase Structure of Higher-Dimensional Black Rings and Black Holes,” *JHEP* **0710** (2007) 110, [arXiv:0708.2181 \[hep-th\]](#).
- [49] M. M. Caldarelli, R. Emparan, and M. J. Rodriguez, “Black Rings in (Anti)-deSitter space,” *JHEP* **0811** (2008) 011, [arXiv:0806.1954 \[hep-th\]](#).
- [50] J. Armas and N. A. Obers, “Blackfolds in (Anti)-de Sitter Backgrounds,” *Phys.Rev.* **D83** (2011) 084039, [arXiv:1012.5081 \[hep-th\]](#).
- [51] M. M. Caldarelli, R. Emparan, and B. Van Pol, “Higher-dimensional Rotating Charged Black Holes,” *JHEP* **1104** (2011) 013, [arXiv:1012.4517 \[hep-th\]](#).
- [52] M. M. Caldarelli, J. Camps, B. Goutéraux, and K. Skenderis, “AdS/Ricci-flat correspondence and the Gregory-Laflamme instability,” *Phys.Rev.* **D87** (2013) no. 6, 061502, [arXiv:1211.2815 \[hep-th\]](#).
- [53] M. M. Caldarelli, J. Camps, B. Goutéraux, and K. Skenderis, “AdS/Ricci-flat correspondence,” *JHEP* **1404** (2014) 071, [arXiv:1312.7874 \[hep-th\]](#).
- [54] I. Kanitscheider and K. Skenderis, “Universal hydrodynamics of non-conformal branes,” *JHEP* **0904** (2009) 062, [arXiv:0901.1487 \[hep-th\]](#).
- [55] M. Rangamani, “Gravity and Hydrodynamics: Lectures on the fluid-gravity correspondence,” *Class.Quant.Grav.* **26** (2009) 224003, [arXiv:0905.4352 \[hep-th\]](#).
- [56] V. E. Hubeny, S. Minwalla, and M. Rangamani, “The fluid/gravity correspondence,” [arXiv:1107.5780 \[hep-th\]](#).
- [57] J. D. Brown and J. W. J. York, “Quasilocal energy and conserved charges derived from the gravitational action,” *Phys. Rev. D* **47** (1993) 1407–1419, [arXiv:gr-qc/9209012 \[gr-qc\]](#).
- [58] S. Hawking and G. Ellis, “The Large Scale Structure of Space-Time,”
- [59] R. C. Myers and M. Perry, “Black Holes in Higher Dimensional Space-Times,” *Annals Phys.* **172** (1986) 304.
- [60] R. Emparan and H. S. Reall, “A Rotating black ring solution in five-dimensions,” *Phys.Rev.Lett.* **88** (2002) 101101, [arXiv:hep-th/0110260 \[hep-th\]](#).
- [61] R. Emparan, “Rotating circular strings, and infinite nonuniqueness of black rings,” *JHEP* **0403** (2004) 064, [arXiv:hep-th/0402149 \[hep-th\]](#).
- [62] R. Emparan, T. Harmark, V. Niarchos, and N. A. Obers, “New Horizons for Black Holes and Branes,” *JHEP* **1004** (2010) 046, [arXiv:0912.2352 \[hep-th\]](#).
- [63] R. Emparan, “Blackfolds,” [arXiv:1106.2021 \[hep-th\]](#).

- [64] J. Camps, R. Emparan, P. Figueras, S. Giusto, and A. Saxena, “Black Rings in Taub-NUT and D0-D6 interactions,” *JHEP* **0902** (2009) 021, [arXiv:0811.2088 \[hep-th\]](#).
- [65] M. Duff, B. Nilsson, and C. Pope, “Kaluza-Klein Supergravity,” *Phys. Rept.* **130** (1986) 1–142.
- [66] C. N. Pope, “Lectures on Kaluza-Klein theory,” 2000. <http://people.physics.tamu.edu/pope/ihplec.pdf>.
- [67] B. Gouteraux, J. Smolic, M. Smolic, K. Skenderis, and M. Taylor, “Holography for Einstein-Maxwell-dilaton theories from generalized dimensional reduction,” *JHEP* **1201** (2012) 089, [arXiv:1110.2320 \[hep-th\]](#).
- [68] M. Smolic, “Holography and hydrodynamics for EMD theory with two Maxwell fields,” *JHEP* **1303** (2013) 124, [arXiv:1301.6020 \[hep-th\]](#).
- [69] J. de Boer and S. N. Solodukhin, “A Holographic reduction of Minkowski space-time,” *Nucl. Phys. B* **665** (2003) 545–593, [arXiv:hep-th/0303006 \[hep-th\]](#).
- [70] G. Arcioni and C. Dappiaggi, “Exploring the holographic principle in asymptotically flat space-times via the BMS group,” *Nucl. Phys. B* **674** (2003) 553–592, [arXiv:hep-th/0306142 \[hep-th\]](#).
- [71] R. B. Mann and D. Marolf, “Holographic renormalization of asymptotically flat spacetimes,” *Class. Quant. Grav.* **23** (2006) 2927–2950, [arXiv:hep-th/0511096 \[hep-th\]](#).
- [72] V. Mukhanov, *Physical Foundations of Cosmology*. Cambridge University Press, Cambridge, UK, 2005.
- [73] **Planck Collaboration** Collaboration, P. Ade *et al.*, “Planck 2013 results. XVI. Cosmological parameters,” *Astron. Astrophys.* **571** (2014) A16, [arXiv:1303.5076 \[astro-ph.CO\]](#).
- [74] A. Strominger, “The dS / CFT correspondence,” *JHEP* **0110** (2001) 034, [arXiv:hep-th/0106113 \[hep-th\]](#).
- [75] A. Strominger, “Inflation and the dS / CFT correspondence,” *JHEP* **0111** (2001) 049, [arXiv:hep-th/0110087 \[hep-th\]](#).
- [76] S. Nojiri and S. D. Odintsov, “Conformal anomaly from dS / CFT correspondence,” *Phys. Lett. B* **519** (2001) 145–148, [arXiv:hep-th/0106191 \[hep-th\]](#).
- [77] A. Ghezelbash and R. B. Mann, “Action, mass and entropy of Schwarzschild-de Sitter black holes and the de Sitter / CFT correspondence,” *JHEP* **0201** (2002) 005, [arXiv:hep-th/0111217 \[hep-th\]](#).
- [78] D. Klemm, “Some aspects of the de Sitter / CFT correspondence,” *Nucl. Phys. B* **625** (2002) 295–311, [arXiv:hep-th/0106247 \[hep-th\]](#).

- [79] M. Spradlin and A. Volovich, “Vacuum states and the S matrix in dS / CFT,” *Phys. Rev. D* **65** (2002) 104037, [arXiv:hep-th/0112223](#) [[hep-th](#)].
- [80] D. Anninos, T. Hartman, and A. Strominger, “Higher Spin Realization of the dS/CFT Correspondence,” [arXiv:1108.5735](#) [[hep-th](#)].
- [81] J. Maldacena, “Einstein Gravity from Conformal Gravity,” [arXiv:1105.5632](#) [[hep-th](#)].
- [82] P. McFadden and K. Skenderis, “Holography for Cosmology,” *Phys. Rev. D* **81** (2010) 021301, [arXiv:0907.5542](#) [[hep-th](#)].
- [83] P. McFadden and K. Skenderis, “Holographic Non-Gaussianity,” *JCAP* **1105** (2011) 013, [arXiv:1011.0452](#) [[hep-th](#)].
- [84] P. McFadden and K. Skenderis, “Cosmological 3-point correlators from holography,” *JCAP* **1106** (2011) 030, [arXiv:1104.3894](#) [[hep-th](#)].
- [85] A. Bzowski, P. McFadden, and K. Skenderis, “Holography for inflation using conformal perturbation theory,” *JHEP* **1304** (2013) 047, [arXiv:1211.4550](#) [[hep-th](#)].
- [86] W. P. Thurston *et al.*, “Three dimensional manifolds, Kleinian groups and hyperbolic geometry,” *Bull. Am. Math. Soc. (New Series)* **6** (1982) no. 3, 357–381.
- [87] N. Kaloper, J. March-Russell, G. D. Starkman, and M. Trodden, “Compact hyperbolic extra dimensions: Branes, Kaluza-Klein modes and cosmology,” *Phys. Rev. Lett.* **85** (2000) 928–931, [arXiv:hep-ph/0002001](#) [[hep-ph](#)].
- [88] S. Nasri, P. J. Silva, G. D. Starkman, and M. Trodden, “Radion stabilization in compact hyperbolic extra dimensions,” *Phys. Rev. D* **66** (2002) 045029, [arXiv:hep-th/0201063](#) [[hep-th](#)].
- [89] V. Balasubramanian and P. Kraus, “A Stress tensor for Anti-de Sitter gravity,” *Commun. Math. Phys.* **208** (1999) 413–428, [arXiv:hep-th/9902121](#) [[hep-th](#)].
- [90] S. de Haro, S. N. Solodukhin, and K. Skenderis, “Holographic reconstruction of space-time and renormalization in the AdS / CFT correspondence,” *Commun. Math. Phys.* **217** (2001) 595–622, [arXiv:hep-th/0002230](#) [[hep-th](#)].
- [91] C. Fefferman and C. R. Graham, “Conformal invariants,” in *Élie Cartan et les Mathématiques d’aujourd’hui*, Astérisque, hors série, p. 95. Lyon, 1985.
- [92] R. C. Myers, “Stress tensors and Casimir energies in the AdS / CFT correspondence,” *Phys. Rev. D* **60** (1999) 046002, [arXiv:hep-th/9903203](#) [[hep-th](#)].
- [93] F. Kottler, “Über die physikalischen Grundlagen der Einsteinschen Gravitationstheorie,” *Ann. Phys.* **361** (56) (1918) 401–462.

- [94] S. L. Bazański and V. Ferrari, “Analytic extension of the Schwarzschild-de Sitter metric,” *Il Nuovo Cimento B* **91** (1986) no. 1, 126–142.
- [95] D. Birmingham, “Topological black holes in Anti-de Sitter space,” *Class. Quant. Grav.* **16** (1999) 1197–1205, [arXiv:hep-th/9808032 \[hep-th\]](#).
- [96] R. Emparan, “AdS / CFT duals of topological black holes and the entropy of zero energy states,” *JHEP* **9906** (1999) 036, [arXiv:hep-th/9906040 \[hep-th\]](#).
- [97] G. Gibbons, H. Lu, D. N. Page, and C. Pope, “The General Kerr-de Sitter metrics in all dimensions,” *J. Geom. Phys.* **53** (2005) 49–73, [arXiv:hep-th/0404008 \[hep-th\]](#).
- [98] M. H. Dehghani, “Kerr-de Sitter space-times in various dimensions and dS / CFT correspondence,” *Phys. Rev. D* **65** (2002) 104003, [arXiv:hep-th/0112002 \[hep-th\]](#).
- [99] R. Dijkgraaf, H. L. Verlinde, and E. P. Verlinde, “String propagation in a black hole geometry,” *Nucl. Phys. B* **371** (1992) 269–314.
- [100] E. Kiritsis, “Exact duality symmetries in CFT and string theory,” *Nucl. Phys. B* **405** (1993) 109–142, [arXiv:hep-th/9302033 \[hep-th\]](#).
- [101] M. Gromov, “Hyperbolic manifolds according to Thurston and Jørgensen,” in *Séminaire Bourbaki vol. 1979/80 Exposés 543 – 560*, vol. 842 of *Lecture Notes in Mathematics*, p. 40. Springer-Verlag, Berlin, Heidelberg, 1981.
- [102] I. Kanitscheider, K. Skenderis, and M. Taylor, “Precision holography for non-conformal branes,” *JHEP* **0809** (2008) 094, [arXiv:0807.3324 \[hep-th\]](#).
- [103] I. Kanitscheider and K. Skenderis, “Universal hydrodynamics of non-conformal branes,” *JHEP* **0904** (2009) 062, [arXiv:0901.1487 \[hep-th\]](#).
- [104] G. T. Horowitz and T. Wiseman, “General black holes in Kaluza-Klein theory,” [arXiv:1107.5563 \[gr-qc\]](#).
- [105] B. Gouteraux and E. Kiritsis, “Generalized Holographic Quantum Criticality at Finite Density,” *JHEP* **1112** (2011) 036, [arXiv:1107.2116 \[hep-th\]](#).
- [106] I. Kanitscheider, K. Skenderis, and M. Taylor, “Precision holography for non-conformal branes,” *JHEP* **0809** (2008) 094, [arXiv:0807.3324 \[hep-th\]](#).
- [107] R. Emparan, T. Harmark, V. Niarchos, and N. A. Obers, “Blackfolds in Supergravity and String Theory,” *JHEP* **1108** (2011) 154, [arXiv:1106.4428 \[hep-th\]](#).
- [108] J. Bhattacharya, S. Bhattacharyya, S. Minwalla, and A. Yarom, “A Theory of first order dissipative superfluid dynamics,” *JHEP* **1405** (2014) 147, [arXiv:1105.3733 \[hep-th\]](#).
- [109] A. Buchel, “Bulk viscosity of gauge theory plasma at strong coupling,” *Phys.Lett.* **B663** (2008) 286–289, [arXiv:0708.3459 \[hep-th\]](#).

- [110] P. Kovtun, D. T. Son, and A. O. Starinets, “Holography and hydrodynamics: Diffusion on stretched horizons,” *JHEP* **0310** (2003) 064, [arXiv:hep-th/0309213 \[hep-th\]](#).
- [111] T. Harmark, V. Niarchos, and N. A. Obers, “Instabilities of black strings and branes,” *Class.Quant.Grav.* **24** (2007) R1–R90, [arXiv:hep-th/0701022 \[hep-th\]](#).
- [112] B. Kol, “Topology change in general relativity, and the black hole black string transition,” *JHEP* **0510** (2005) 049, [arXiv:hep-th/0206220 \[hep-th\]](#).
- [113] H. S. Reall, “Classical and thermodynamic stability of black branes,” *Phys.Rev.* **D64** (2001) 044005, [arXiv:hep-th/0104071 \[hep-th\]](#).
- [114] P. Bostock and S. F. Ross, “Smeared branes and the Gubser-Mitra conjecture,” *Phys.Rev.* **D70** (2004) 064014, [arXiv:hep-th/0405026 \[hep-th\]](#).
- [115] O. Aharony, J. Marsano, S. Minwalla, and T. Wiseman, “Black hole-black string phase transitions in thermal 1+1 dimensional supersymmetric Yang-Mills theory on a circle,” *Class.Quant.Grav.* **21** (2004) 5169–5192, [arXiv:hep-th/0406210 \[hep-th\]](#).
- [116] A. Buchel and J. T. Liu, “Universality of the shear viscosity in supergravity,” *Phys.Rev.Lett.* **93** (2004) 090602, [arXiv:hep-th/0311175 \[hep-th\]](#).
- [117] I. Bredberg, C. Keeler, V. Lysov, and A. Strominger, “Wilsonian Approach to Fluid/Gravity Duality,” *JHEP* **1103** (2011) 141, [arXiv:1006.1902 \[hep-th\]](#).
- [118] I. Bredberg, C. Keeler, V. Lysov, and A. Strominger, “From Navier-Stokes To Einstein,” *JHEP* **1207** (2012) 146, [arXiv:1101.2451 \[hep-th\]](#).
- [119] S. Bhattacharyya, R. Loganayagam, I. Mandal, S. Minwalla, and A. Sharma, “Conformal Nonlinear Fluid Dynamics from Gravity in Arbitrary Dimensions,” *JHEP* **0812** (2008) 116, [arXiv:0809.4272 \[hep-th\]](#).
- [120] R. Argurio, F. Englert, and L. Houart, “Intersection rules for p-branes,” *Phys.Lett.* **B398** (1997) 61–68, [arXiv:hep-th/9701042 \[hep-th\]](#).
- [121] R. Argurio, “Intersection rules and open branes,” [arXiv:hep-th/9712170 \[hep-th\]](#).
- [122] A. W. Peet, “TASI lectures on black holes in string theory,” [arXiv:hep-th/0008241 \[hep-th\]](#).
- [123] M. Huq and M. Namazie, “Kaluza-Klein Supergravity in Ten-dimensions,” *Class.Quant.Grav.* **2** (1985) 293.
- [124] F. Giani and M. Pernici, “N=2 SUPERGRAVITY IN TEN-DIMENSIONS,” *Phys.Rev.* **D30** (1984) 325–333.
- [125] I. Campbell and P. C. West, “N=2 D=10 Nonchiral Supergravity and Its Spontaneous Compactification,” *Nucl.Phys.* **B243** (1984) 112.

-
- [126] E. Cremmer, B. Julia, and J. Scherk, “Supergravity Theory in Eleven-Dimensions,” *Phys.Lett.* **B76** (1978) 409–412.
- [127] A. A. Tseytlin, “Composite black holes in string theory,” [arXiv:gr-qc/9608044 \[gr-qc\]](#).
- [128] S. S. Gubser and I. Mitra, “Instability of charged black holes in Anti-de Sitter space,” [arXiv:hep-th/0009126 \[hep-th\]](#).
- [129] S. S. Gubser and I. Mitra, “The Evolution of unstable black holes in anti-de Sitter space,” *JHEP* **0108** (2001) 018, [arXiv:hep-th/0011127 \[hep-th\]](#).
- [130] S. F. Ross and T. Wiseman, “Smeared D0 charge and the Gubser-Mitra conjecture,” *Class.Quant.Grav.* **22** (2005) 2933–2946, [arXiv:hep-th/0503152 \[hep-th\]](#).
- [131] T. Harmark, V. Niarchos, and N. A. Obers, “Instabilities of near-extremal smeared branes and the correlated stability conjecture,” *JHEP* **0510** (2005) 045, [arXiv:hep-th/0509011 \[hep-th\]](#).
- [132] R. Gregory, “Black string instabilities in Anti-de Sitter space,” *Class.Quant.Grav.* **17** (2000) L125–L132, [arXiv:hep-th/0004101 \[hep-th\]](#).
- [133] A. Buchel, “Violation of the holographic bulk viscosity bound,” *Phys.Rev.* **D85** (2012) 066004, [arXiv:1110.0063 \[hep-th\]](#).
- [134] T. Hirayama, G. Kang, and Y. Lee, “Classical stability of charged black branes and the Gubser-Mitra conjecture,” *Phys.Rev.* **D67** (2003) 024007, [arXiv:hep-th/0209181 \[hep-th\]](#).
- [135] J. Erdmenger, M. Rangamani, S. Steinfurt, and H. Zeller, “Hydrodynamic Regimes of Spinning Black D3-Branes,” *JHEP* **1502** (2015) 026, [arXiv:1412.0020 \[hep-th\]](#).

